THE EFFECTS OF AN ARTIFICIAL SKIN ON SCARRING AND CONTRACTION IN OPEN WOUNDS

by

DENNIS P. ORGILL

B.S., University of California, Berkeley
(1978)

S.M., Massachusetts Institute of Technology
(1980)

Submitted to the Harvard-M.I.T.
Division of Health Sciences and Technology
in Partial Fulfillment of the
Requirements of the Degree of

DOCTOR OF PHILOSOPHY

at the

MASSACHUSETTS INSTITUTE OF TECHNOLOGY

April 1983

Signature of Author _____
Harvard-M.I.T. Division of Health Sciences
and Technology, April 29, 1983

Certified by _____
/ / Thesis Supervisor

Accepted by _____
Chairman, Department Graduate Committee

THE EFFECTS OF AN ARTIFICIAL SKIN ON SCARRING AND CONTRACTION IN OPEN WOUNDS

by

DENNIS PAUL ORGILL

Submitted to the Harvard-M.I.T. Division of Health Sciences and Technology on April 29, 1983 in partial fulfillment of the requirements for the Degree of Doctor of Philosophy

ABSTRACT

A bilayer polymeric membrane consisting of a top layer of silicone elastomer bonded to a bottom layer of a highly porous collagen-glycosaminoglycan (GAG) matrix was seeded with a suspension of epidermal cells. Seeding of the bilayer membrane was accomplished by constructing a special centrifuge bucket which was machined to the size of the membrane and maintained the plane of the membrane perpendicular to the centrifugal force vector. When applied to the open wound of the guinea pig, these membranes maintained wounds free from infection and exudation. Mesenchymal cells and capillaries from the woundbed invaded the collagen-GAG matrix which acted as a biodegradable template for the formation of a dermal-like tissue (neodermis). Within two weeks of grafting, the seeded epidermal cells had divided and formed a confluent keratinizing epidermis (neoepidermis) just below the silicone layer. This allowed the silicone layer to be removed. The neoepidermis maintained the wounded areas free from infection and developed a water permeability comparable to normal skin.

The neodermis formed had a collagen fiber morphology different from scar, but lacked skin accessory organs such as hair follicles and sebaceous glands. The skin produced, as a result of the application of these membranes, was soft, supple, resilient and formed a smooth transition with normal skin. Measurements of mechanical properties in guinea pigs showed the neodermis to have an ultimate tensile strength of 2,000 p.s.i., about 45% of the value for normal dermis adjacent to the graft. Samples of neodermis were slightly stiffer than the adjacent dermis. Both stiffness and strengths of the neodermis were similar to those of a mature full-thickness autograft.

The gross appearance of the new skin 200 days after grafting with 1.5 by 3 cm membranes showed that the wound area was about 70% of the original. This area was much greater than that observed with ungrafted wounds (23%) and wounds grafted with unseeded membranes (27%, $p < 0.005$),

but significantly less than that seen in the full-thickness autograft (121%, $p < 0.005$). This suggests that the neo-epidermal-neodermal interaction is an important parameter in the control of contraction.

The time at which neoepidermal confluence occurred was dependent on the number of cells seeded. Seeding membranes with 500,000 cells/cm^2 graft area resulted in epidermal confluence in 12 ± 3 days, whereas seeding with 50,000 cells/cm^2 yielded confluence in 21 ± 8 days. Increasing the cell density above 500,000 cells/cm^2 graft did not reduce the time required to achieve neoepidermal confluence. About 2,000,000 viable cells were isolated from each square centimeter of the thin split-thickness skin biopsies. This resulted in expansion factors of 4:1 and 40:1 when 500,000 and 50,000 cells/cm^2 were used respectively. The cell isolation and seeding procedure was performed in a period of less than two hours. These results suggest that it may be possible to close large wounds of a burn victim in a single operative procedure without extensive use of autografts. These results also suggest that long-term disfigurement resulting from scarring and contraction may also be reduced.

Preliminary studies using epidermal cells of a heterologous origin showed in 38% of the grafts gross evidence of the production of a functional neoepidermis without cell mediated rejection over at least 17 days of observation. No immunosuppression was used and in three animals, immunocompetence was demonstrated by subsequent rejection of a full-thickness homograft from the same donor in a period of about 10 days. It was proposed that the elimination of Langerhans cells from the epidermal cell suspension may result in neoepidermal survival without the use of immunosuppressive drugs. Further work will be required to determine the optimal treatment of the donor epidermal cell suspension so as to reduce its immunogenicity.

Thesis Supervisor: Ioannis V. Yannas, Ph.D.

Title: Professor, Harvard, M.I.T. Division of Health Sciences and Technology

Professor of Polymer Science and Engineering, Department of Mechanical Engineering and the Department of Materials Science and Engineering, Massachusetts Institute of Technology

TABLE OF CONTENTS

FIGURE LEGENDS

FIGURE LEGENDS (cont.)

FIGURE LEGENDS (cont.)

TABLES

ACKNOWLEDGMENTS

This thesis has required the cooperation of many individuals from many disciplines. I would like to thank my thesis advisor, Professor I.V. Yannas for the many hours he spent with me discussing this project. Each member of my thesis committee has contributed their area of expertise to this thesis: Dr. Burke with his clinical knowledge of artificial skin and surgery, Professor Cravalho for his expertise in cryopreservation, and Professor Backer for his advice on mechanical measurements.

Dr. James Murphy has spent many hours preparing, analyzing and interpreting the histologic specimens with assistance in the area of neuropathology and special stains from Dr. William Schoene. I would like to thank Ms. Blanca Lusetti for the preparation of histologic specimens.

I am grateful to Mr. Eugene Skrabut for assistance in the preparation of the grafts, culturing cells, and advice on many of the experimental aspects of this thesis. I would like to thank Don Costa, Jude Colt, Susan Flynn, Pam Phillips, and Dr. Christian Newcomber for their assistance with grafting and caring for the animals. I would like to acknowledge the help of Mrs. Betsy Goeke with the Scanning Electron Microscope and Dr. Irving Blank of the Department of Dermatology at Massachusetts General Hospital for the use of the evaporimeter.

I would like to thank the Whitaker Foundation for

the support they provided me throughout the duration of this thesis. Finally, I would like to thank my wife Nancy for her help and encouragement on many aspects of this work as well as her assistance with the manuscript.

ABBREVIATIONS

ACD	Acid Citrate Dextrose
DMEM	Dulbecco's Modified Eagle's Medium
DMSO	Dimethyl sulfoxide
EDTA	Ethylenediaminotetraacetic Acid
FCS	Fetal Calf Serum
GAG	Glycosaminoglycan
PBS	Phosphate Buffered Saline
SEM	Scanning Electron Microscope
TCM	Tissue Culture Medium

INTRODUCTION

The need for a synthetic replacement for the skin has long been recognized. A suitable replacement would aid the treatment of skin loss due to a variety of diseases and trauma and would be particularly helpful in the treatment of burn victims. Over 130,000 persons (1) are hospitalized each year in the United States due to burns, and 10,000 die as a result of their burn injuries (2). Of the patients who are hospitalized, many have burns over half of the body surface which demand months of medical treatment and often years of physical therapy and reconstructive surgery to restore function and reduce disfigurement.

The acute burn victim presents the physician with two major problems which are a direct result of loss of skin: 1) fluid loss due to water evaporation from open wounds, and 2) infection related to access of microoorganisms to the body through the wounded areas. Current burn therapy (3,4,5) is directed at treating these problems as well as using various surgical techniques and devices to close these potentially devastating wounds.

Being the largest organ in the body, the skin covers about 1.7 square meters of the average adult. Normally, it acts as a protective barrier to prevent bacteria, toxic materials, and ultraviolet light from entering the body and to keep fluid and electrolytes within the body. The skin also acts as a mechanical barrier by protecting the body from abrasions and minor trauma. It serves in thermo-

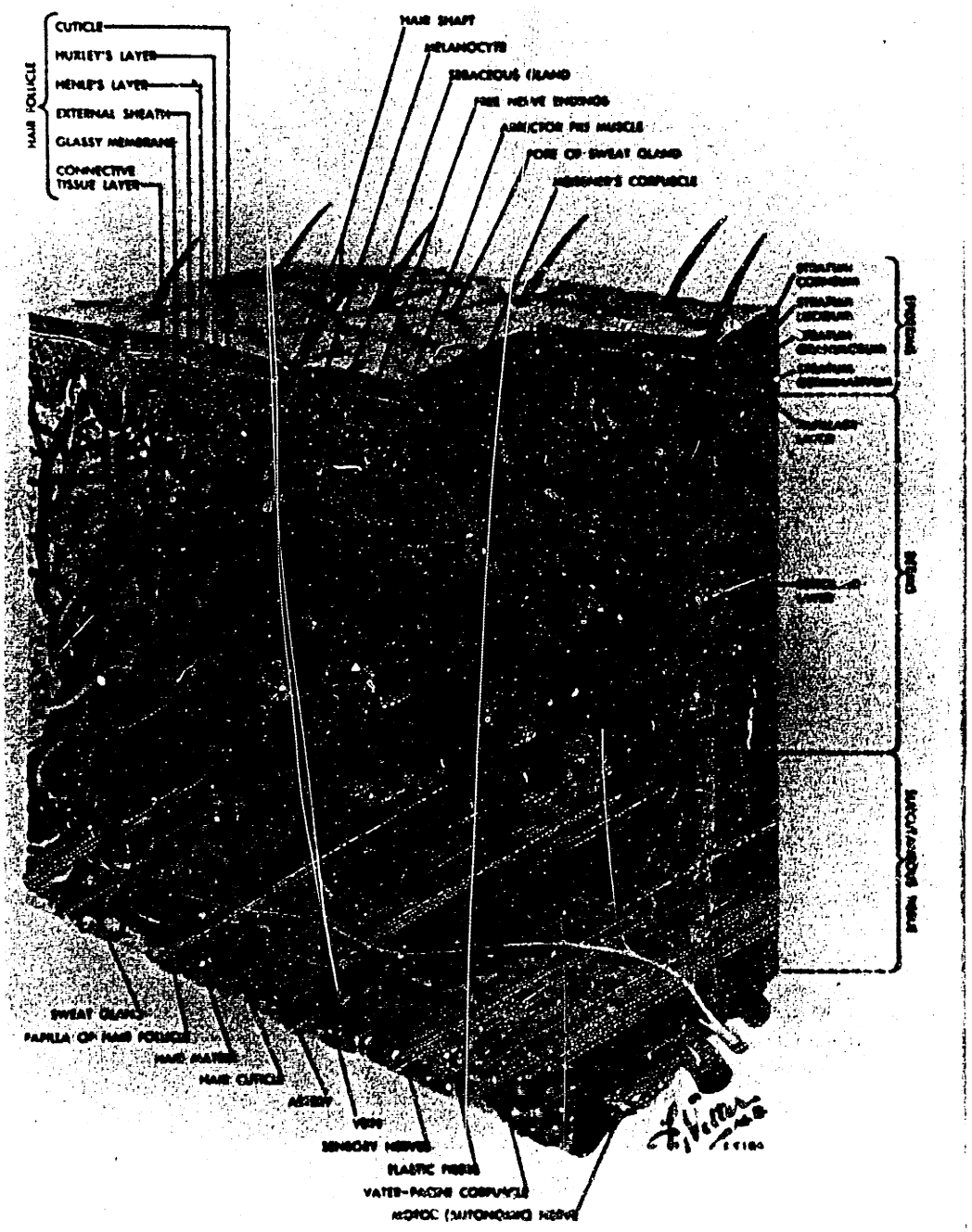

Figure 1. Anatomy of the skin (CIBA Pharmaceutical Co., Division of CIBA-GEIGY Corporation, illustrated by Frank H. Netter, M.D.).

regulation through the use of specialized sweat glands and by the regulation of surface blood flow. The rate of blood flow in skin is also an important regulator of blood pressure. Human skin also plays a small role in excreting toxic metabolites such as urea from sweat glands.

The skin is composed of two basic layers, the dermis and epidermis. The epidermis, derived from the embryonic ectoderm, is a multicellular layer about 80 μm thick consisting of four sublayers (Figure 2): the stratum basalis, the stratum spinosum, the stratum granulosum, and the stratum corneum (6). Cells of the stratum basalis, or basal cell layer, are the stem cell population of the epidermis and lie in close proximity to the dermis. As cells mature, they pass upwards in the epidermis through the stratum spinosum and stratum granulosum. Finally, cells at the top of the stratum granulosum die, become anuclear and join together to form the stratum corneum. The stratum corneum, therefore, is being replaced continously by cells below it as the upper levels of the stratum corneum slough off. The stratum corneum acts as the barrier to mass transport between the body and the environment. Skin appendages such as hair, sweat glands, sebaceous glands and apocrine glands are specialized organs derived from the epidermis (7).

The dermis, derived from the embryonic mesoderm, is a much thicker layer (1-2 mm thick) and is responsible for the mechanical properties of the skin. It is composed primarily of water, collagen, glycosaminoglycans, elastin,

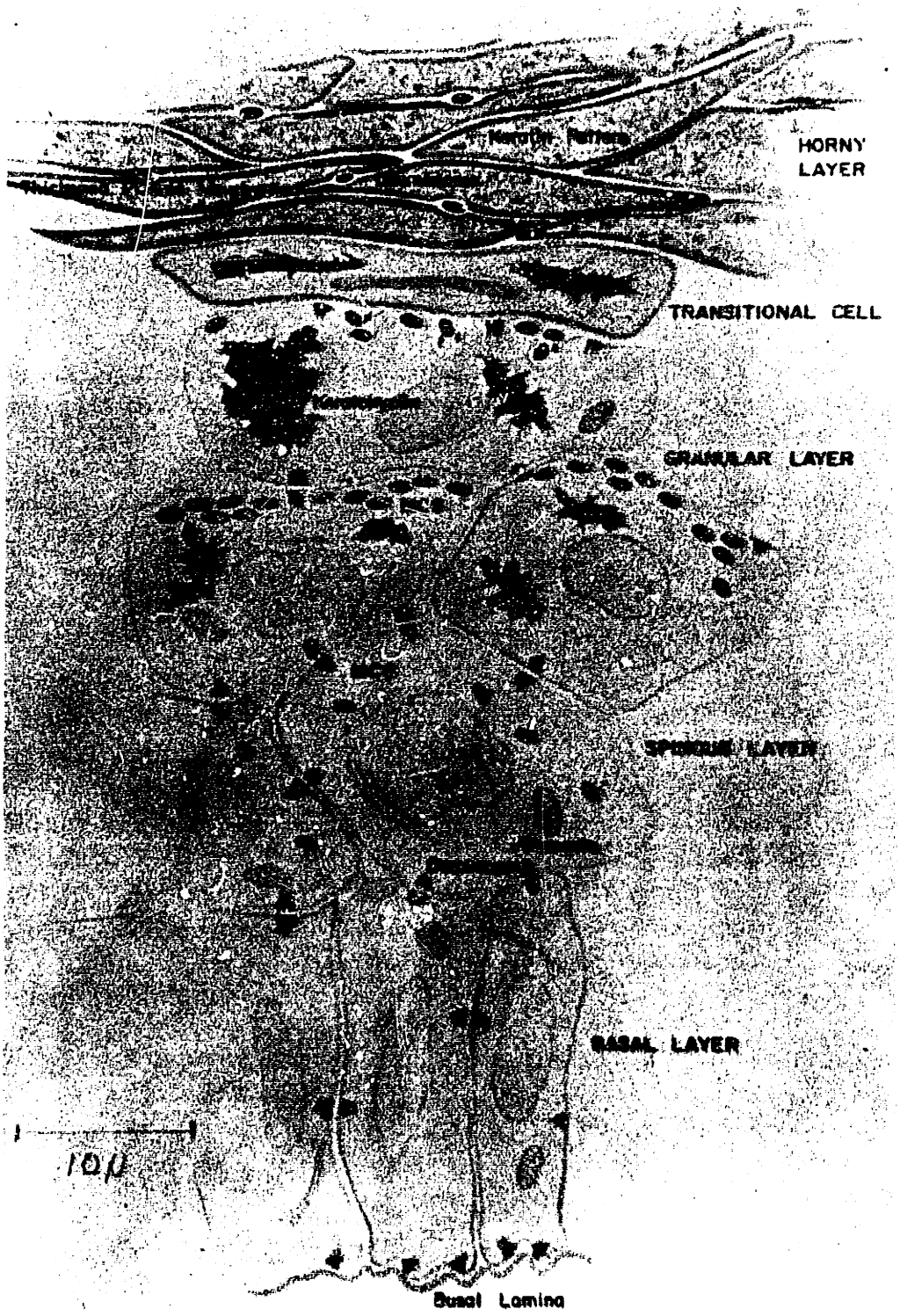

Figure 2. Anatomy of the epidermis. The maturation sequence for an epidermal cell is from the basal layer to the horny layer or stratum corneum. From: Montagna, W., Parakkal, P.F. The Structure and Function of Skin, 3rd ed., New York, Academic Press, 1974.

and reticulum (8). The dermis is a relatively strong viscoelastic structure with tensile strengths ranging from 500 to 10,000 p.s.i. (9,10) depending on species, location in the body, and orientation of the specimen. Many of the mechanical properties of the dermis can be ascribed to the collagen fibers present. Because of the rich vascularity of the dermis, body temperature can be maintained over a variety of environmental conditions by regulation of the skin blood flow (Figure 3).

The replacement of skin and the process of wound healing have long intrigued man (11). Mammalian skin seems to have lost its ability to regenerate (12). This is in contrast to lower animal species such as the salamander where it is well known that complete limbs can regenerate without any evidence of scarring (12). Anecdotes in the human, and a recently documented study in the mouse (13), suggest that perhaps the regenerative capacity in mammals is not completely lost. In this study, structures such as bone, nail and dermis were shown to regenerate when the distal portion of the digit of a mouse was amputated (13). Other than these isolated instances, the mammalian species seem to react quite differently to wounds than the amphibian counterpart. The mammal reacts to an open wound by two important processes: contraction and scarring. Contraction is the reduction in wound area which occurs during healing. Contraction may be a mammalian adaptation to defend against the potential lethal effects of an open

IMPORTANT FUNCTIONS OF SKIN AS AN ORGAN

1. Protection of the Body from Trauma
2. Controls flux of H_2O, O_2, CO_2, etc.
3. Prevents Microorganisms from entering the Body
4. Regulates body temperature
5. Activates Vitamin D
6. Receptors for hot, cold, pain, touch, etc.

Figure 3. Physiology of the Skin.

wound. Skin from the edges of the wound is pulled together helping to close the wound. Contraction has been studied in many animal models and differences in the rate of contraction have been found due to species, nutrition, and the administration of drugs (14-26).

Many theories have been proposed to explain the mechanism of contraction. One popular theory states that contraction is due to the action of myofibroblasts, cells present in granulation tissue, which exert forces on the surrounding tissue. Majno et al showed the contractility of strips of granulation tissue in vitro when exposed to pharmacologic agents such as bradykinin, vasopressin, and epinephrine (27). Myofibroblasts are also found around blood clots and in Dupuytren's contracture. Myofibroblasts have characteristics both of fibroblasts and smooth muscle cells when viewed with the electron microscope (28-30) and are probably derived from either fibroblasts or mesenchymal cells. The administration of a smooth muscle inhibitor has been observed to delay wound contraction by 10 to 14 days (31). Corticosteroids have also been shown to be effective in delaying contraction (16), although the mechanism of their action has not been proven. Due to the toxic effects of smooth muscle inhibitors and other agents such as corticosteroids, a clinically acceptable pharmacologic blockade to wound contraction has not been identified to date.

The result of the contraction process is an area of disfigurement referred to as a contracture. These are areas

of the body which lack sufficient skin to permit a full range of motion around the affected joints. Thus, contractures can often be crippling and require reconstructive surgery to restore function. As an open wound contracts, fibroblasts in the woundbed secrete various compounds such as collagen and glycosaminoglycans which are invaded by a rich bed of capillaries. This fragile tissue which forms on top of the woundbed, termed granulation tissue, is thought to be a precursor of scar tissue. Scar formation is thought to arise as a consequence of contraction and granulation tissue synthesis. Histologically, scar has close packed collagen fibers which lack the wavy appearance of collagen fibers in normal dermis (32,33). This close-packed and oriented geometry of collagen fibers in scar is conceivably responsible for the observation that scar is much stiffer than normal skin (10).

Hypertrophic scar and keloid are peculiar phenomena seen only in human skin without any comparable animal model (34). These unsightly exacerbations of scars are reflected by hyperplasia of fibroblasts and an excess synthesis of collagen tissue. Hypertrophic scarring is often associated with wound contractures and is often seen in the burn patient. Keloid in many respects is a more severe form of hypertrophic scarring. It frequently has a genetic predisposition, and often only a minor injury is required to produce a large lesion (34).

Scarring has been extensively studied by many

investigators using biochemical, cellular, morphological, and mechanical techniques. These investigations have further classified scar into categories such as early scar, mature scar, hypertrophic scar and keloid. Biochemical comparisons of many of the components of dermis have been made with scar including the chondroitin-4-sulfate content and the amount of Type III collagen present (32,35-41). Comparison of the nature of collagen crosslinks and the content of elastin have also been made (32,33,42-45). A careful review of this biochemical literature indicates that, although some differences in composition between scar and dermis have been reported, these tissues are, in fact, quite similar biochemically (Table I). Mechanical studies show scar to be much stiffer than dermis (10). This increased stiffness is reflected at a histological level by increased orientation of collagen fibers. A constituitive relation for connective tissues can be derived by modeling them as a swollen proteoglycan matrix reinforced with collagen and elastin fibers (46). This type of relationship can explain some of the differences in mechanical properties of scar and dermis based on collagen fiber morphology.

In 1970, Professor I.V. Yannas and Dr. J.F. Burke began a collaborative effort to design an artificial skin which would address both the short-term and long-term needs of the burn victim. The autograft had been used successfully for many years in replacing skin loss (47); however,

SOME BIOCHEMICAL COMPARISONS OF SCAR AND DERMIS

Component	Human Scar	Dermis
Percent Water (38)	65.8	65.2
Total Collagen (38) mg hydroxyproline/g dry wt.	69.6	72.8
Insoluable Collagen (38) % weight of total collagen	36	50.5
Elastin (38)	<0.1%	<0.1%
Acid Soluable Collagen (41)		
Total hydroxylysine residues	2.31	2.81
Ratio of Glc-Gal-Hyl to Gal-Hyl	1.53	2.16
% Glycosylation	16.2	16.6
Gelatinized Insoluable Collagen (41)		
Total Hydroxylysine Residues	2.69	2.81
Ratio of Glc-Gal-Hyl to Gal-Hyl	2.51	2.38
% Glycosylation	16.9	17.0
Relative Percentages of GAGs (36)		
Hyaluronic Acid	21	41.5
Dermatin Sulfate	70.5	54.0
Chondrotin 4-sulfate	8.5	4.5

TABLE I. Please refer to references for methods, type of scar used, age of scar, and number of samples used.

in the severely burned patient, the autograft was in short supply and a substitute was desired. Skin grafts from cadavers (47,48) or pig skin grafts (49,50) were not considered acceptable due to their rapid immunologic rejection which required frequent replacement. Because of the complexity of this problem, the research effort was divided into two design stages (51): Stage 1 and Stage 2 (Figure 4). Stage 1 of the design was to meet the short-term needs of the burn patient. Specifically, it was to close the wound, regulate fluid loss, and maintain the wound free from infection over a period of at least 30 days. Stage 2 of the design addressed itself to the long-term problems of scarring and contraction, as well as satisfying the Stage 1 criteria. In order to accomplish this, certain physical and biological specifications were outlined (Figure 4). After several years of work, a bilayer membrane was developed which met the Stage 1 objectives (52-54). This consisted of an outer layer of a silicone elastomer and an inner layer of a highly porous collagen-glycosaminoglycan (GAG) copolymer. The silicone layer served as an inert membrane regulating transport between the environment and the woundbed. In contrast, the collagen-GAG layer reacted with the woundbed and was gradually degraded enzymatically.

Stage 1 membranes have been shown to achieve their objectives both in the guinea pig model (50-53) and in preliminary clinical trials (55). In both cases, exudation and infection were controlled. In addition, there was no

Summary of Design Objectives of Stages 1 and 2 Artificial Skin

Stage 1

Physicial Properties	Biologic Properties
Moisture Flux Rate	Control fluid loss
Bending Rigidity	Barrier to bacteria
Tear Strength	Non-toxic metabolites
Surface Energy	Low or obsent antigenicity
Suturabe	Lack of inflamatory or foreign body reaction
Shelf Life	Allow ingrowth of tissue
Pore Structure	Synthesis of neodermis
	Peel Strength

Stage 2

Physical Properties	Biological Properties
Same as Stage 1	Same as Stage 1
	Control of Contraction
	Reduction in scarring
	Simultaneous synthesis of neodermis and neoepidermis

Figure 4

evidence of graft rejection, and immunosuppressive agents were not required. Mesenchymal cells and capillaries from the woundbed invaded the collagen-GAG matrix during the first week. Epidermal cells from normal adjacent skin migrated between the silicone and collagen-GAG layers by the end of the first week (Figure 5). Epidermal cell migration led to closure of 1.5 x 3.0 cm guinea pig wounds in 30 to 45 days; however, in large wounds, this rate of epidermal migration (approximately 0.25 mm/day) proved to be too slow to be clinically acceptable. To speed up the process of wound closure, thin split-thickness grafts (0.1 mm) were meshed and placed over the vascularized collagen-GAG membrane after the silicone layer had been removed. This procedure closed the wound in about two weeks and gave an aesthetically more pleasing result than the conventional mesh graft treatment (55) of open wounds. The histologic results at 60 days showed a neodermis which differed from conventional scar tissue. Using very thin split-thickness skin grafts (0.1 mm), as compared to the conventional split-thickness skin grafts (0.3 to 0.4 mm), also resulted in minimal or no scarring at the donor site. Studies in humans and in guinea pigs indicate that these membranes performed at the level required of Stage 1 membranes and, with the addition of the autoepidermal grafts, approached the Stage 2 design criteria.

One major disadvantage of the Stage 1 procedure is that it requires two traumatic surgical procedures to cover a

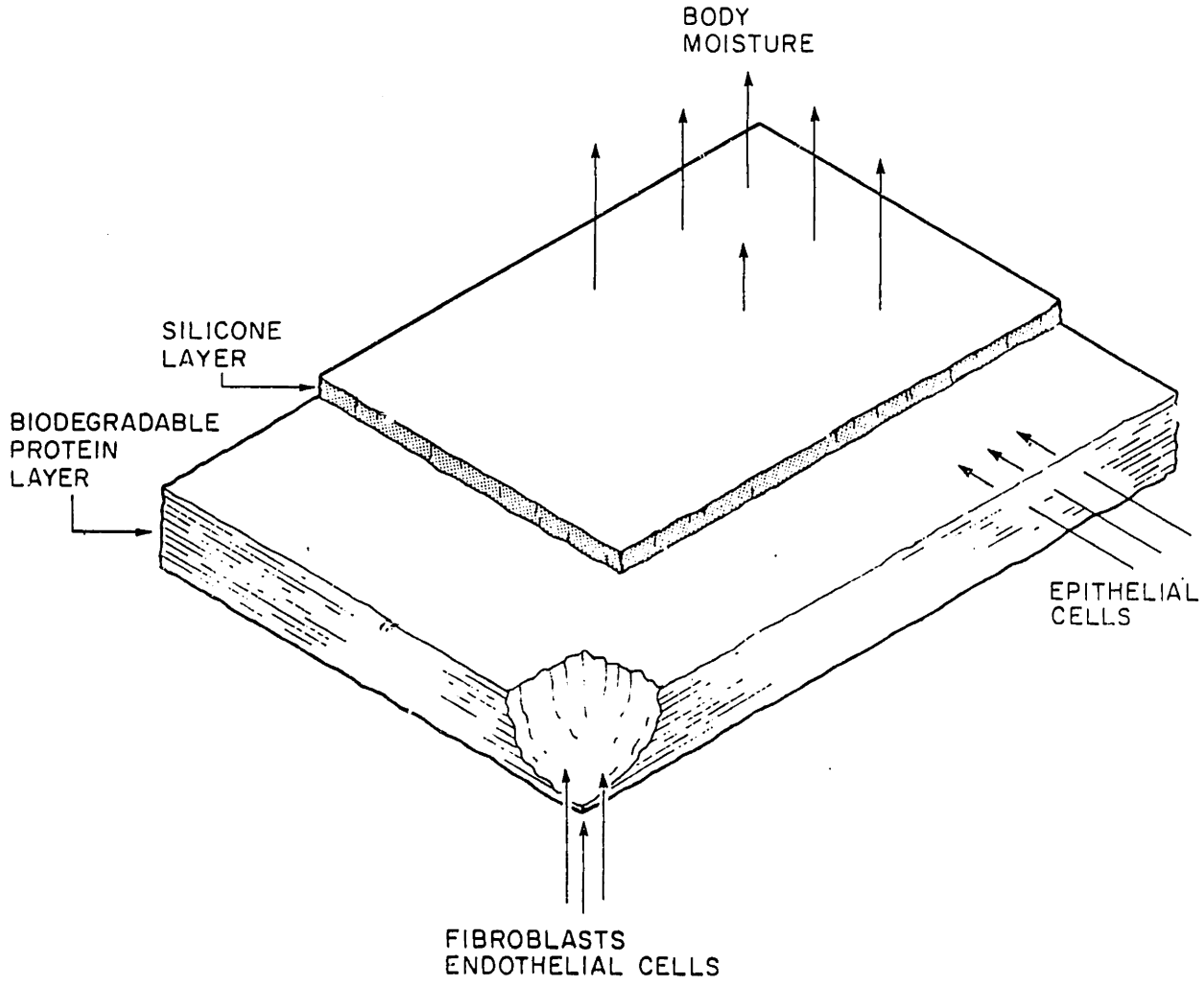

Figure 5. Schematic of bilayer membrane.

given area of skin. One goal of the research described in this thesis was to design a procedure which would eliminate one of these operations. The second goal of the thesis was to investigate scarring and contraction which occur as a result of the application of these bilayer membranes. The combination of these two goals was to lead to the development of a Stage 2 membrane.

To test hypotheses related to the goals of the thesis, the guinea pig model was chosen. A considerable amount of data had been generated with the guinea pig model in developing membranes which satisfied the Stage 1 design criteria. Although there are significant differences in anatomy and physiology of the guinea pig skin and human skin, it was felt that this convenient animal model would answer many of the design questions. Specifically, it was recognized that the guinea pig has a panniculus carnosus, a thin muscle layer of the skin, which makes the skin of the rodent very mobile. In addition, the guinea pig has much more hair than humans and lacks sweat glands.

Previous work with Stage 1 membranes has shown that when applied to 1.5 by 3.0 cm wounds, contraction is delayed by 10 to 15 days when compared to ungrafted controls. Varying several of the physicochemical parameters of the collagen-GAG matrix, including porosity (56), degree of cross-linking (57), and content of glycosaminoglycan (56) have shown to influence the contraction kinetics. In contrast to the guinea pig model, Stage 1 membranes applied to open

wounds in humans showed no evidence of contraction when used in conjunction with autoepidermal grafts (55). Therefore, it was felt that the guinea pig provided a more sensitive assay for contraction than did human subjects.

As different methods were being proposed to achieve the Stage 2 design criteria, it became necessary to provide a method to evaluate the efficacy of the various membranes tested. The Stage 1 design criteria could be easily assessed by frequent gross observation of the membranes. Membranes which had a low infection rate and an appropriate moisture flux would be likely candidates for future studies. In contrast, the evaluation of the efficacy of Stage 2 membranes in reducing disfigurement would be more difficult. To evaluate the long-term disfigurement caused by open wounds, it was proposed that disfigurement could be modeled as a function of contraction and scarring (Figure 6). Contraction is the quantity most easily measured since it can be obtained from gross observations. Scarring, in contrast, is most readily assessed by histologic examination of the tissue (58-61). The collagen fiber morphology, the elastin content, the direction of dermal capillaries, the presence of hair follicles, and morphology of the dermal-epidermal junction are all classic criteria used to distinguish scar from dermis microscopically (Table II).

In developing a Stage 2 membrane, the initial emphasis of this research was to evaluate the factors which influenced the contraction pattern of these grafts. It was

$$\text{Disfigurement} = \text{Fn}(\text{Scarring}, \text{Contraction})$$

Figure 6. The long-term disfigurement which results from open wounds can be modeled as a function of two components, scarring and contraction. Contraction is grossly observable as the change in wound area with time. Scarring is most accurately assessed by histologic examination.

CLASSIC HISTOLOGIC CRITERIA OF SCAR TISSUE

Structure	Morphology
Collagen Bundles	Close packed, oriented parallel to the plane of skin
Small Blood Vessels	Extend perpindicularly between epidermis and subcutis
Hair Follicles and other Adenexa	Absent
Elastin	Absent or thin fibers running parallel to collagen
Dermal-Epidermal Junction	Rete Pegs absent in Humans No difference in the Guinea Pig

TABLE II.

hoped that understanding the effects of many of the parameters of the graft could lead to a separation of the two phenomena of scarring and contraction.

To achieve the Stage 2 design criteria, it became necessary to devise a method which would close the wound with a functional epidermis within a clinically acceptable time. Several approaches to this problem were considered including the use of agents such as epidermal growth factor (62) or the use of epidermal sheets grown from cultures in vitro (63-65). Before resorting to these techniques, it was felt that a bilayer membrane suitably seeded with epidermal cells might provide the most straightforward solution to the problem. It was hoped that, with the aid of growth factors present in the woundbed, the epidermal cells would multiply within the graft and form a confluent sheet of epidermis (Figure 7). Several seeding approaches were proposed including the inoculation of the bilayer membrane with a hypodermic syringe, "painting" the collagen-GAG layer with a cellular suspension prior to assembly, and centrifugal inoculation. Of these possibilities, centrifugal inoculation offered the most uniform cell distribution and appeared to give the most reproducible results (66-71).

As an extension of the Stage 2 design, the possible use of cells derived from a heterologous source was proposed. The incorporation of heterologous cells in artificial skin grafts would be advantageous for several reasons. It would

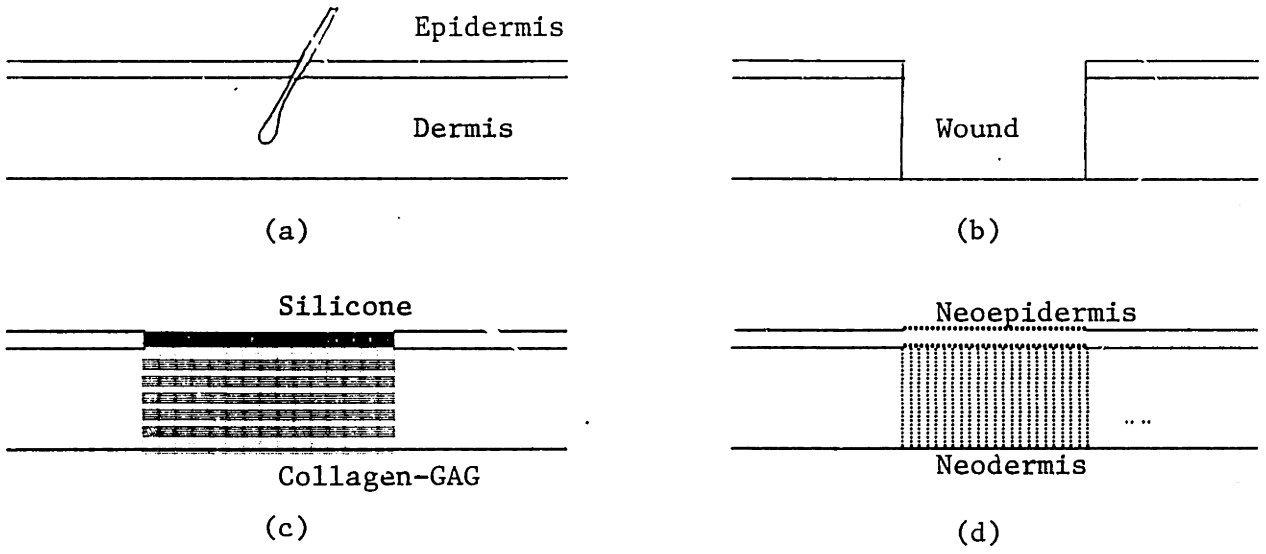

Figure 7. Animal model of Stage 2 design. a) shows normal skin, b) an excised wound, c) a seeded bilayer membrane in place, d) the seeded cells have multiplied to form a confluent neoepidermis allowing removal of the silicone layer. The collagen-GAG layer is replaced by neodermis.

eliminate the need for a biopsy as well as the need to have a nearby laboratory with trained personnel to perform the cell separation and seeding processes. With the advances of cryobiology, a method to allow storage and shipment of frozen seeded membranes could be developed.

It has been suggested by Rogers as early as 1950 (72) that homografts of pure epidermal origin, being avascular like transplants of the cornea or cartilage, might be exaempted from immunologic rejection. Later studies have shown, however, that even intact epidermal sheet homografts, as suggested by Rogers (72), are rejected (73). It is well-known that full-thickness homografts are rejected (74) over a period of about two weeks. Immunosuppressive drugs were not considered as a possible solution due to their high incidence of side effects. The recipient, in addition, would probably be required to take such drugs indefinitely to avoid eventual rejection.

There is some recent evidence (65,75-84) that epidermal cells isolated from skin biopsies can be treated to reduce their immunogenicity. Transplantation antigens have been divided into two classes: Class I major histocompatability complex (MHC) and Class II MHC (Ia alloantigens in mice). Class I MHC alloantigens are expressed by virtually all nucleated cells, whereas Class II antigens are restricted to cell populations such as B lymphocytes, macrophages, subpopulations of T lymphocytes, and certain dendritic cells (78), including Langerhans cells. Langerhans cells are

derived from the bone marrow and reside in the suprabasal portion of the epidermis. Cumulative evidence suggests that these cells are the primary immunocompetent cell of the epidermis (65,75-84). They have been implicated in initiating the immune response in contact hypersensitivity and in stimulating the epidermal cell lymphocyte reaction (75). Corneal allografts, an epithelial tissue devoid of Langerhans cells have been used successfully without the need for immunosuppressive agents. Therefore, it was felt that the elimination of Langerhans cells from the epidermis would result in a tissue that could be transplanted without rejection. Several approaches have been used to separate Langerhans cells from epidermal cells. Eisinger (65) has grown sheets of epidermis for several weeks in culture and grafted them on dog open wounds. Even though these were allografts, no lymphoid infiltrate was seen during the six weeks of the study. Faure et al (76) showed an in vitro decrease in expression of cytologic antibodies in cultured epidermal cells. Elmets et al (77) reported an absence of Langerhans cells in epidermal cells beyond 0.3 mm from explants of skin in organ culture. It may be that the increased proliferation rates of epidermal cells relative to Langerhans cells in culture depletes the population of Langerhans cells. Several methods have been developed to separate, in vitro, Langerhans cells from epidermal cells. Morhenn et al (75) used velocity sedimentation to separate out epidermal cells. Streilein et al (78) reports success

in removing significant populations of Langerhans cells by repeatedly stripping the skin with tape. Recently the specificity of a monoclonal antibody for Langerhans cells (79-81) has been utilized to enrich populations of Langerhans cells using a fluorescence-activated cell sorter (82). Density centrifugation has also been shown to be an effective physical method to separate out the Langerhans cells (74).

In addition to these physical methods, treating an epidermal cell suspension with ultraviolet light (83) or with corticosteroids (84) has also been shown to reduce the ability of Langerhans cells to present antigens effectively. Although there have been these multiple approaches to eliminating the effect of Langerhans cells, no one to date has proven that this hypothesis will work in actual allograft transplants. Although the preliminary work by Eisinger (65) is likely to be valid, grafting epidermal sheets onto open wounds is a difficult procedure to evaluate due to problems of contraction and epidermal ingrowth from the edges. In contrast, by seeding a selected cell population into a Stage 1 membrane, it was hoped that much of the immunology of these allogenic epidermal cells could be determined by histologic examination. By examining the tissue surrounding the seeded epidermal clusters, one could assess the presence of an immune response microscopically.

MATERIALS AND METHODS

Preparation of Bilayer Membranes

The preparation of the bilayer membrane has been previously described in detail (51-52). Briefly, 0.5% by weight bovine hide collagen (Eastern Regional Center, U.S. Department of Agriculture, Philadelphia, PA) was dispersed in 0.05 M acetic acid and precipitated with chondroitin-6-sulfate (sodium salt, Type C, Sigma Chemical, St. Louis, MO). The co-precipitate was then freeze-dried into a highly porous solid and then treated in a vacuum oven at 105° C for 24 hours. Silicone (Dow Corning Silastic, Medical Adhesive Type A) was then spread over the membrane to form a thin layer (0.2-0.4 mm) and allowed to cure at room temperature in an acetic acid bath (0.05 M). The collagen-glycosaminoglycan (GAG) portion was further crosslinked by treatment in a glutaraldehyde bath. Excess glutaraldehyde was removed by exhaustive dialysis, and the membrane was stored in a sterile container (Figure 8).

As a variant of this procedure, some collagen-GAG membranes were prepared by freeze-drying a more concentrated co-precipitate of collagen and condroitin-6-sulfate (0.8% collagen in acetic acid) as described in detail by Chen (56). Another set of membranes was prepared using preformed silicone sheeting (Dow Corning Silastic Sheeting 501-1; reinforced - 0.18 mm thick, or Dow Corning Silastic Sheeting 500-3; non-reinforced - 0.25 mm thick). These preformed membranes were adhered to the collagen-GAG layer by

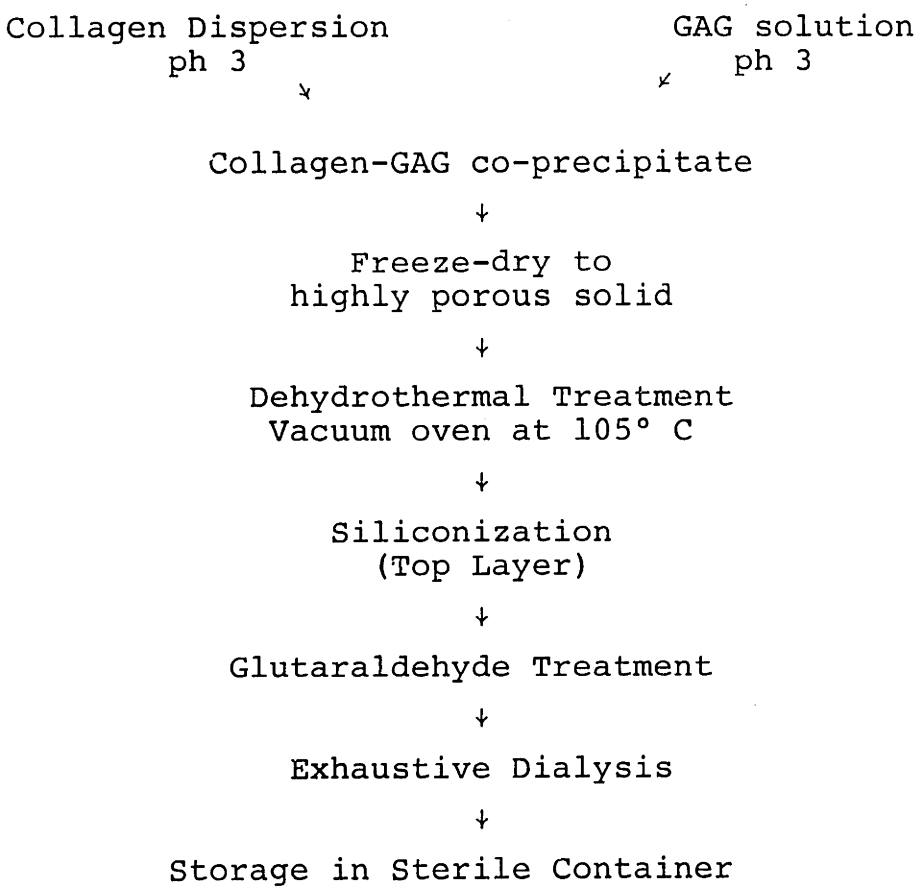

Figure 8. Preparation of bilayer Stage 1 membrane.

spreading a thin layer (approximately 0.1 mm) of polydimethylsiloxane (18.5%) in trichlorotrifluoroethane (Dow Corning, 355 Medical Adhesive) over the preformed sheet. This sheet was then secured to the collagen-GAG membrane by rolling a sterile 3/4" diameter rod slowly across the bilayer assembly.

Preparation of Membranes Seeded With Epidermal Cells

Harvesting of Skin

Hair from the guinea pig was removed by clipping and by chemical depilation (Nair, Carter Products, Irvine, CA). The area where the donor site was to be taken was scrubbed with povidone iodine (Betadine, Perdue Frederick Co., Norwalk, CT) and rinsed with 70% isopropanol twice. Thin split-thickness skin grafts (0.2 to 0.3 mm) were taken with either a Goullian Knife (Edward Weck and Co., Research Park, NC) or with a Brown Electrodermatome (Zimmer U.S.A., Warsaw, IN) under sterile conditions. This was generally performed under general anesthesia (Halothane); however, it was possible to take small areas of skin using a local anesthetic (Xylocaine). The split-thickness skin grafts were stored in sterile 0.9% saline at 4° C. Donor sites were treated with a petroleum dressing (Xeroform, Cheesebrough-Ponds, Inc., Greenwich, CT) or a Stage 1 graft covered with a 3 x 3 in. sterile cotton gauze (Topper Sponge, Johnson and Johnson, New Brunswick, NJ). Animals were bandaged in two layers of Elastoplast (Beiersdorf, Inc., South Norwalk, CT) each containing a 3 x 3 cotton gauze (50).

Cell Isolation Procedure

Basal cells are isolated from the graft following procedures modified from the literature (85-87). Split-thickness skin grafts, previously rinsed in saline, were incubated in 0.25-2.5% trypsin (GIBCO, Grand Island, N.Y., 1:250) in phosphate-buffered saline (PBS, pH 7.2) without calcium or magnesium at 37° for 40 minutes. The grafts floated in the trypsin with the dermal portion of the graft facing down. The dermis was most easily distinguished from the epidermis by the presence of blood. With watchmakers forceps, the epidermis was then carefully removed from the underlying dermis. The dermal portion of the graft was placed in a 50 ml polypropylene conical tube (Falcon 2098, Becton Dickenson, Oxnard, CA) filled with 20-30 ml of tissue culture medium (TCM) which consisted of Dulbecco's Modified Eagle's Medium (DMEM) containing 10% fetal calf serum (FCS), penicillin (100 U/ml) and streptomycin (100 µg/ml). This was then vortexed with a Vortex Genie (Model K-550-G, Scientific Products, McGraw Park, IL) at a setting of 10 for 30 to 90 seconds. The dermal portion of the graft was removed by filtering the cellular suspension through a sterile gauze. Cell yield was determined by the addition of an equal volume of trypan blue (0.4%, GIBCO, Grand Island, NY) to a small aliquot of the cellular suspension and counting cells in a hemocytometer. The percent viability was determined by dividing the number of cells which excluded the dye by the total number of cells. The cell

suspension was then centrifuged (500 g x 10 min) and the volume of TCM adjusted so that the desired density of viable cells was obtained (85,86). Epidermal cells were occasionally isolated from the epidermal portion of the graft post-trypsinization by an additional 20 minute incubation in trypsin-EDTA at 37° C followed by repeated pipetting (88,89). One variant of this procedure used TCM containing DMEM with 10% human AB serum rather than 10% FCS. In another experiment, PBS with 12% acid citrate-dextrose (ACD) was used instead of TCM. Cells were washed twice in this medium to dilute the trypsin.

After the dermal portion of the graft had been filtered, fibroblasts were isolated by washing the graft in PBS and then incubating it in collagenase (Sigma #C-3267, 1500 Units/5 ml PBS) for 25 minutes at 37° C. The dermal portion was then placed in TCM and vortexed for two minutes (Vortex Genie, setting of 10) and filtered. Cell counts of fibroblasts were made using trypan blue exclusion and a hemocytometer.

Cryopreservation of Cells

Cells were cryopreserved with dimethylsulfoxide (DMSO) using a modification of a procedure described by Skrabut (91). After centrifugation of epidermal cells (500 g x 10 min), the cells were resuspended in fetal calf serum containing 12% acid citrate-dextrose (ACD) to a final concentration of 1.0×10^6 cells/ml. To this cell suspension was added an equal volume of 15% DMSO in fetal calf serum,

dropwise with agitation over a period of 5 minutes. The cell suspension was divided into 4 ml aliquots (Cryule Vial, Wheaton Scientific, Millville, NJ). The tubes were placed in dry ice (-80° C) for 1 hour after which they were transferred to a liquid N_2 freezer (-196° C) and stored for 4 days, 43 days or 6 months. Following storage, the cell suspension was thawed by immersion in a 37° C water bath until ice was no longer visible. Each aliquot was diluted with an equal volume of DMEM with 10% FCS and centrifuged at 500 x g for 8 minutes after which one half of the supernatant was removed. The cells were washed three more times by addition of an equal volume of DMEM with 10% FCS followed by centrifugation and removal of half of the supernatant. After the third centrifugation, the supernatant was completely removed and the cells resuspended in TCM to the desired cell concentration. Viability was assessed by using trypan blue exclusion.

Fractionation of Epidermal Cells

Epidermal cells isolated were run on commerical density gradients (Percoll, Pharmacia; 500 g x 30 min or Ficoll-Paque, Pharmacia; 500 g x 20 min). The cell suspension was carefully layered on top of the gradient in a 50 ml conical tube. After centrifugation, cells from the interface of the cell culture medium and the gradient, as well as cells from different locations within the gradient, were removed with a spinal needle, washed, and resuspended in TCM. The various layers within the tube were used for cell culture

or seeded into grafts for animal experiments.

Hair Follicle Isolation and Seeding

After a split-thickness skin graft was removed, a portion of the wounded skin was excised down to the panniculus carnosa and washed in saline. This lower layer of the dermis was placed in 2.5% trypsir for 40 minutes at 37° C after which it was added to DMEM with 10% FCS, vortexed and filtered. Hair follicles were counted using trypan blue exclusion and a hemocytometer. After the basal cells had been seeded into the membrane by centrifugation, the excess supernatant was removed and the hair follicle suspension added on top of the graft. This was allowed to settle for at least 20 minutes without centrifugation into the graft before being grafted onto the animal.

Cell Cultures

Several of the epidermal cell suspensions were cultured using standard cell culture techniques. The cell culture medium (TCM) consisted of Dulbecco's Modified Eagle's Medium (DMEM) with 10% heat inactivated fetal calf serum, 100 IU/ml penicillin, and 100 µg/ml streptomycin. The concentration of epidermal cells was adjusted to 3.4×10^5 cells/ml and placed in standard tissue culture flasks. Cells were examined and the medium changed twice weekly.

Cell Seeding Procedure

Cell free bilayer membranes previously prepared were equilibrated in TCM for at least 30 minutes and then placed in a polycarbonate (Lexan, General Electric Co., Pittsfield,

MA) holder specially designed to maintain the centrifugal force vector perpendicular to the plane of the membrane (Figure 9). The membranes were placed with the silicone side facing downwards, and the cellular suspension was added on top of the collagen-GAG matrix and centrifuged typically for 15 minutes at 64 g. Excess cell culture media was removed from the centrifuge cup with a pipette.

Cell Distribution in Graft

The distribution of cells which were centrifugally inoculated into the collagen-GAG membrane was estimated as follows. 1.5 x 3.0 cm cell free Stage 1 grafts were seeded with 500,000 viable cells/cm^2 (trypan blue exclusion) for a predetermined time and spinning speed in the centrifuge. After being seeded, the grafts were removed from the specially designed centrifuge cup and stored for 48 hours in 10% formalin with the plane of the silicone parallel to the gravitational vector. The specimens were frozen in liquid nitrogen and freeze-dried. Specimens were then cut and mounted so as to visualize sections of the top and side of the collagen-GAG membrane as well as planar (en face) view of the silicone following careful removal of the collagen-GAG layer. They were then covered with a carbon and gold vapor coating and examined under the scanning electron microscope JSM-U3 (Jeolco Co., Japan). From the number of cells counted in a known area viewed under the SEM, the percentage of the number of cells seeded per unit area was calculated. When possible, a large enough area of each

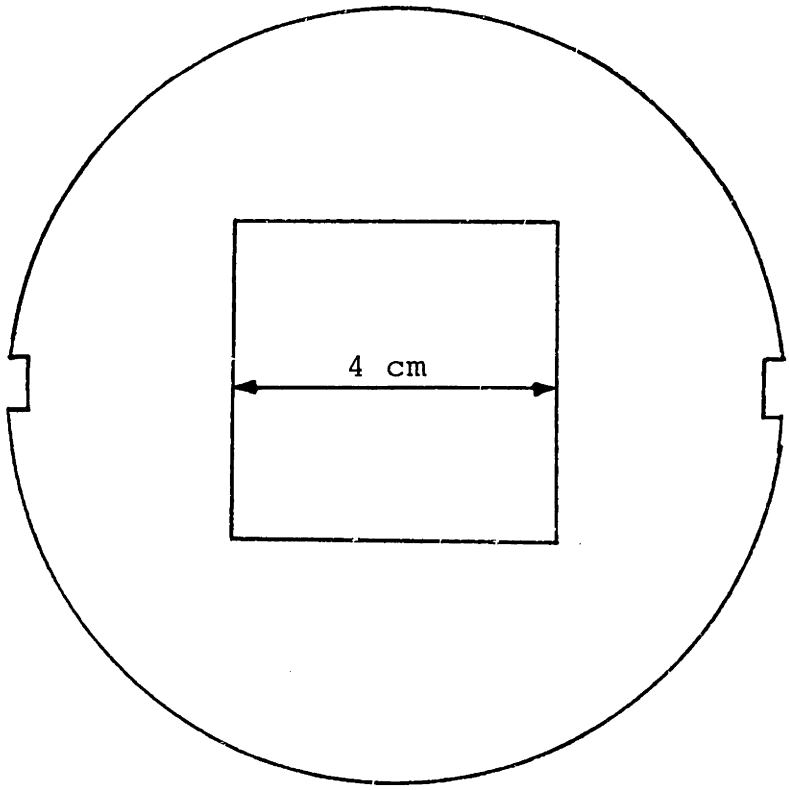

TOP VIEW

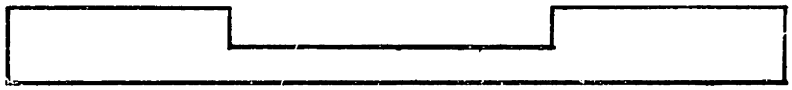

SIDE VIEW

Figure 9. Top and side views of polycarbonate graft holder for a 4 x 4 cm graft. Drawing is actual size.

sample was scanned to include 20-30 epidermal cells.

Animal Model

Animal Grafting and Observation

White female Hartley Guinea Pigs (400-450 grams, Charles River, Boston, MA) were individually caged for at least one week on a standard diet before surgery. Animals were shaved, chemically depilated, and given a pre-operative dose of antibiotic (intramuscular tetracycline, Pfizer; 0.1 mg/kg or intramuscular Keflin, Lilly; 50 mg/kg). Animals were anesthetized using a combination of nitrous oxide (0-80%) and halothane (Fluothane), 1-3% in oxygen. The skin was prepared by scrubbing with Betadine and washing with isopropanol. The grafting was carried out under aseptic conditions. Standard rectangular wounds of 1.5 x 3.0 cm, 3.0 x 3.0 cm, 4.0 x 4.0 cm, and 5.0 x 6.0 cm were made by excising down to but not including the panniculus carnosus on the dorsum of the guinea pig. The panniculus was most easily distinguished from the dermal layer by its red color in contrast to the white color of the dermis. After hemostasis was achieved, by blotting with a gauze, the graft was applied to the open wound with the silicone facing outwards, being secured with several interrupted nylon sutures (5-0 Ethilon, Ethicon Inc., Sommerville, NJ) (Figure 10). The animal was photographed, bandaged as described above, weighed, and returned to the cage. As controls, some animals were not grafted, but their wounds

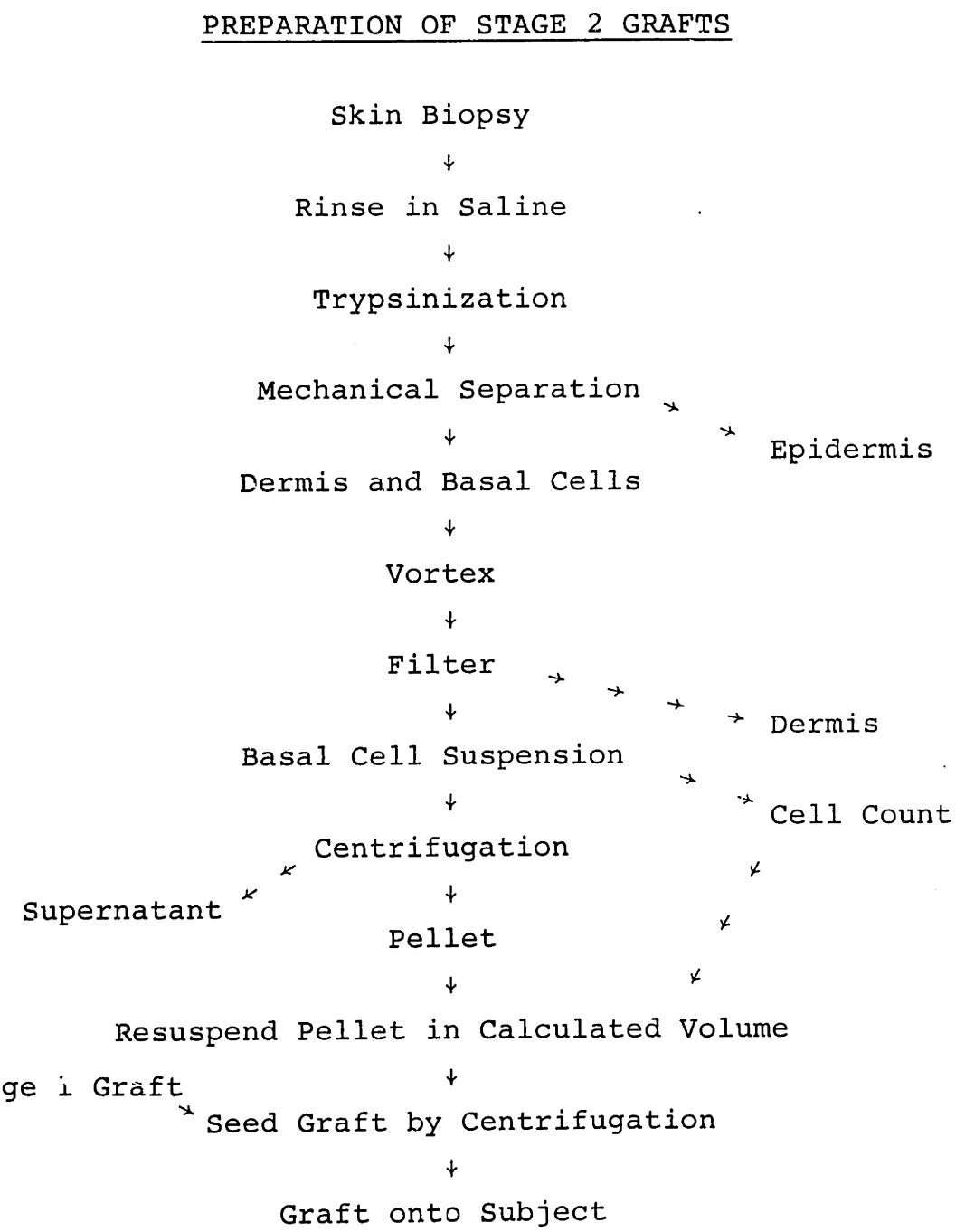

Figure 10. Preparation of seeded (Stage 2) membranes.

left open and treated with a Xeroform gauze. In other animals, the excised full-thickness skin was rotated 180° and replaced on the wound to serve as autograft controls. Full-thickness excised skin from a donor animal grafted onto an excised open wound of a recipient animal served as allograft controls. In several animals, tattoo marks were made in the skin adjacent to the wound by injecting India ink intradermally with a 25 gauge needle. By locating the needle in the dermis parallel to the skin surface, line segments could be made by injecting small amounts of ink as the needle was withdrawn.

Wounds were inspected every 1 to 14 days for bleeding, exudation, color and consistency of the graft. No immunosuppressive agents or systemic antibiotics were used except for an initial pre-operative dose of antibiotics. Wounds which had a purulent exudate were presumed to be infected and the animals were usually sacrificed. In some cases, the infections were treated by removing the exudate with sterile gauze and covering the wound with a gauze soaked with povidone iodine or covered with Neosporin (Burroughs Wellcome Co., Research Triangle Park, NC, a topical mixture of neomycin, bacitracin, and polymyxin B). Cultures were taken with a sterile swab to confirm suspected infections. The wound was photographed, measured and replaced with a new dressing. Wound areas were calculated as a product of an average length and an average width between the hairline or by planimetry of photographs and plotted as a function

of time. This method was consistent with the bulk of the wound contraction literature (14-20). This allowed the measurement of contraction of autografts, and enabled the observation of reexpansion of wound areas. In contrast, Chen (56) departed from this method and plotted the percentage of the wound remaining open as a function of time.

For membranes seeded with basal cells, normally between 9 and 14 days, the silicone of these membranes was removed. When possible, the original bandage was left undisturbed until it was felt that the silicone layer would be ready for removal. A reduced rate of infection was associated with not examining the wounded area until day 10 through day 14. Criteria for removal was dehiscence of the silicone from the underlying neoepidermis or the presence of a purulent exudate. After about 30 to 40 days, the bandages were permanently removed. Sensory innervation was tested by the use of the pin-prick test (90). Histological specimens were stored in 10% buffered formalin prior to standard histopathologic imbedding in paraffin and sectioning into five micron sections (55). All specimens were stained with hematoxylin and eosin and a few were stained with special stains including Masson's Trichrome, Bodian, Bieilkowsky, reticulum, and elastin stains (58-61).

Peel Strength

A method was developed to quantify the force of attachment of the graft to the underlying tissue based on standard 90° peel tests. The guinea pig was anesthetized and

situated such that the plane of the graft was perpendicular to the peel force. A metal clip was attached to the silicone of the anterior edge of a 1.5 x 3.0 cm graft. The grip was hung by a perpendicular string which was counterbalanced through a pulley (Figure 11). By slowly adding water to a graduated cylinder, the force applied to the grip increased slowly. Water was added over a one to two minute interval during which several photographs of the peeling event were taken. The peel strength was calculated as the force required to completely detach the graft from the woundbed divided by the original width of the graft (1.5 cm). The original width of the graft was used rather than the actual width since as the wound contracted, both the force to remove the silicone and the width of the wound went to zero. Dividing two small numbers resulted in a large scatter of the data as the wound contracted. In addition, the fracture plane was noted during the peel experiment.

Mechanical Measurements of Skin

Skin specimens were obtained by excising down to, but not including, the panniculus carnosus of an anesthetized animal and stored in chilled PBS at 4° C. Specimens were cut to a dumbbell shape similar to that described by Ridge and Wright (92) with a gauge length of 1.0 in. Specimens were obtained from the dorsum of the animal and cut parallel to the longitudinal axis of the animal and tested within 24 hours of removal. Widths and thicknesses of the samples were measured with a micrometer. Specimens were mounted in

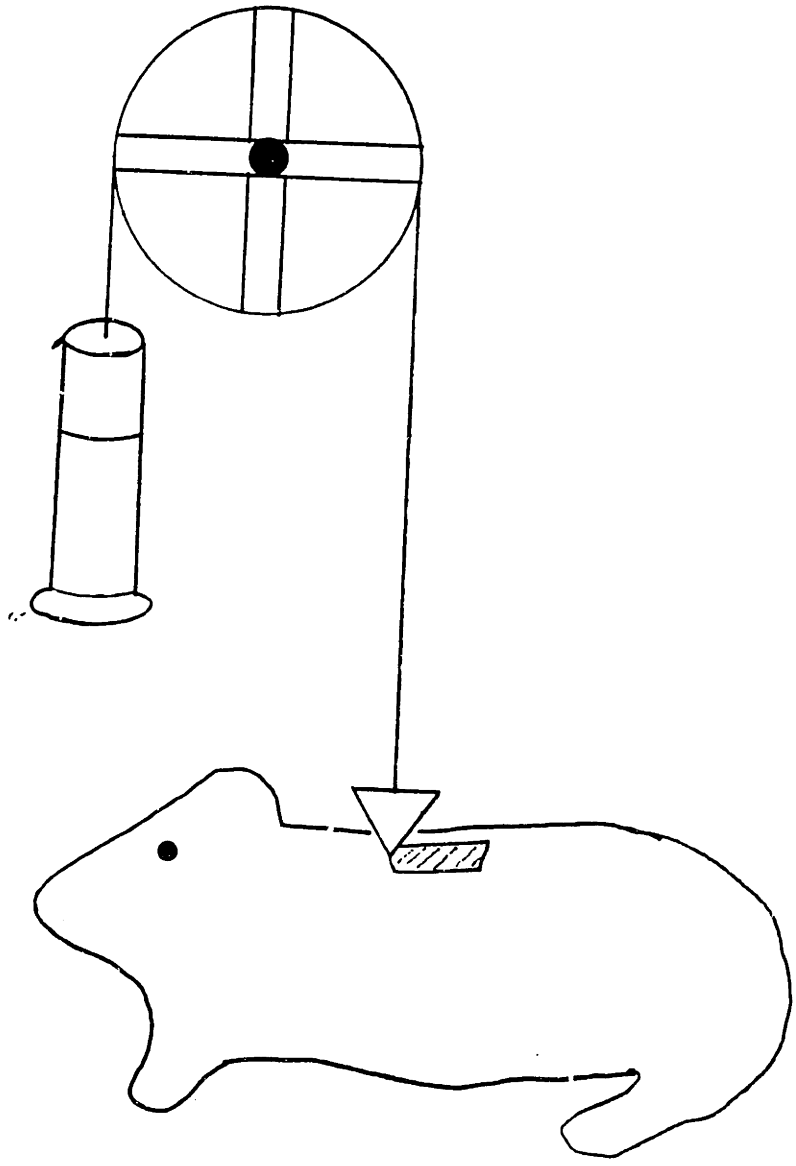

Figure 11. 90° Peel Strength Test. The upward force of the clip is slowly increased over a period of 1-2 minutes until the graft is removed from the anesthetized animal.

pneumatic serrated grips and extended at a constant rate of 1 in/min (Instron Model TT-C). One grip was fixed and the other was connected to a load cell (Instron Tensil Load Cell B or C). The output of the load cell was plotted on a calibrated chart recorder moving at a rate of 10 inches per minute. Stress-strain curves and ultimate tensile strengths were calculated from the chart recordings for samples of normal skin, autograft and Stage 2 skin.

In Vitro Measurement of Permeability

Aluminum permeability cups with an inside diameter of 3.5 cm were filled with distilled water within 3-5 mm of the top of the cup, fitted with the test material, and placed in a desiccator. The weights of these cups were measured at periodic intervals and the permeability calculated. The temperature was recorded at each weighing, and a free water surface standard was also used.

In Vivo Measurement of Skin Permeability

Hair from the dorsum of guinea pigs was clipped close to the skin. A calibrated Servo-Med Evaporimeter (Stockholm, Sweden, courtesy of Dr. Irwin Blank, Department of Dermatology, Massachusetts General Hospital) was used to measure the moisture flux (93,94) over the area grafted with a Stage 2 membrane or autograft. A control measurement was made over normal skin on the contralateral dorsum of the guinea pig.

RESULTS

Seeded Grade Preparation

Cell Isolation Procedure

The cell isolation procedure used initially was one adopted from Prunieras, Delescluse, Regnier, and Jepson (85-87). As animal studies were being conducted, concomitant *in vitro* studies were made to improve the efficiency of this method. Two important parameters characterize the trypsinization step: 1) the thickness of the biopsy and 2) the time interval since the skin had been harvested. Trypsin migrated to the dermal-epidermal junction by diffusion through the dermis. Since this time is roughly proportional to the square of the thickness of the biopsy, thin split-thickness skin biopsies were suitable for rapid trypsinization. For guinea pig skin, it was found that a biopsy specimen thickness of 0.2 mm provided a thin specimen which was easily removed from the animal. Biopsies trypsinized within a few hours of removal took much longer to separate the dermis from the epidermis using a dilute concentration of trypsin (0.25%) than biopsies which had equilibrated in saline for several hours. This was presumably due to trypsin inhibitor present in serum which diffuses out of the graft over a period of hours. It was found that by using a more concentrated trypsin solution (2.5%), the effect of the trypsin inhibitor could be overcome.

TABLE III

Time from Biopsy	%Trypsin Used	Time Required for Separation of dermis from dermis	Temp.	Mean Viability, Trypsin Blue
2 days	0.25%	40 minutes	37° C	54%*
0-2 hours	2.5%	40 minutes	37° C	73%*
0-2 hours	0.25%	>2 hours	37° C	
0-2 hours	2.5%	24 hours	4° C	56%
0-2 hours	2.5%	22 hours	22° C	65.4%

*$p < 10^{-5}$ t-test, two-tailed

Trypsin had a maximum activity near body temperature. Using 2.5% trypsin for 40 minutes, soon after the skin biopsy had been taken, rapid separation was accomplished with a high proportion of viable cells (trypan blue exclusion). The skin biopsies trypsinized within a few hours of the biopsy (2.5% trypsin for 40 minutes) had a significantly greater viability than grafts trypsinized two days after the biopsy (0.25% trypsin for 40 minutes; see Table I and Figure 12).

To remove the basal cells from the dermal-epidermal junction, and around the hair follicles, the dermal portion of the biopsy was vortexed in TCM. To determine the optimal time to vortex the skin specimen, samples were vortexed for 30,60 and 90 seconds (Vortex Genie, setting of 10), and cell counts and viabilities were made using the trypan blue exclusion method. The cell counts for these three times were not significantly different, but the 60 second

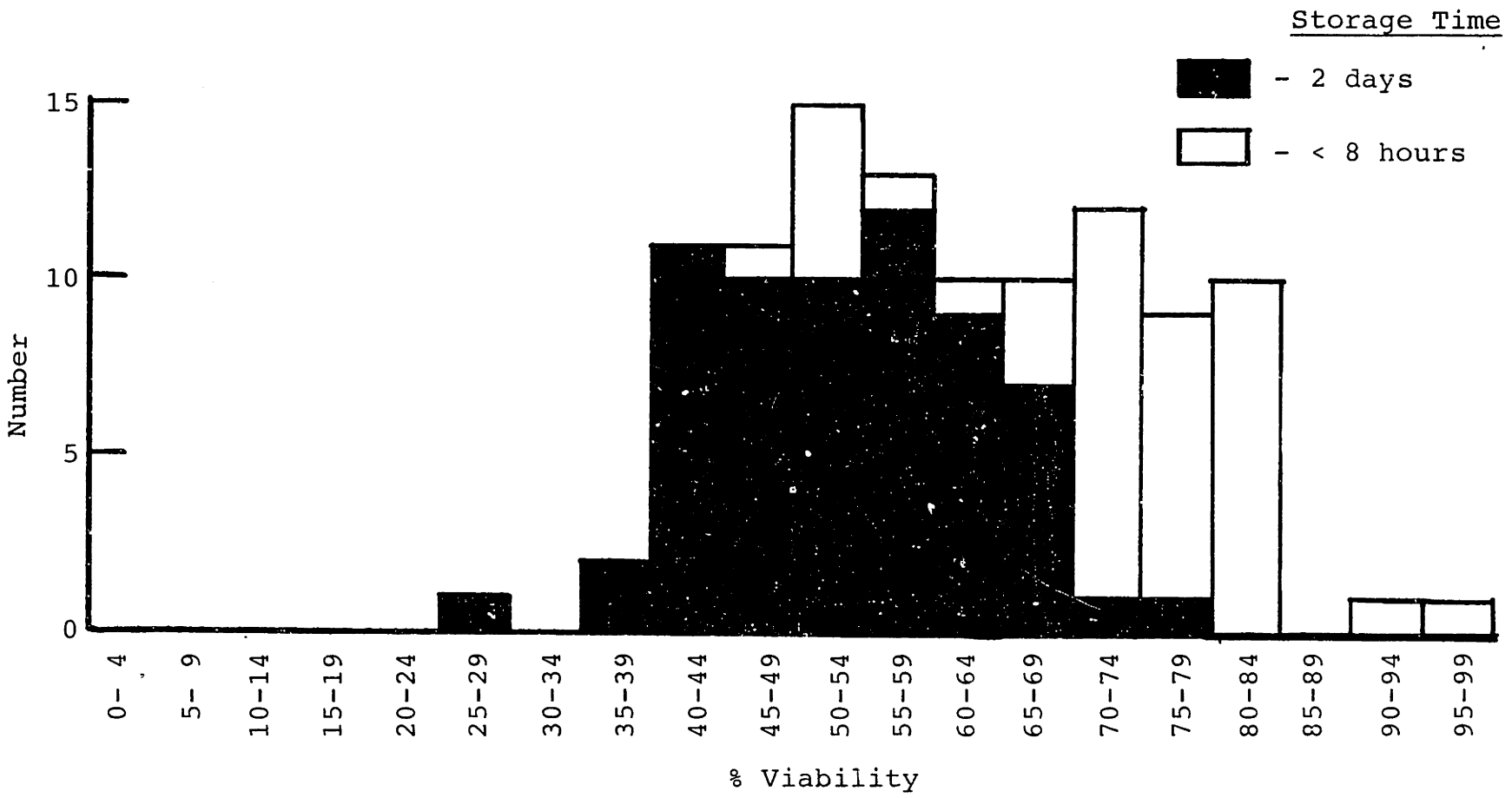

Figure 12. Histogram of trypan blue viability of epidermal cells isolated from split-thickness skin biopsies. Cells isolated within a few hours of the biopsy show higher viabilities than those stored for 2 days.

vortexing time consistently gave the highest cell viability. Histologic sections of the dermal portions after vortexing showed most of the basal cells had been removed by 30 seconds, and a few additional cells were removed by 60 seconds. The 60 second and 90 second samples were comparable histologically.

TABLE IV

Vortex Time	Viability
30 sec.	68
60 sec.	77
90 sec.	55

It appeared somewhat wasteful to throw away the epidermal portion of the graft after it was manually separated (Figure 13). However, this segment appeared microscopically to consist mainly of stratum spinosum, stratum granulosum, and stratum corneum. Cells isolated from this segment by additional incubation in trypsin-EDTA, when put in cell culture, formed very few epidermal colonies. This was in contrast to epidermal cells derived from the "dermal" portion of the biopsy which formed many colonies in culture within one to two weeks. Since basal cells are by definition epidermal cells with the capacity to divide, it appeared that most of the basal cells were attached to the "dermal" portion of the biopsy split by trypsin. Figure 13 shows where trypsin split the biopsy.

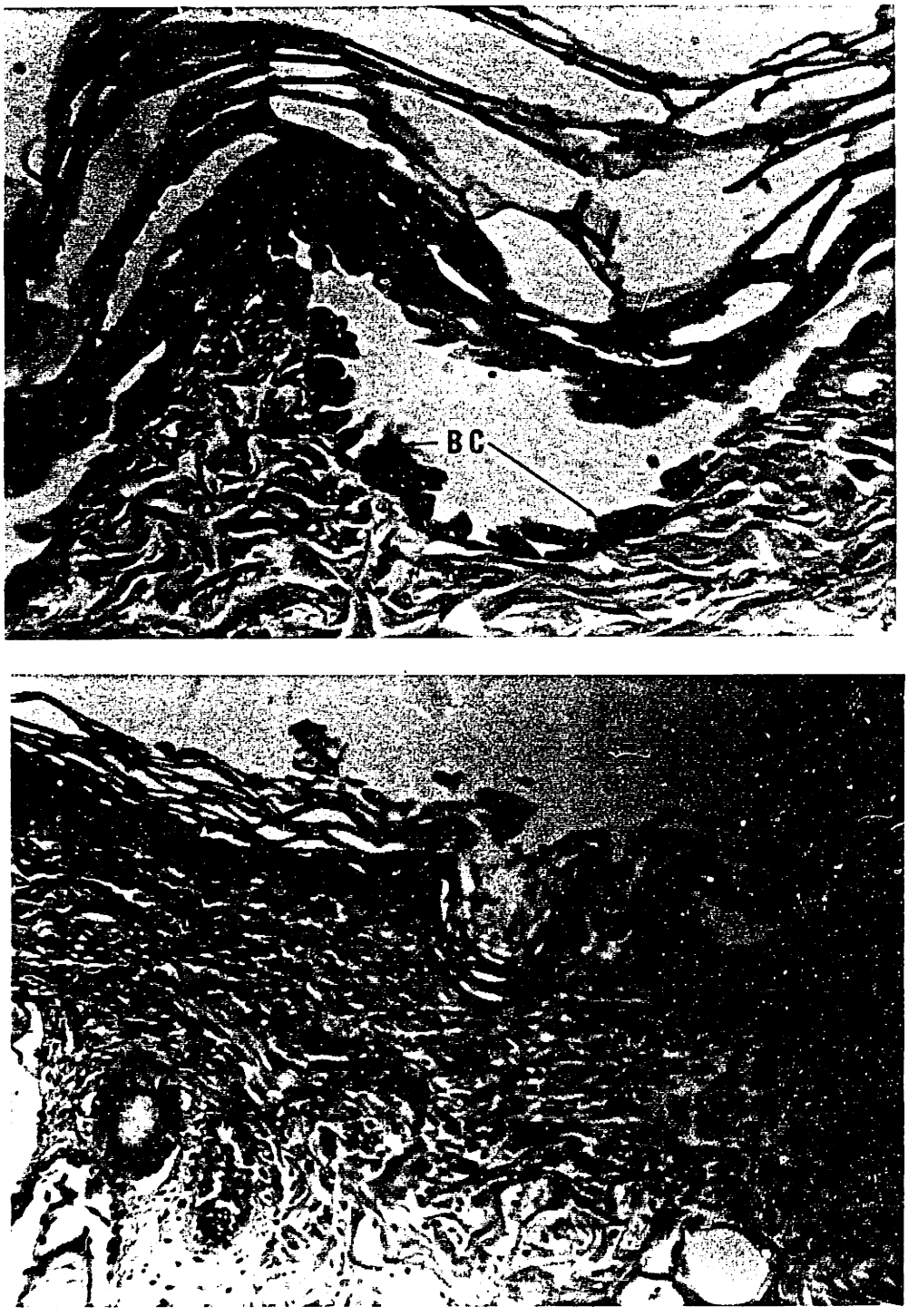

Figure 13. High (675 X) and low (150 X) view of a skin biopsy after 40 minutes in trypsin. The epidermis (E) is beginning to separate from the dermis (D). The basal cell layer (BC) of the epidermis is adherent to the dermal layer. These cells are subsequently removed by vortexing.

Scanning Electron Microscopic Analysis of Cell Seeding

The scanning electron microscope (SEM) provided a convenient technique for visualizing the distribution of cells within the grafts. Figure 14 shows the effect of the centrifuge speed on the distribution of cells within the graft. In this series of experiments, the time of centrifugation was held constant at 15 minutes while the speed of the cenfuge was varied. Very little centrifugal force was required to derive the cells into the graft. Even without centrifugation (1 g x 15 min), cells were visualized resting on the silicone membrane. However, with centrifugation, the number of cells visualized on the silicone increased by a factor of 6 to 8 (Figures 16 and 17). There was a slight decline in the number of cells seen on the silicone as the centrifuge was spun at 2,000 rpm. Some of the cells in these samples were pleomorphic suggesting that at this high acceleration (800 g), some of the cells were damaged. Most of the cells seen in the SEM were visible on the silicone surface or near the surface of the collagen-GAG membrane which would face the woundbed. Cells which had not penetrated deep within the graft appeared to be trapped in areas of the collagen-GAG matrix as shown in Figure 18 and 19. Very few cells were visualized in the center of cross-sectional cuts of the membrane.

In a second series of experiments, the centrifuge speed was held constant while the time in the centrifuge was varied. Figure 15 shows that, at a constant speed of

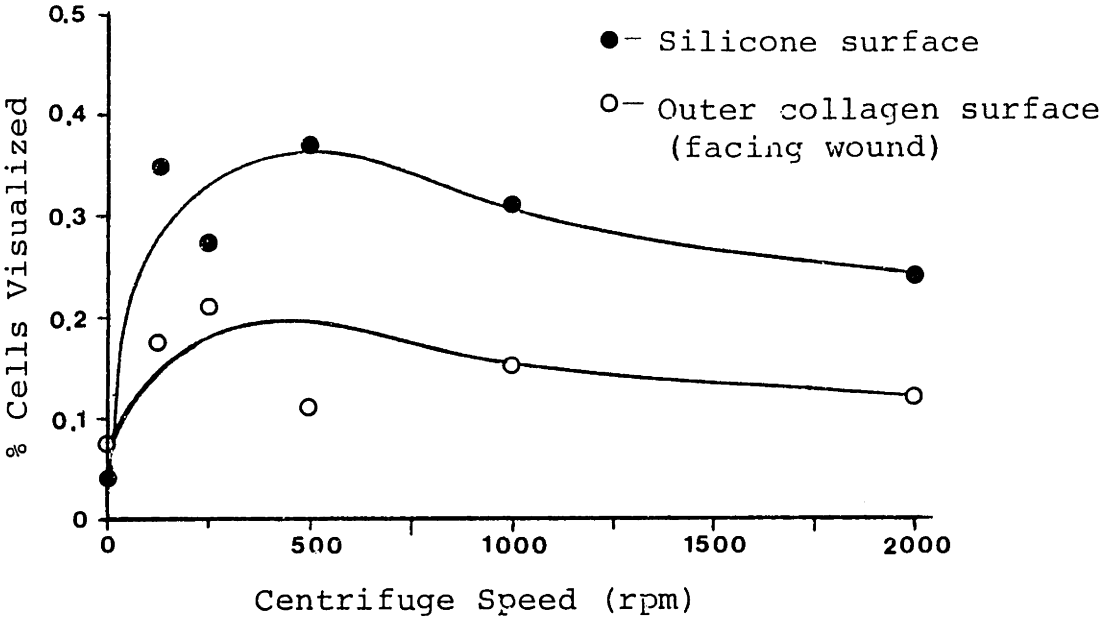

Figure 14. The effect of centrifuge speed on cell distribution.

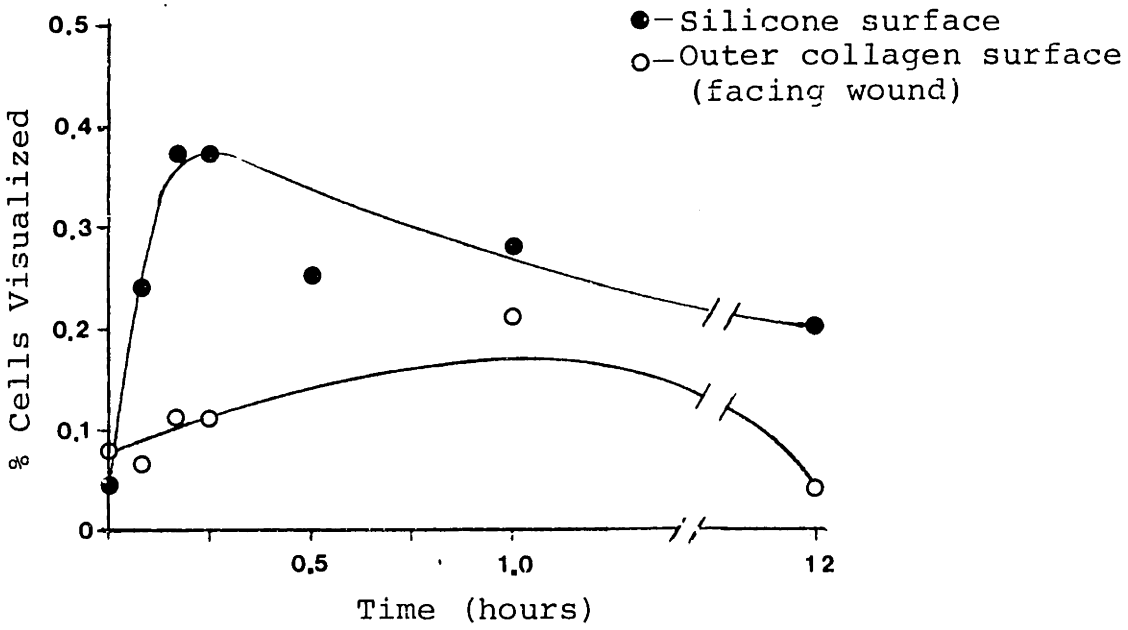

Figure 15. The effect of time in the centrifuge on cell distribution.

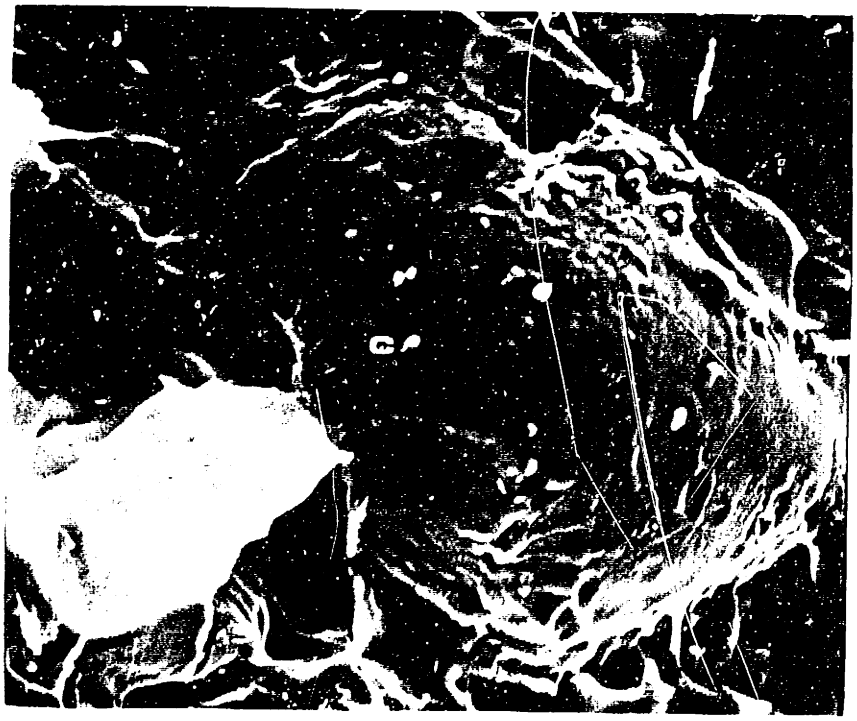

Figure 16. Low power (300 X) SEM of cells seeded into a bilayer membrane. View is of silicone surface with some collagen-GAG attachments. Several cells (C) are visible. 20 kV.

Figure 17. High power (1000 X) SEM of cells located on the silicone surface of a bilayer membrane. A deformed red blood cell is present in the center. 20 kV.

Figure 18. View of a cluster of epidermal cells located on the silicone membrane of a bilayer membrane (1000 X). This membrane had a more vertical pore structure resulting in epidermal cells appearing in clumps on the silicone membrane. Membrane was freeze dryed from 0.8% collagen-GAG (see ref. 56). 20 kV, SEM.

Figure 19. SEM of epidermal cells attached to fibers of the collagen-GAG matrix (1000 X). This is the collagen-GAG surface furthest from the silicone layer. 20 kV.

500 rpm (64 g), an increase in the number of cells at the silicone interface is seen by 10 minutes. After 15 minutes in the centrifuge, a gradual decline in the number of cells visualized on the silicone was observed. Pleomorphic cells were also seen in the 12 hour sample indicating possible damage of the cells after prolonged periods in the centrifuge. For the 1.5 x 3.0 cm grafts, most of the cells in the cellular suspension ended up in the graft after centrifugation. Figures 20 and 21 show the percentage of cells which remained in the centrifuge bucket after the graft had been removed. After very little centrifugation, there were consistently between 5% and 10% of the cells in the suspension left in the centrifuge bucket. These cells most likely came from near the edges of the graft where the contact with the centrifuge bucket was not perfect. The SEM method provided a quantitative method to compare the number of cells visualized; however, in the preparation of the specimens for SEM, most of the cells seeded were dislodged from the specimen since only a fraction of the cells seeded was visualized. These results support the usage of cell centrifugation in the range of 10-15 minutes at 20-200 g.

Time Analysis of Cell Separation and Seeding Procedure

Current times for the cell separation and seeding procedure are as follows:

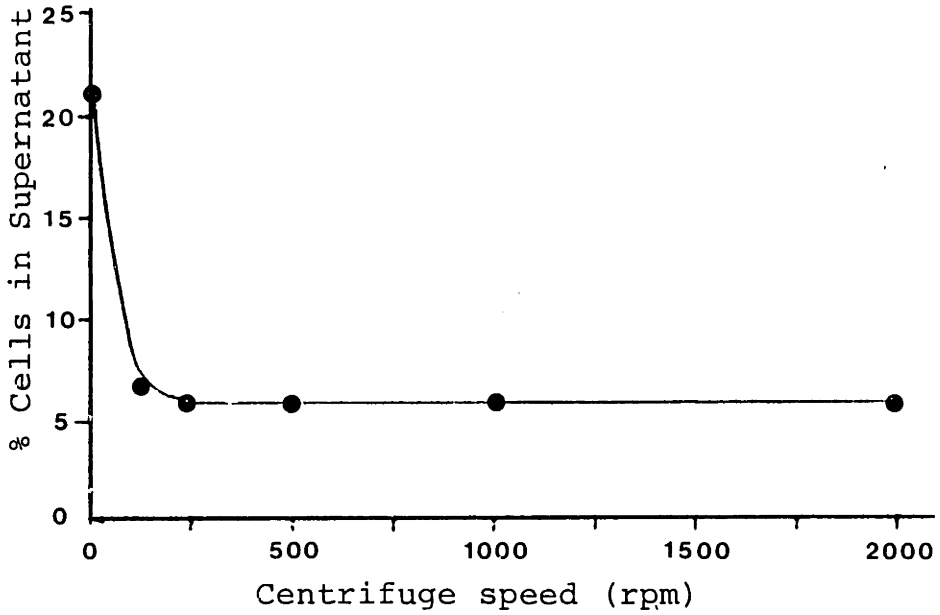

Figure 20. The effect of centrifuge speed on the number of cells in the supernatant.

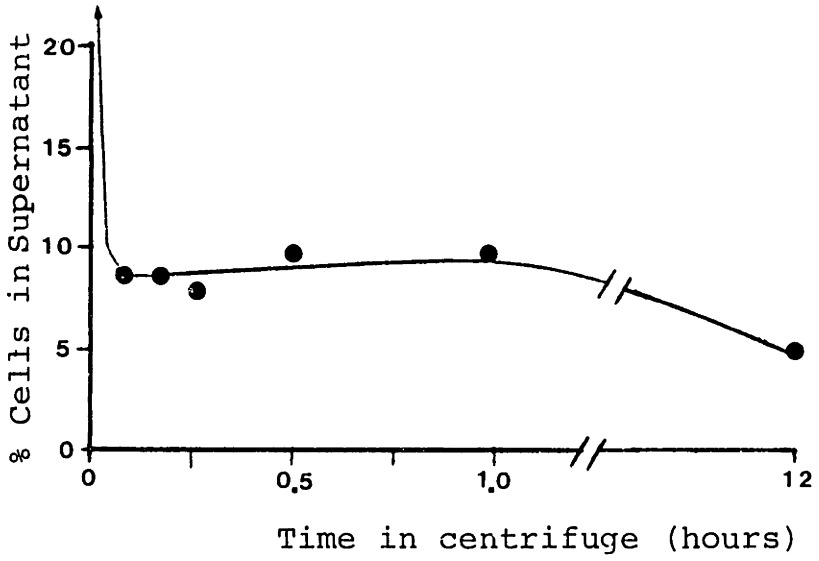

Figure 21. The effect of time in the centrifuge on the number of cells in the supernatant.

TABLE V

	Minutes
Rinse in Saline	3
Trypsinization	45
Mechanical Separation	7
Vortex	2
Filtering	2
Centrifuging (concentration)	17
Preparation of Cell Suspension	2
Centrifugation (seeding)	22
TOTAL	100 min

The preparation of the seeded membranes from the time of the initial biopsy requires less than two hours of preparation. About half of this time is required to isolate the epidermal cells from the biopsy, and the rest of the time is that required to seed these cells into the biospy. With increased experience over the course of two years, this preparation time has been reduced significantly from about 4 hours to less than 2 hours.

Results of Animal Model

Contraction Kinetics

The contraction kinetics of Stage 2 membranes were compared with those of ungrafted controls, full-thickness autografts, and Stage 1 (unseeded artificial skin grafts) controls. In each set, there were four animals all grafted in the same series. All animals in the comparison had similar 1.5 x 3.0 cm full-thickness wounds on the left dorsum of the guinea pig and were cared for in the same manner. Measurements of tattooed animals were made as shown in Figure 22, and the day when the wounded area or graft reached 50% of its original was recorded in Tables VI-XI.

Ungrafted Wounds

1.5 x 3 cm open wounds closed in all four animals by the 21st day. Contraction was delyaed for four days after excision of the full-thickness segment of skin, but then proceeded at a rate of 5-8% per day over the next 13 days. Linear regression of the data from the four animals in the series between day 4 and 15 resulted in a slope of -7.2%/day, an X-intercept of 18.0 days, and a correlation coefficient $r = 0.97$. The woundbeds reached 50% of the original area between day 10 and 12 and were closed by the 21st day. The long-term scars, which formed as a result of the contraction process, showed an area similar to that seen on the 21st day (Figure 23). The measured lengths of the woundbed suggest an anisotropy of the forces present in the woundbed (Figure 24). The anterior-posterior length

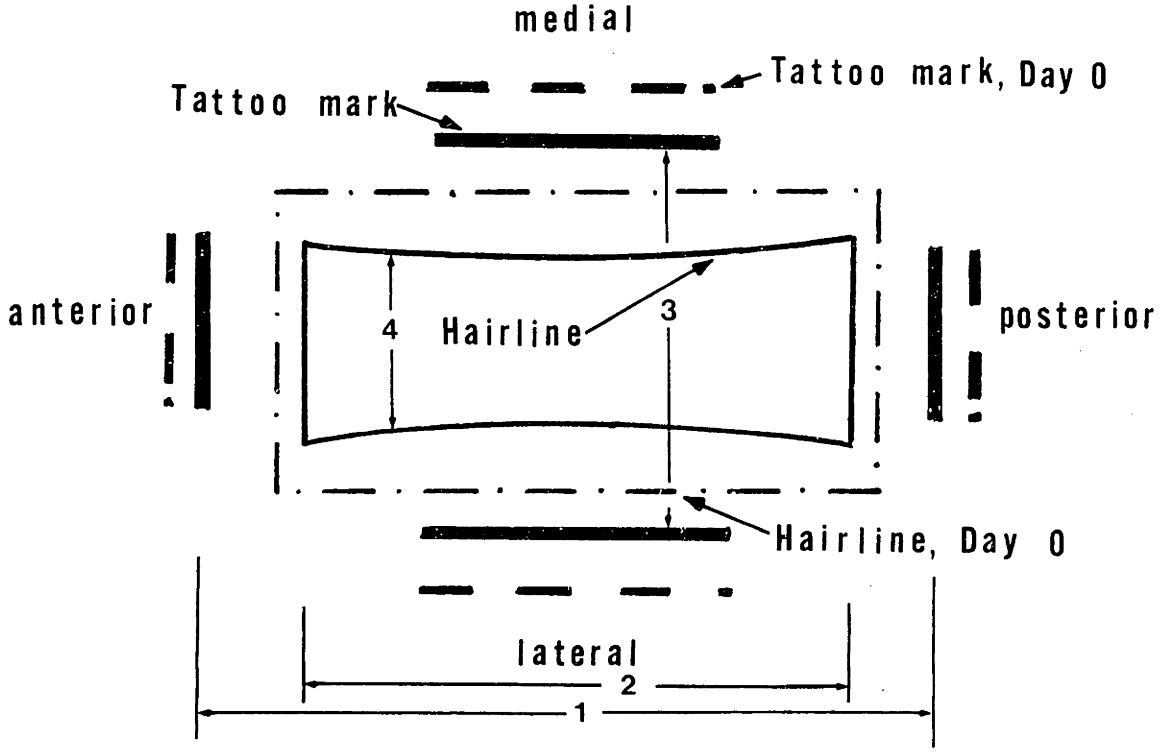

Figure 22. Direct measurements made of guinea pig wounds. The dashed lines show the geometry of the tattoo lines and the margin of the 1.5 x 3.0 cm excised wound (hairline) on Day 0. After a few days the tattoo lines and the hairline borders have moved closer together (solid lines). Each time the wound was examined, four measurements were made as marked on the diagram:

1) the anterior-posterior (A-P) distance between tattoo marks.
2) the average A-P distance between the hairline.
3) the medial-lateral (M-L) distance between tattoo marks.
4) the average M-L distance between the hairline.

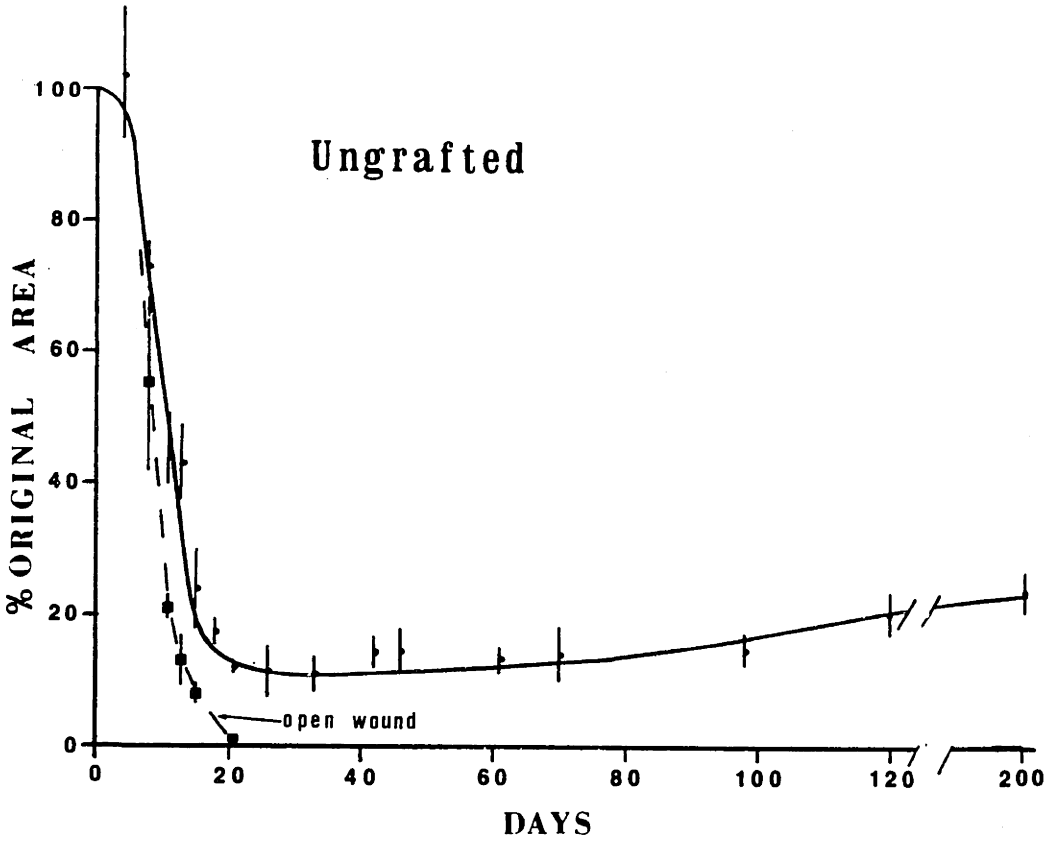

Figure 23. Contraction curve for ungrafted wounds. The top curve is calculated by measuring the area within the hairline as a function of time. The lower curve (dashes) shows the percentage of the original wound area which is open (not covered by epidermis). Error bars indicate ± 1.0 standard deviation from the mean. 1.5 x 3.0 cm guinea pig wounds (n=4).

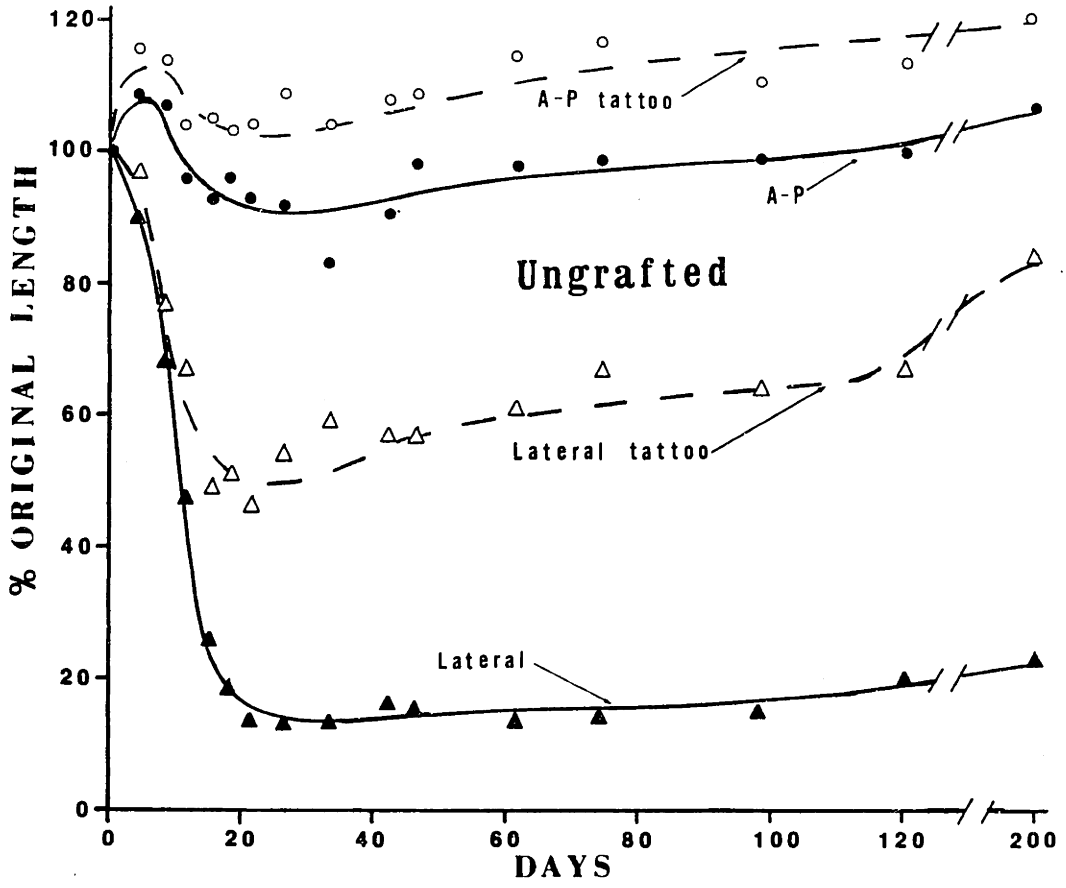

Figure 24. Normalized direct measurements of ungrafted 1.5 x 3.0 cm guinea pig wounds. The A-P and Lateral (M-L) percentages, marked by solid lines, are normalized average perpendicular measurements of the woundbed defined by the hairline. The dashed lines show the percentage of the original length between the tattoo lines. Each symbol represents the average of 4 measurements. Note the anisotropy of the woundbed with contraction being explained primarily due to changes in length occurring in the Lateral (M-L) direction.

maintained a relatively constant value while the lateral dimension reduced to a mere 10-20% of the original length. The tattoo line measurements followed qualitatively the shape of the respective parallel hairline measurements (Figure 24). Tattoo measurements systematically indicated a greater percentage of the original length than hairline measurements (Figure 22).

Autograft

The autograft (full-thickness dermal and epidermal graft) contracted to about 78% of the original area by day 30 and subsequently expanded over the next six months to 120% of the original area (Figure 25). Since most of the contraction occurred in the medial-lateral direction, a first-order estimate of the change in wound area due to the growth of the animal was made by observing changes in the anterior-posterior length of the wound. This typically increased 10-20% over a period of 200 days. The contraction and expansion were primarily due to changes in the lateral dimension (Figure 26). Linear regression of the combined data of the four animal series between day 0 and 26 resulted in a slope of -0.98%/day with a correlation coefficient $r = 0.73$. The distance between tattoo lines slowly expanded over the first 200 days observed to 115-130% of their original length.

Stage 1

Stage 1 membranes delayed the onset of wound contraction for 11 days from the time of grafting (Figure 27).

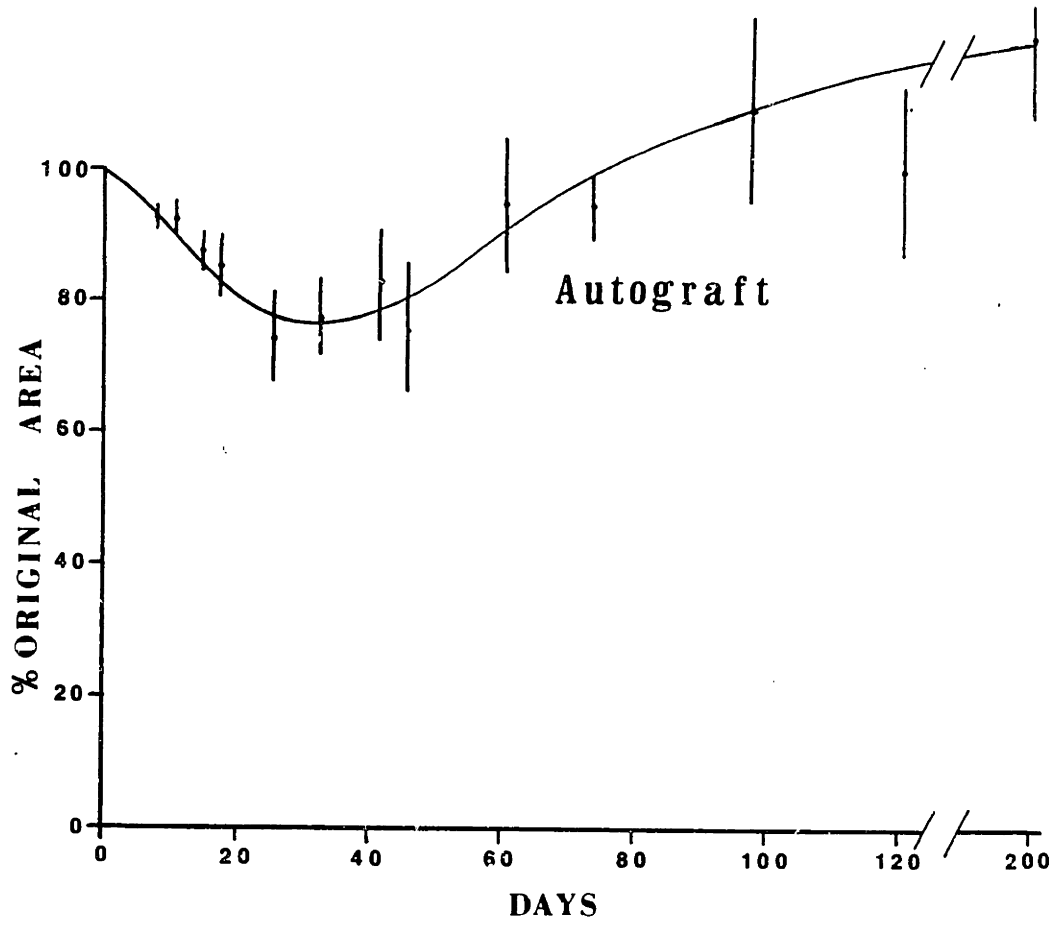

Figure 25. Contraction curve for full-thickness autografts. Error bars indicate mean (n=4) ± 1.0 standard deviation. Note the some contraction occurs during the first 30 days, but this is soon reversed. The full-thickness autograft almost completely inhibits contraction observed in ungrafted wounds (Figure 23). 1.5 x 3.0 cm guinea pig wounds.

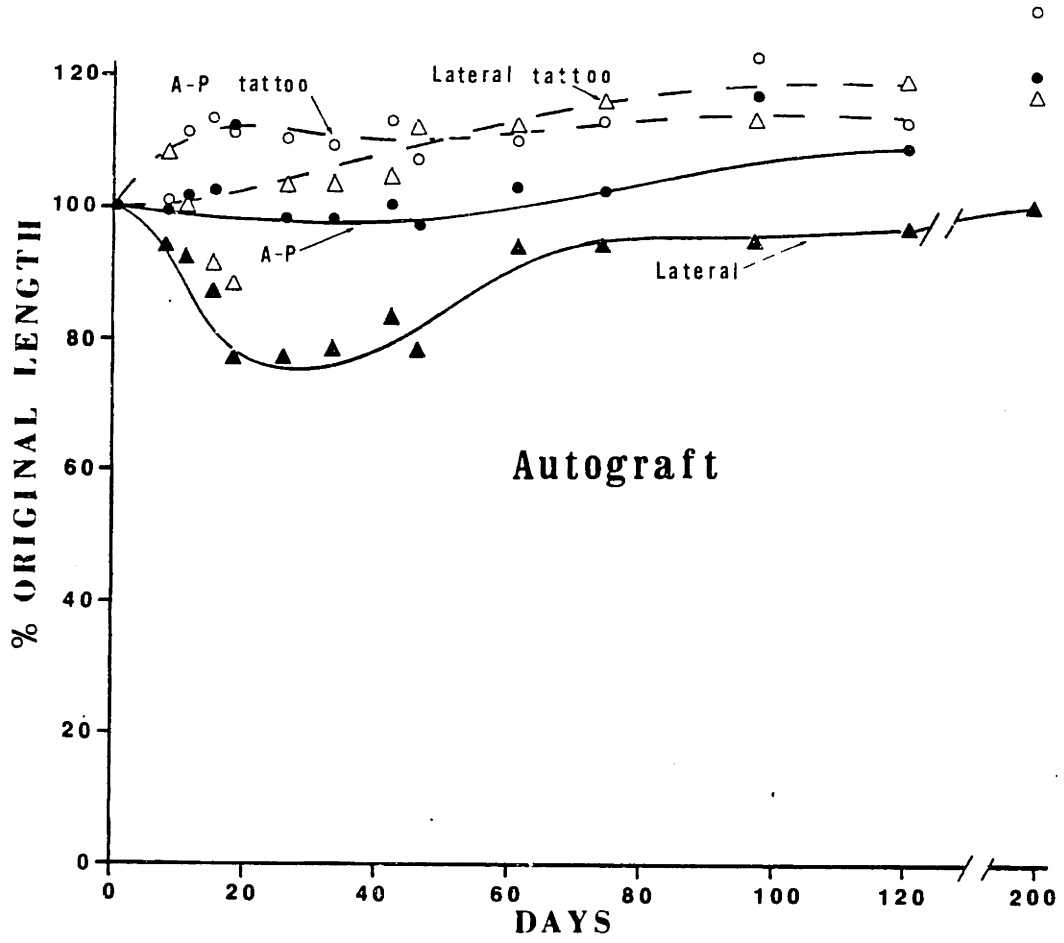

Figure 26. Normalized direct measurements of 1.5 x 3.0 cm full-thickness autografts. Solid lines and symbols represent percentages of original distances measured between the hairline, whereas dashed lines and open symbols represent precentages of the original distances measured between tattoo lines. Each symbol is the average of 4 measurements. Most of the contraction and re-expansion is due to changes in the lateral dimension.

After this time, these wounded areas contracted at a rate of 3-4% per day over the next 30 days. These slopes differed significantly from those observed in the ungrafted controls ($p < 0.025$, t-test, two-tailed). The projected X-intercepts of these slopes were also significantly different than those of the ungrafted controls ($p < 0.025$). Linear regression of the combined data of the four animal series resulted in a slope of -3.6%/day, an X-intercept of 41, and $r = 0.92$. The grafted areas reached 50% of their original areas between day 24 and 28. Wound closure was accomplished by an inward migrating epithelium which preceded the contraction border (hairline). These wounds were closed and the silicone ejected by the 42nd day. After this period, a slow expansion in area was observed. Most of the contraction kinetics could be explained by changes in the lateral dimension (Figure 28). The tattoo dimensions followed a course parallel to those of the corresponding hairline.

Stage 2

Stage 2 grafts followed a contraction curve similar to that observed in Stage 1 grafts over the first 30 days. The grafted area began to contract on about day 10, and between day 13 and 29 contracted at a rate of 2-4% per day. An extension of these slopes resulted in X-intercepts of 39 to 47 days. Neither the slopes of these lines nor the X-intercepts were significantly different than those calculated from the Stage 1 data. However, both the slope

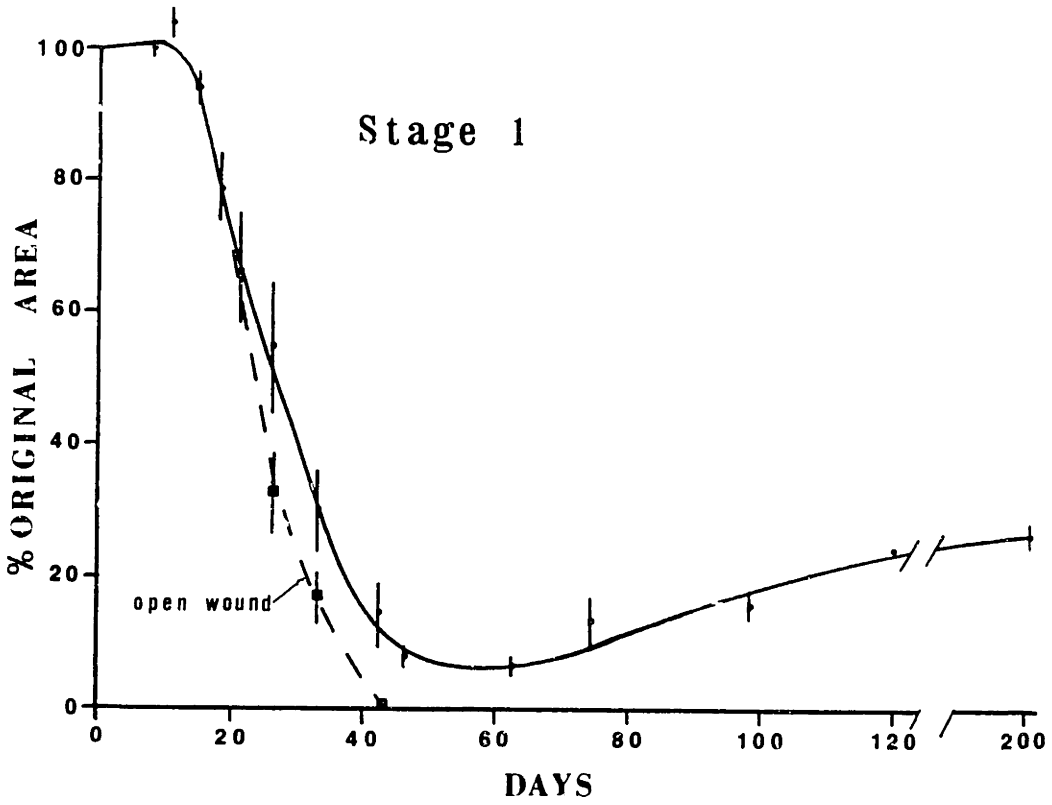

Figure 27. Contraction curve for full-thickness wounds treated with Stage 1 artificial skin grafts. Note the delay in contraction which occurs compared with ungrafted controls (Figure 23). The solid line represents the percent of original area measured within the hairline while the dashed line represents the percentage of original area not covered with epidermis. Error bars show the mean ± 1.0 standard deviation (n=4: day 0-33, n=3: day 42-61, and n=2: day 78 on). 1.5 x 3.0 cm guinea pig wounds.

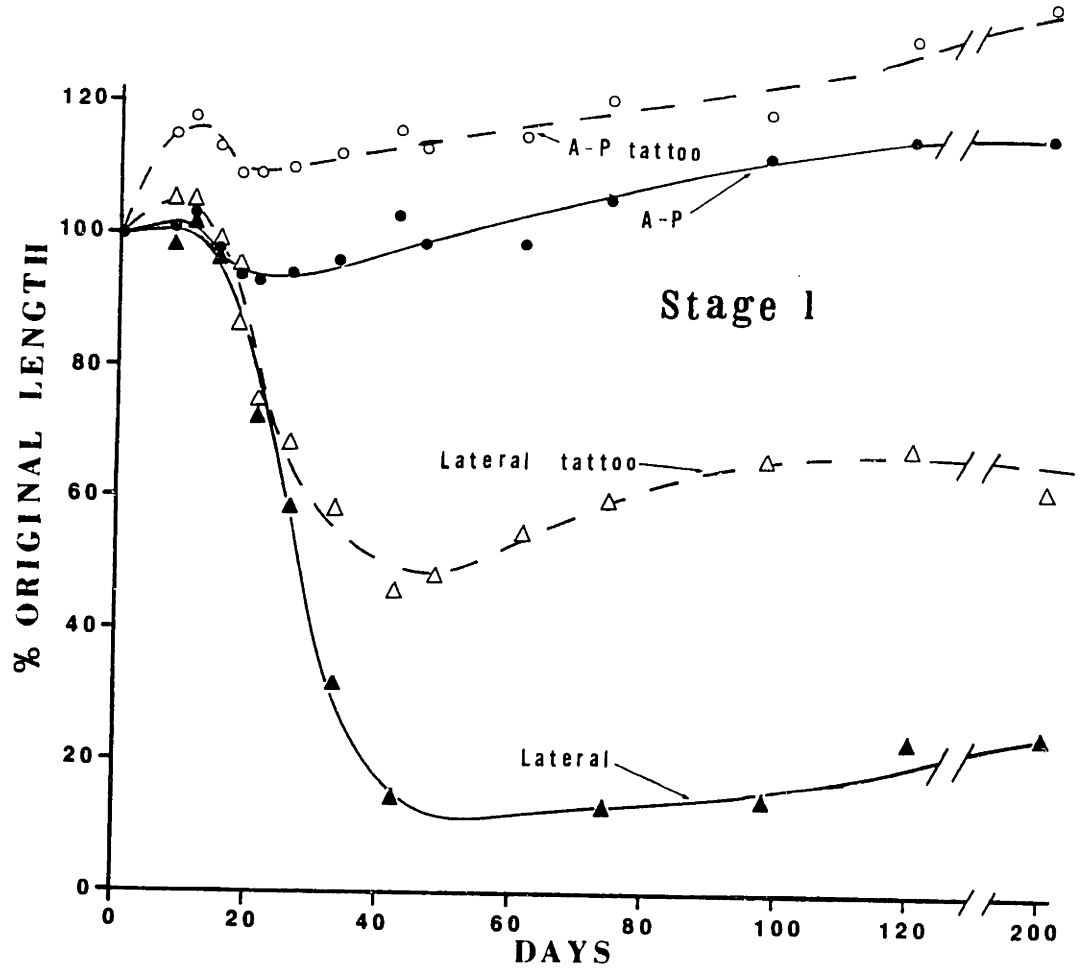

Figure 28. Normalized direct measurements of 1.5 x 3.0 cm full-thickness wounds treated with Stage 1 artificial skin grafts. Solid lines and symbols show hairline measurements; whereas, dashed lines and symbols represent tattoo measurements. Stage 1 membranes show a similar contraction anisotropy as ungrafted wounds (Figure 24), but exhibit a delay in contraction in the Lateral (M-L) dimension.

($p < 0.025$) and the X-intercept ($p < 0.005$) were significantly different than the open wound. Between day 35 and 60, the area of the graft was relatively constant. At two months, the area of the Stage 2 grafts was significantly greater than either the Stage 1 or ungrafted animals ($p < 0.05$). The wound expanded over the next six weeks to about 72% of the original area (Figure 29, $p < 0.005$). At this point, three months post grafting, the autograft was still significantly larger in area than the Stage 2 grafts ($p < 0.05$).

Other long-term Stage 2 grafts with varying size and collagen-GAG composition have been observed and have followed similar contraction curves of those of the standard 1.5 x 3.0 cm Stage 2 grafts (Figure 29). In one series of three animals, the collagen-GAG membrane was prepared by freeze-drying a collagen-GAG slurry 1.6 times the normal concentration (0.8% vs 0.5% by weight collagen-GAG). The performance of these grafts was similar to the Stage 2 grafts described above, however, the expansion between 60 and 100 days was less pronounced. These membranes showed an increased serous exudate when compared with standard Stage 2 membranes during the first two weeks. Long-term observation of larger grafts (4 x 4 cm or 3 x 3 cm) also showed expansion between day 60 and 100. The expansion of area in the "standard grafts" was primarily due to expansion of the M-L direction, although expansion in the A-P direction also occurred (Figure 30).

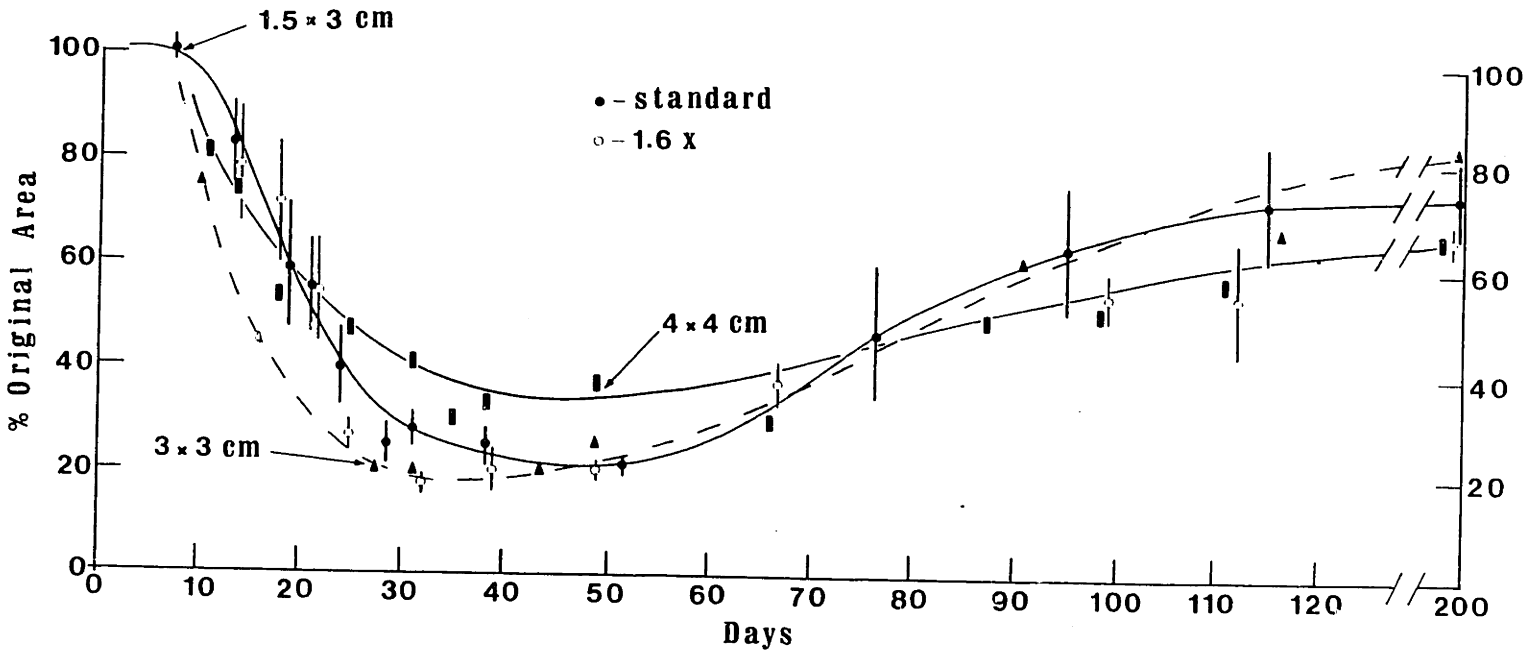

Figure 29. Contraction curves for Stage 2 artificial skin membranes. "Standard" membranes are 1.5 x 3.0 cm Stage 1 grafts seeded with 500,000 autologous epidermal cells/cm^2 graft (trypan blue exclusion). These grafts were prepared by freeze-drying a 0.5% collagen-GAG dispersion. In this four animal series, epidermal confluence was observed by day 12. Note the expansion of wound area between 60 and 100 days. A series of 3 grafts (open circles) was prepared with a 0.8% collagen-GAG dispersion prior to freeze-drying, or 1.6 times the normal concentration of collagen-GAG used prior to freeze-drying. These grafts were seeded with 500,000 cells/cm^2 graft and showed a similar contraction pattern. The contraction curves for a 4 x 4 and a 3 x 3 membrane are also shown.

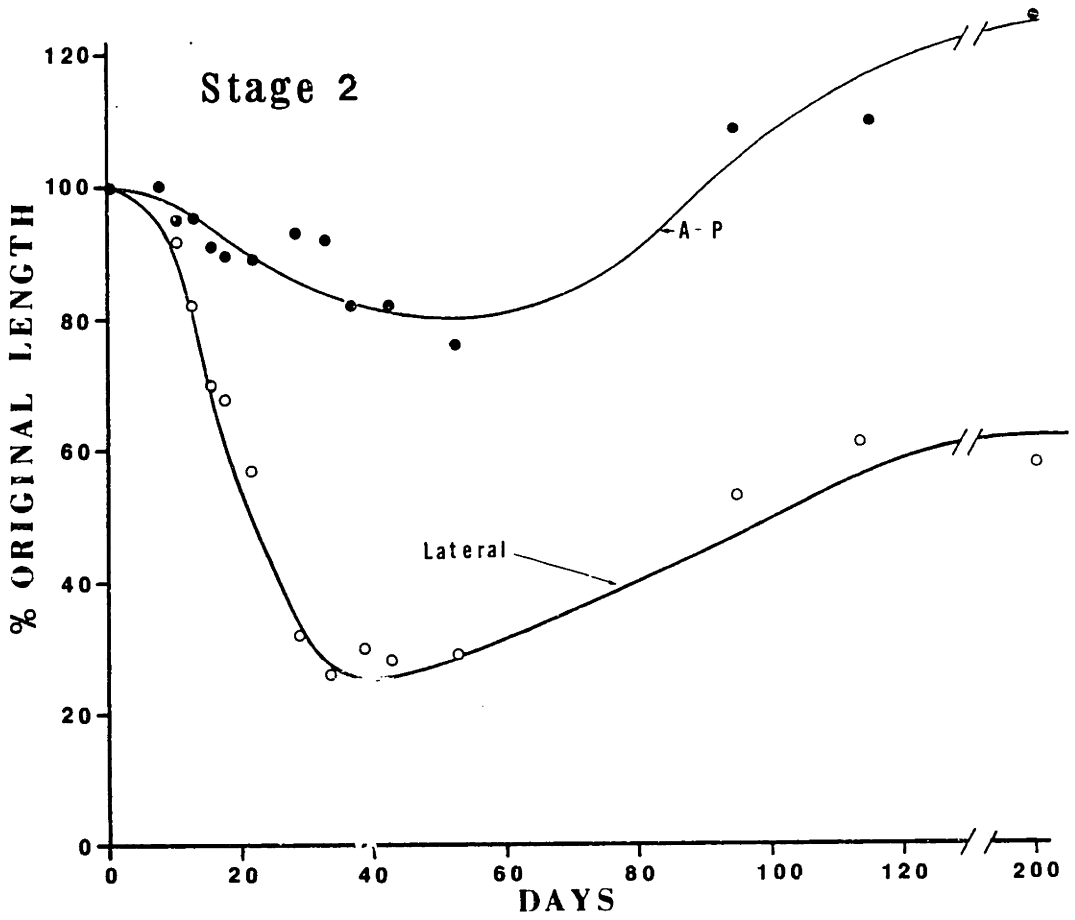

Figure 30. Normalized direct measurements of "standard" 1.5 x 3.0 cm Stage 2 membranes. Most of the contraction and expansion is in the lateral dimension. Each point represents the average of four measurements.

The control experiments with autografts, Stage 1, and ungrafted wounds were important in interpreting the performance of Stage 2 grafts. All grafted woundbeds were prepared in an identical fashion by excising full-thickness 1.5 x 3 cm wounds down to the panniculus carnosus (Figure 31). Grafted wounds with Stage 1 and Stage 2 appeared similar on day 0 (Figure 32).

Stage 2 wounds rapidly achieved confluence between 10 and 14 days with a maturing epidermis. When confluence was achieved, the silicone was removed (Figures 33,34), and the neoepidermis matured and keratinized forming the moisture and bacterial barrier over the wounded area (see below). By day 15, a keratinizing epidermis was present on Stage 2 grafts (Figure 37). This was compared to the control animals 15 days after grafting (Figure 36-39). The autograft appeared healthy with little contraction, whereas the ungrafted wounds were greatly contracted and closing. Stage 1 grafts showed very little contraction by day 15; however, if the silicone was removed, a large open wound was present (Figure 36).

By 60 days, the Stage 1 graft had closed by contraction and epithelialization and had an area comparable with the ungrafted animals (Figures 39,40). The autograft, in contrast, had expanded in area somewhat and approximated the original grafted area (Figure 42). The Stage 2 graft had contracted substantially by day 52 (Figure 41); however, it appeared in shape much more rectangular and was

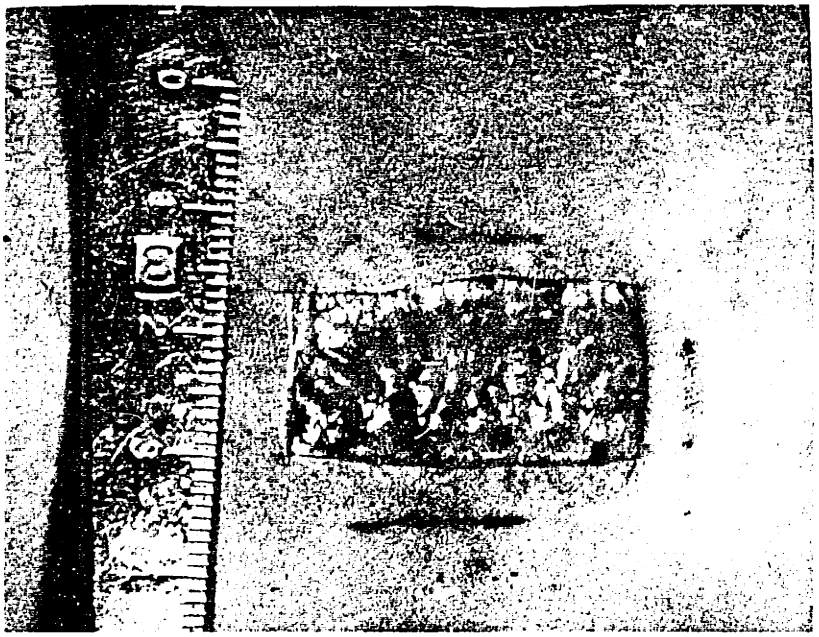

Figure 31. Recently excised 1.5 x 3.0 cm full-thickness wound down to the panniculus carnosus. Note tattoo marks parallel to the wound edges. Hemostasis is obtained before grafting. Animal No. 144-1, day 0.

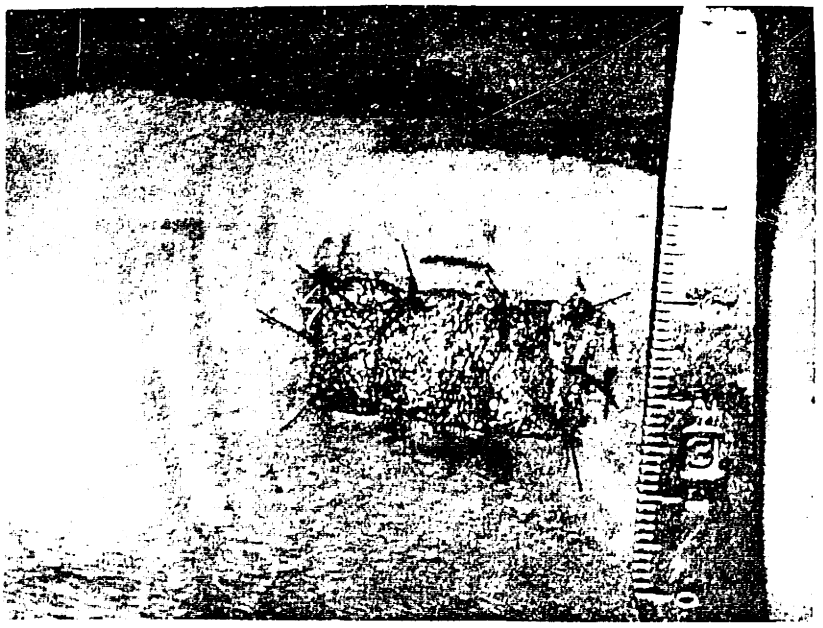

Figure 32. Appearance of artificial skin immediately after grafting. This graft was previously seeded with autologous epidermal cells. Animal No. 146-2, day 0.

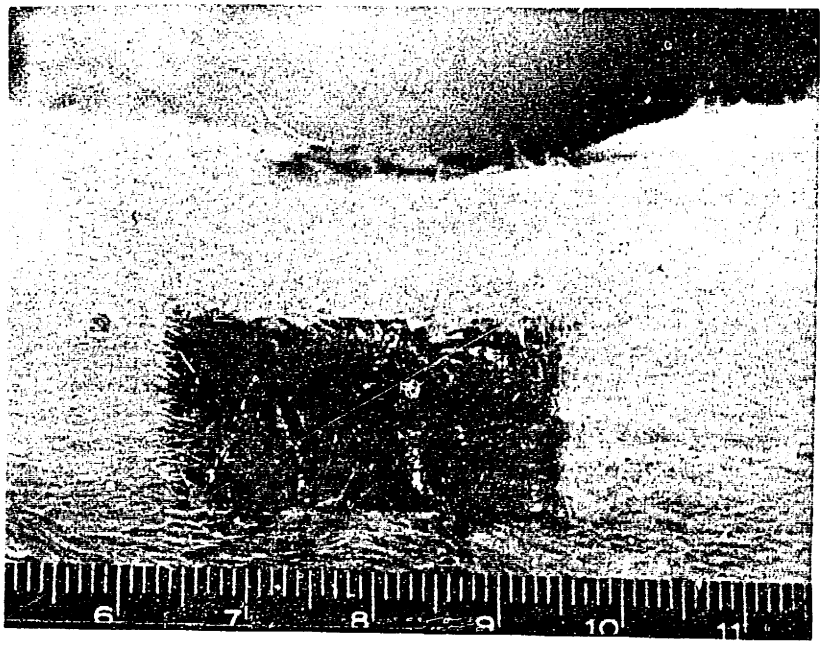

Figure 33. Appearance of a Stage 2 artificial skin graft one day prior to removal of the silicone. Buckling of the silicone is suggestive of some neoepidermal coverage. Animal No. 135-9, day 10.

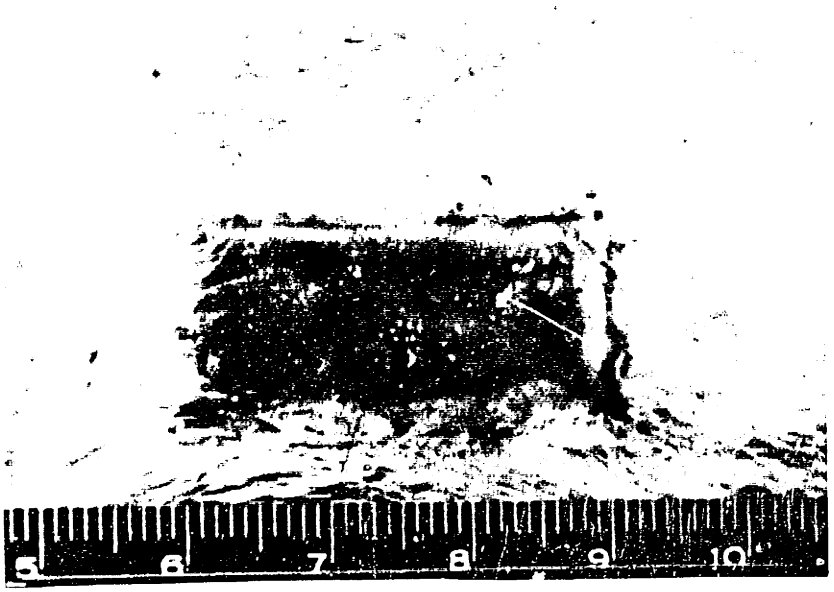

Figure 34. Appearance of wounded area immediately after removal of silicone from a Stage 2 graft. A confluent layer of maturing epidermis is present. Animal No. 135-8, day 10.

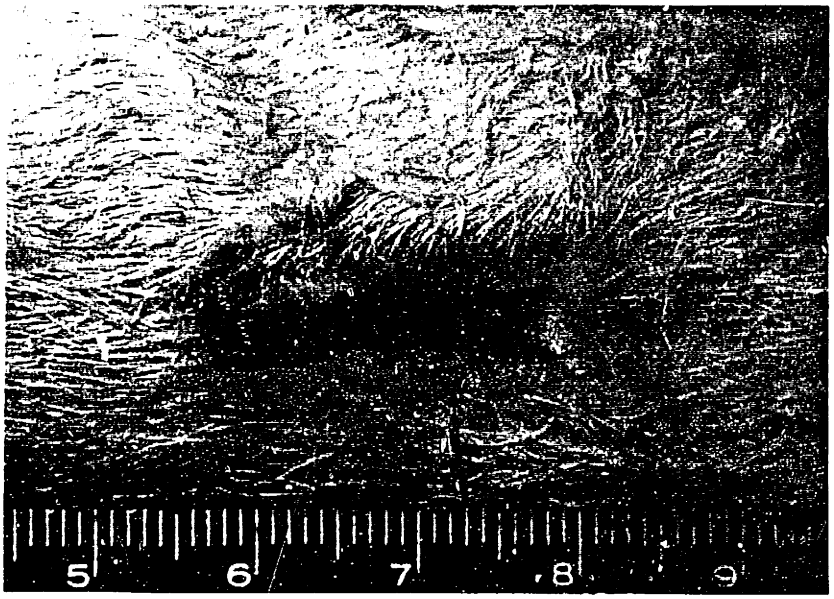

Figure 35. Ungrafted 1.5 x 3.0 cm wound, day 15. Note that most of the wound has closed by contraction. Animal No. 109-6.

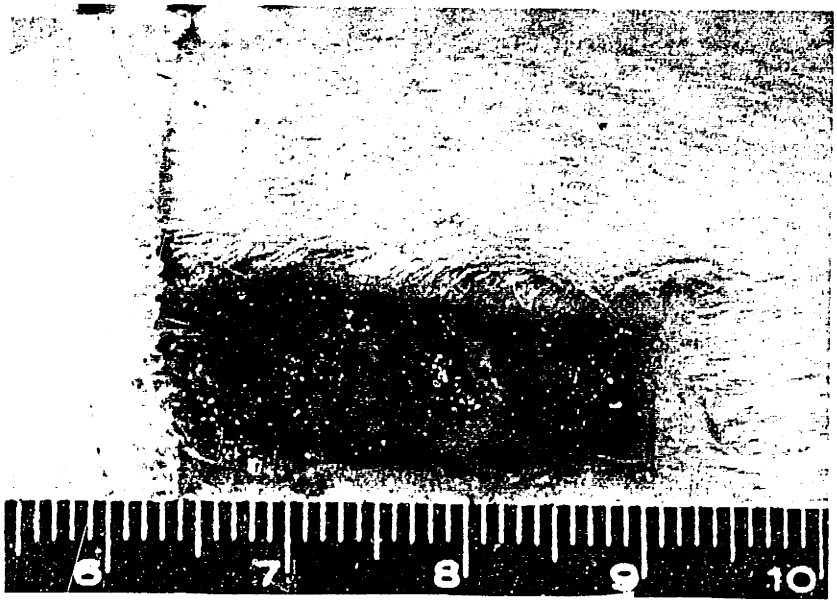

Figure 36. Stage 1, day 15. The silicone was removed to illustrate the large reduction in contraction present due to the application of a Stage 1 membrane. Most of the wound lacks epidermal coverage. Compare with Figure 35. Animal No. 80026A-6.

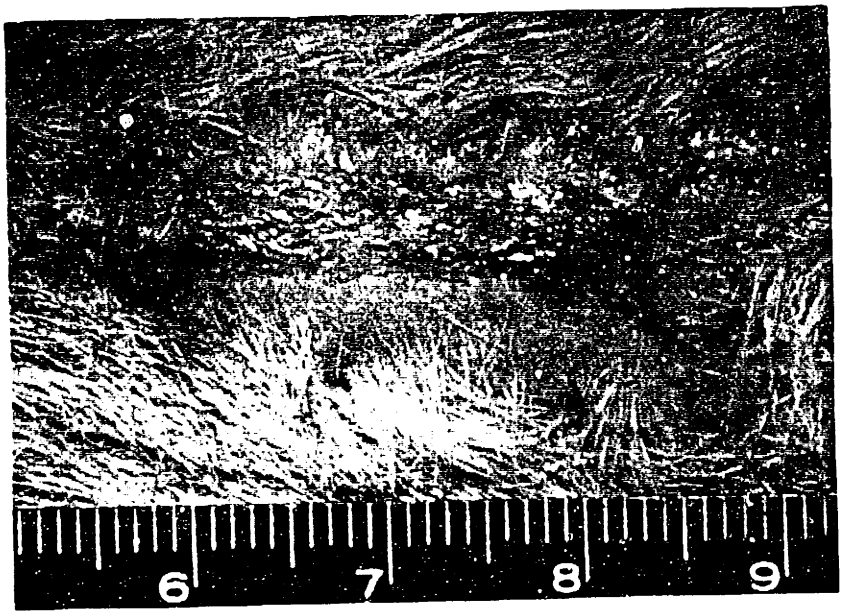

Figure 37. Stage 2, day 15. Note mature epidermis covering the wounded area. Animal No. 133-2.

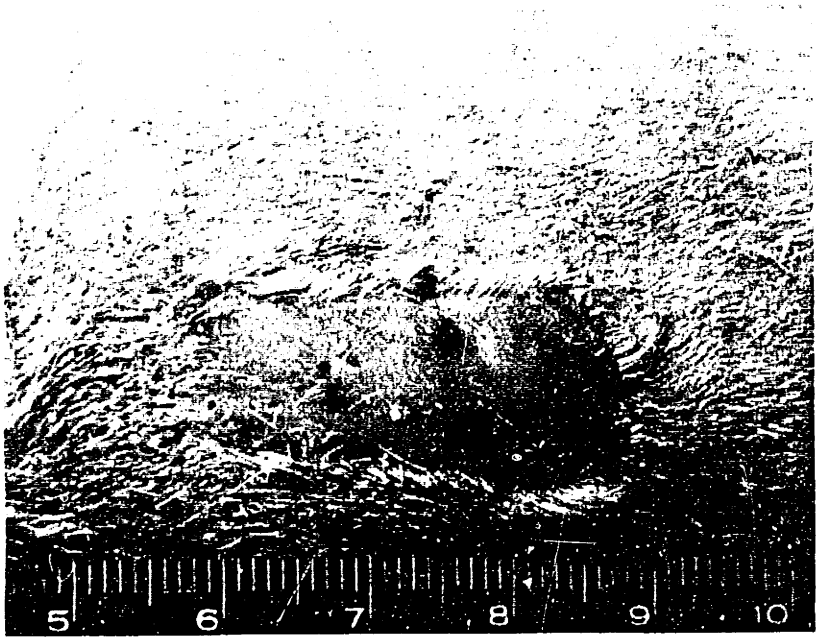

Figure 38. Autograft, day 15. The autograft appears to be vascularized and confluent with the adjacent skin. Animal No. 147-3.

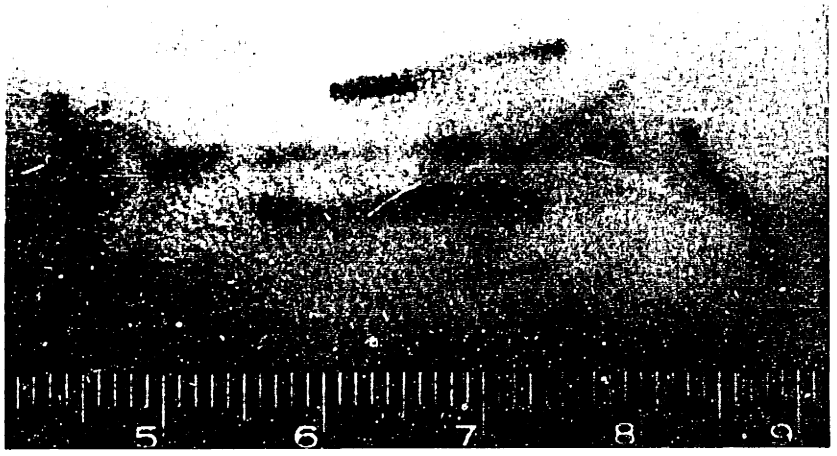

Figure 39. Ungrafted wound, day 61. Wound has closed and has contracted to about 10% of the original area. Animal No. 144-2.

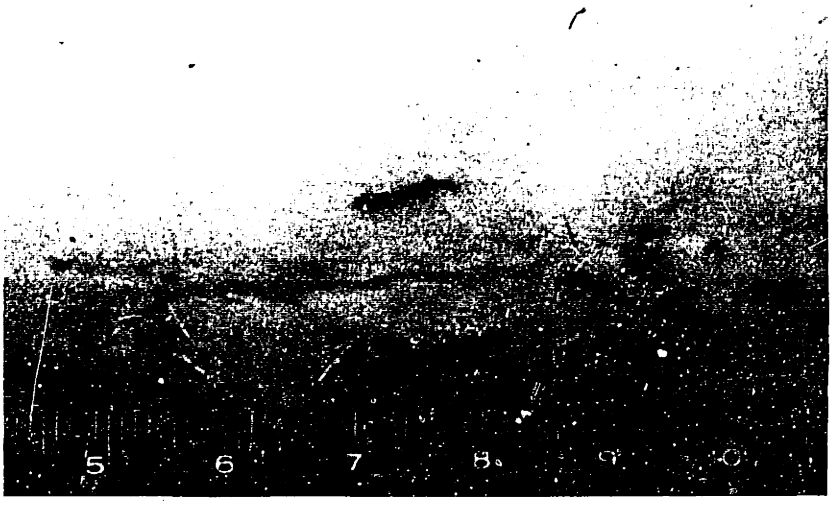

Figure 40. Stage 1, day 61. Wound appears similar to that seen in ungrafted animals. Compare with Figure 39. Animal No. 145-4.

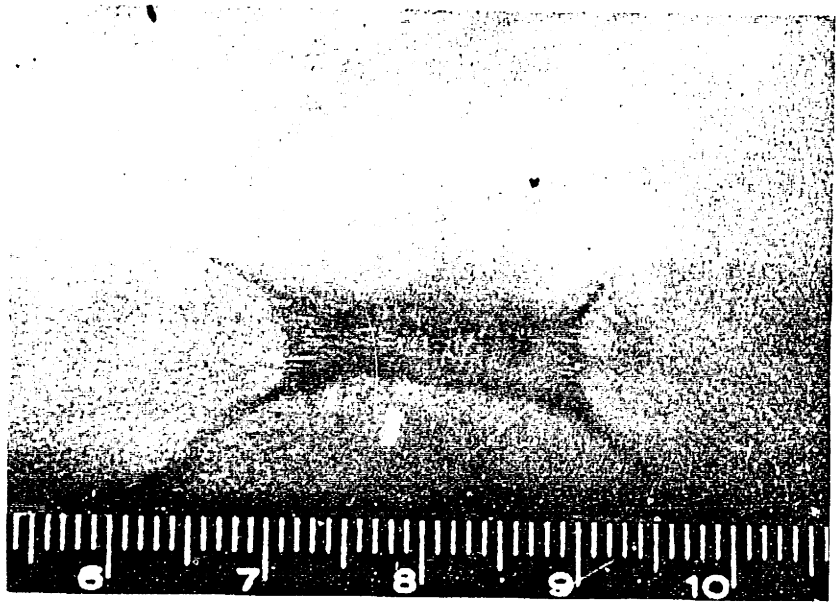

Figure 41. Stage 2, day 52. Note that the grafted area has contracted, but retains a more rectangular shape than either the ungrafted wound or Stage 1. Compare with Figures 39 and 40. Animal No. 135-8.

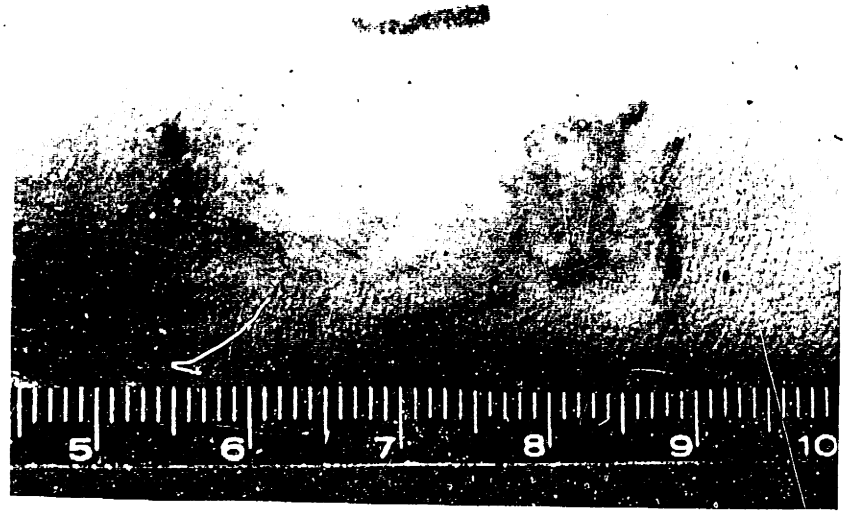

Figure 42. Autograft, day 61. Wound shows very little contraction. Animal No. 147-2.

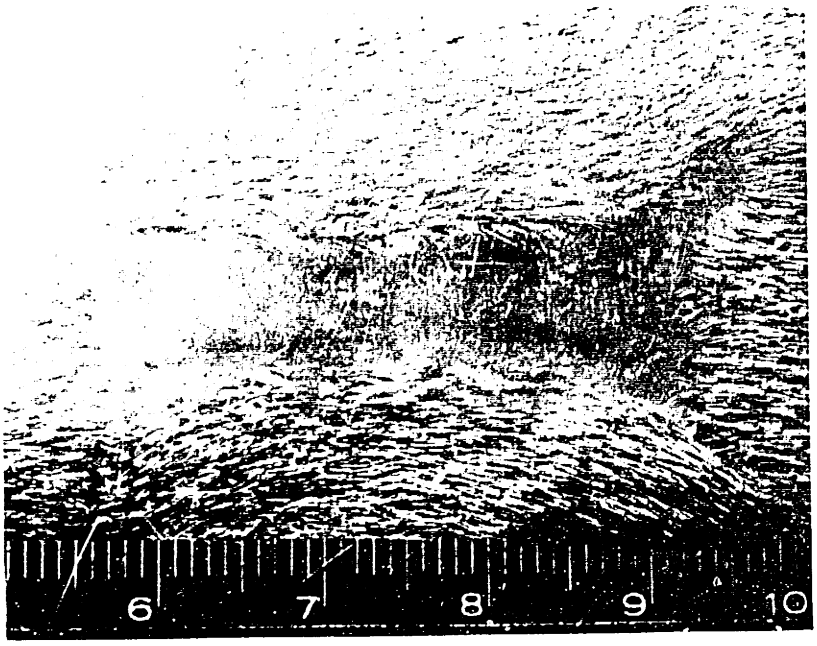

Figure 43. Stage 2, day 139. Grafted area shows significant expansion since seen at day 52 (Figure 41). Animal No. 135-8.

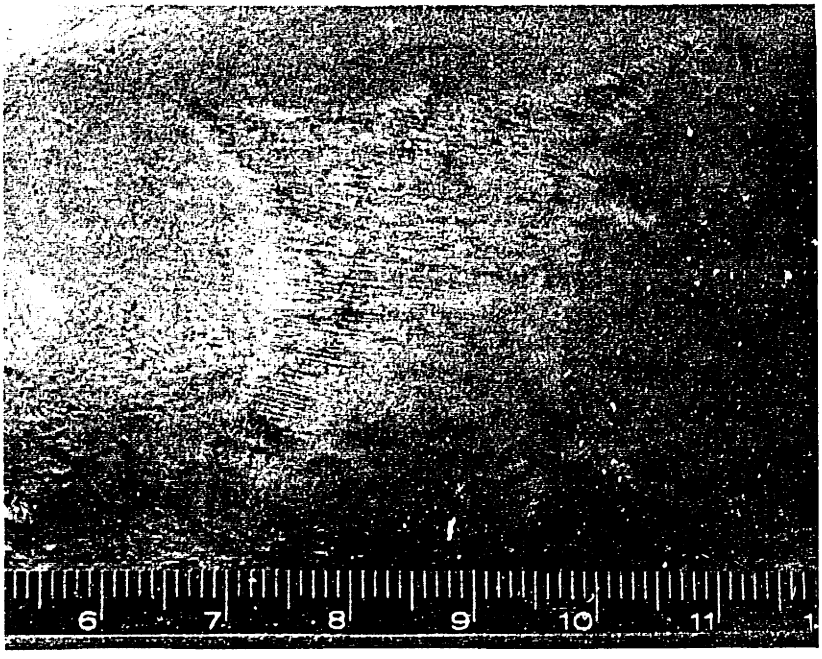

Figure 44. Stage 2, day 111. A larger Stage 2 graft, originally 4 x 4 cm, has also expanded to about 70% of the original area. Animal No. 140-2

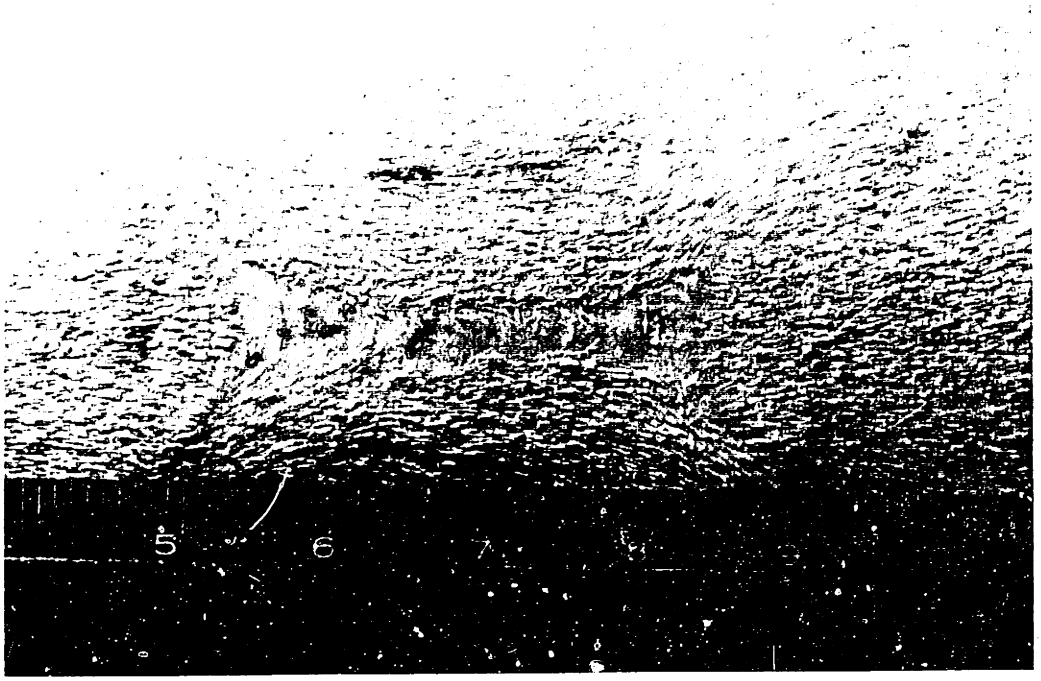

Figure 45. Ungrafted, day 244. Animal No. 144-1.

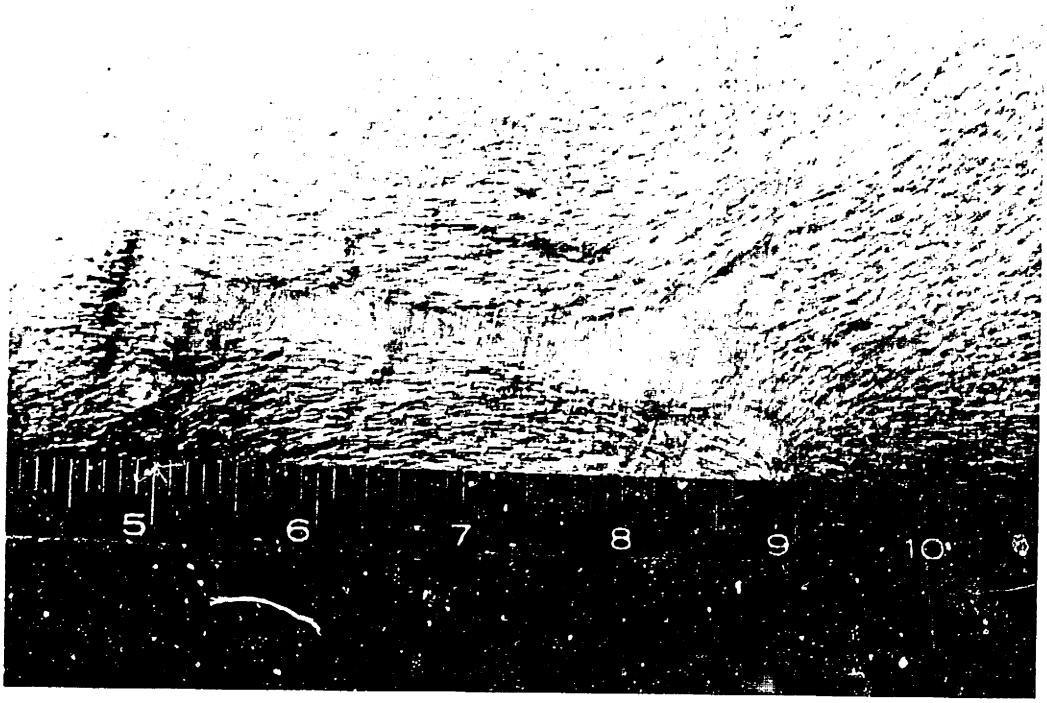

Figure 46. Stage 1, day 244. Animal No. 145-1.

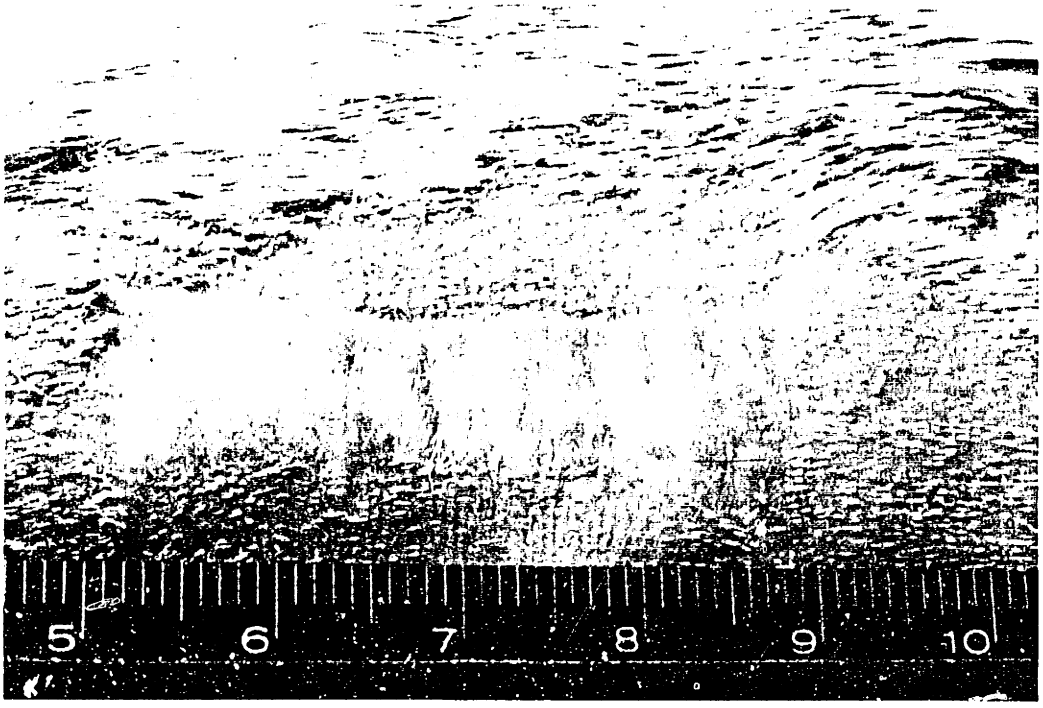

Figure 47. Stage 2, day 164. The Stage 2 graft forms a smooth transition with the normal skin. Animal No. 135-3. Original graft, 3.0 x 1.5 cm.

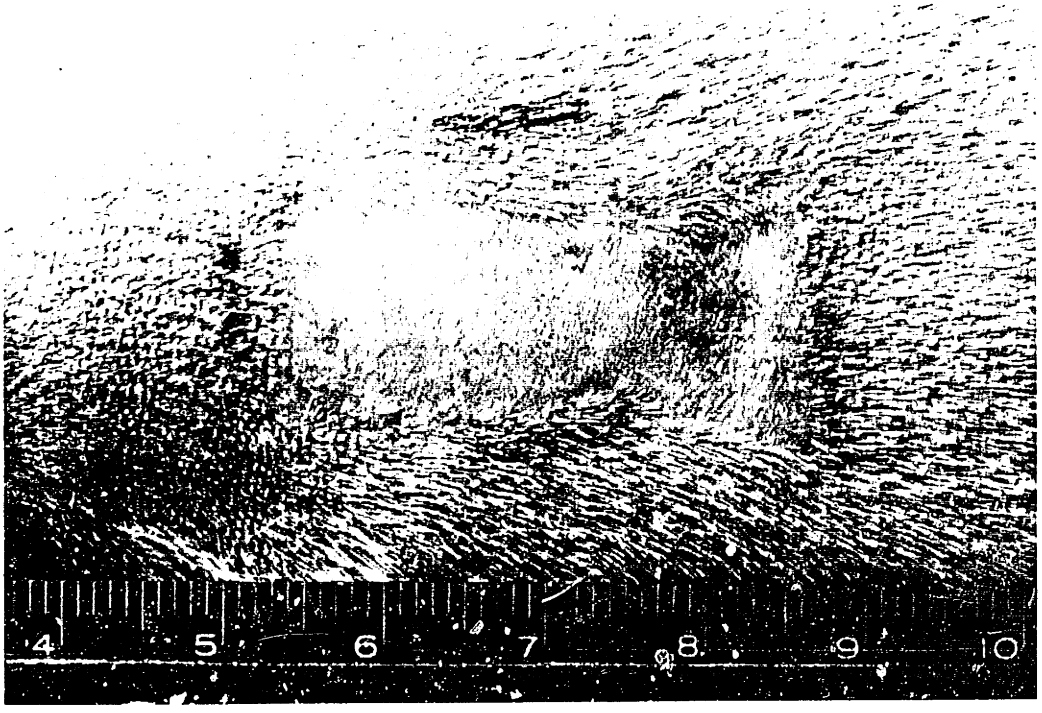

Figure 48. Autograft, day 244. Animal No. 147-3. Original graft, 3.0 x 1.5 cm.

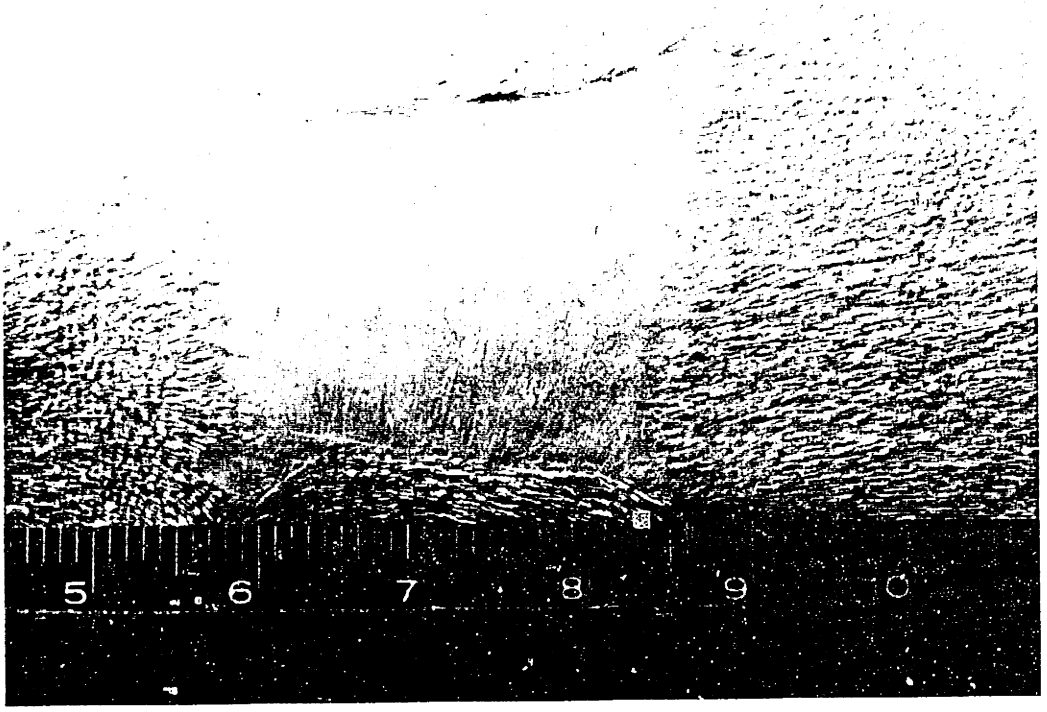

Figure 49. Stage 2, day 155. Originally a 3 x 3 cm graft. Animal No. 153-1.

Stage 2, Animal No. 135-3, day 377. Autograft, Animal No. 147-3, day 244.

Figure 50. Comparison of Stage 2 (left), with autograft (right). Both were originally 1.5 x 3.0 cm wounds. The autograft has retained a greater proportion of the original area and has some hair follicles.

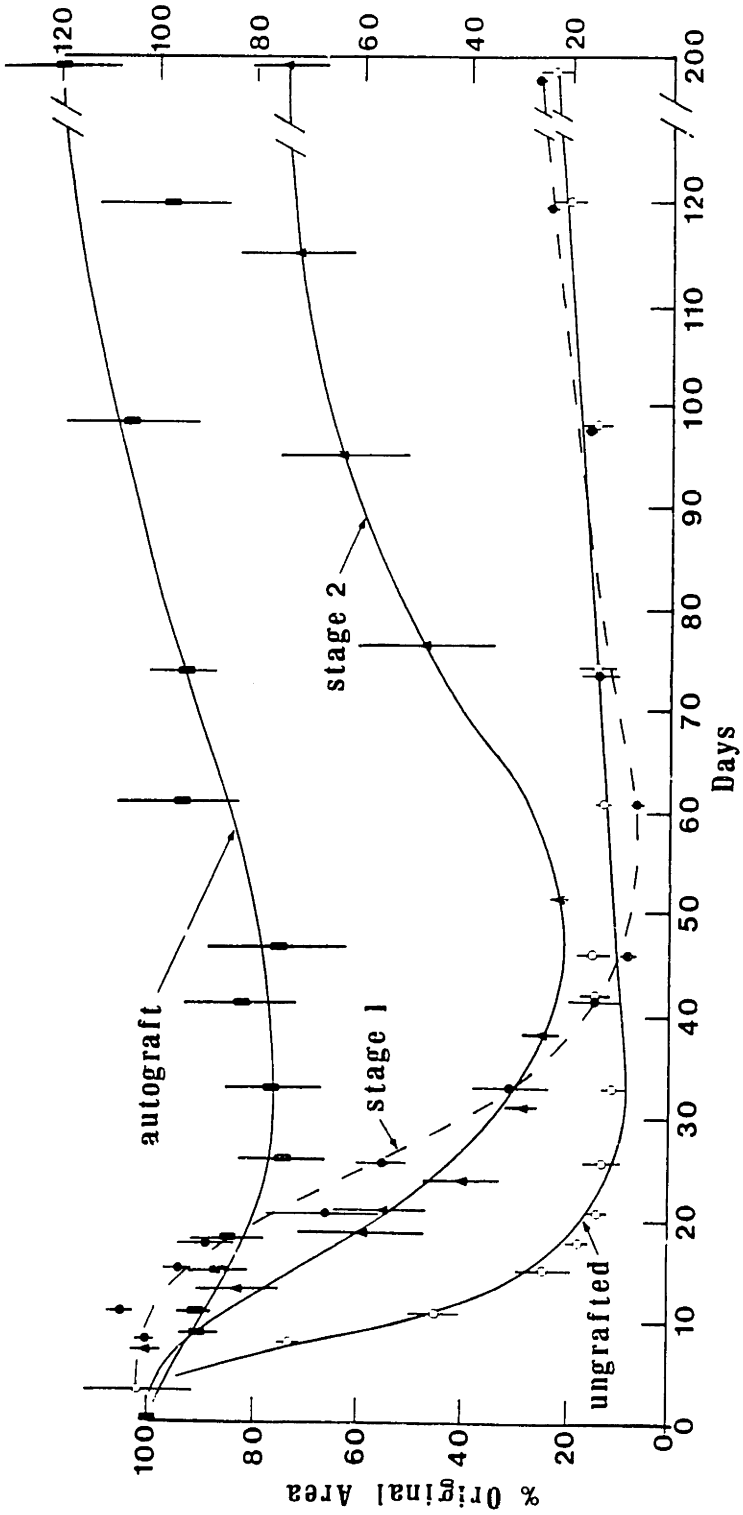

Figure 51. A composite graph comparing the contraction kinetics of 1.5 x 3.0 cm wounds treated with a full-thickness autograft, Stage 1 or Stage 2 artificial skin, or left ungrafted. Error bars represent ± 1.0 standard deviation.

significantly larger in area than either the open wound or Stage 1 graft at comparable dates.

After 60 days, the Stage 2 grafts began a rapid expansion which leveled off at about 70% of the original area by 200 days. This was not only true of the 1.5 x 3.0 cm grafts tested, but also of 4 x 4 cm and 3 x 3 cm grafts which followed similar expansion patterns (Figures 43-51). Both the open wound and Stage 1 areas seem to expand slightly between 120 and 200 days. Figure 51 summarizes the contraction patterns of the artificial skin grafts (Stage 1 and Stage 2) as well as the autograft and ungrafted controls.

D_{50}, An Index of Wound Contraction

The day at which the graft reached 50% of its original area (D_{50}) was considered as an index of contraction. For the grafts where this quantity could be measured, the mean day at which a Stage 2 graft reached 50% of its original area was 17.5 days with a standard deviation of 3.5 days (Figure 52). For Stage 1 (cell free) grafts, the mean D_{50} was 25 days with a standard deviation of 2.2.

The mean D_{50} observed with Stage 2 grafts was significantly longer than that observed for ungrafted controls which had a mean D_{50} of 10.3 days with a standard deviation of 1.0 ($p < 0.001$, t-test, two-tailed). The mean D_{50} observed with Stage 2 grafts was, however, significantly shorter than that observed with Stage 1 controls ($p < 0.005$).

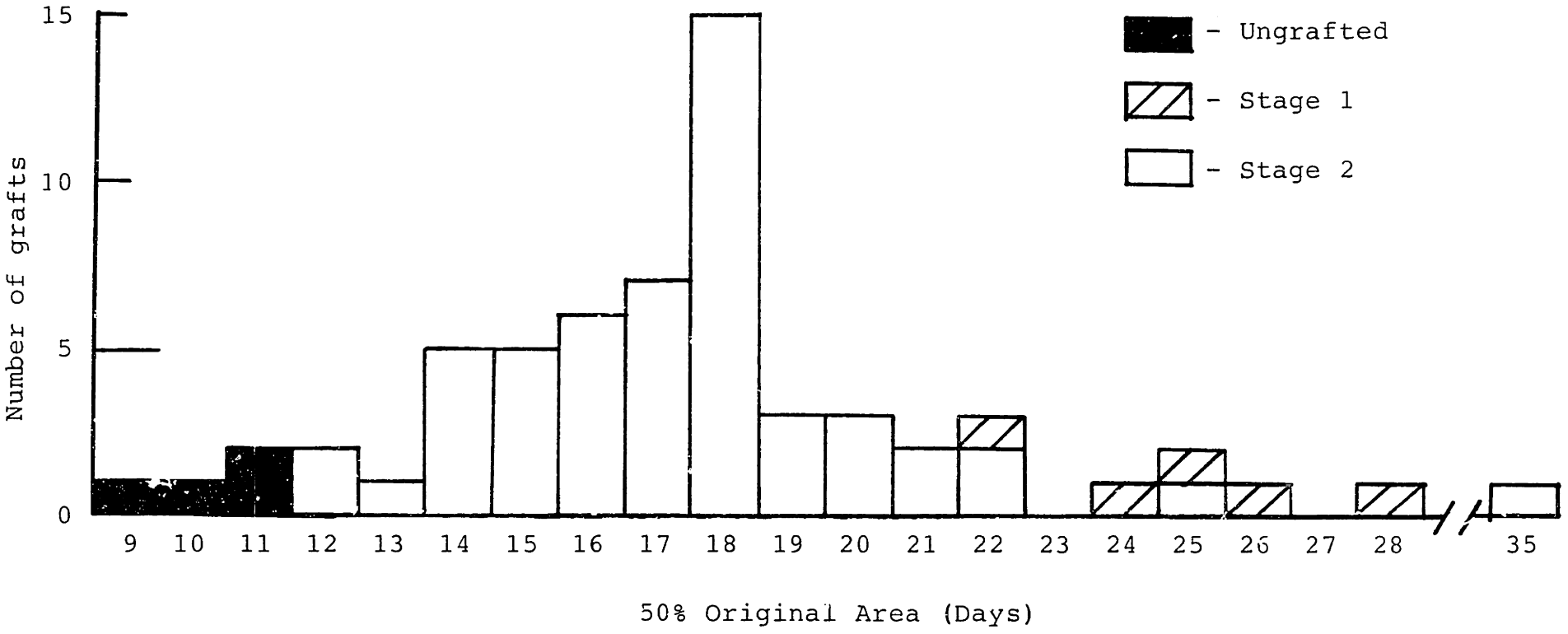

Figure 52. Histogram of the time at which the wound area reaches 50% of the original area. Stage 1 grafts showed the longest times, and ungrafted wounds the shortest.

Stage 2 grafts were observed to be infiltrated with mesenchymal cells and capillaries much earlier than previous studies with Stage 1 grafts. Figures 53 and 54 compare the histology at day 7 of a Stage 1 with a Stage 2 graft.

Effects of Cell Seeding Parameters on Stage 2 Performance

Concentration of Cells in Seeded Graft

The number of cells seeded into the collagen-GAG matrix was an important parameter in reaching neoepidermal confluence. Neoepidermal confluence was defined as the time when at least 75% of the grafted area was covered with neoepidermis (Figure 55). Deciding upon what constituted neoepidermal coverage required substantial experience. When neoepidermal coverage was first observed (Figure 34), it was a very thin shiney surface which was sometimes confused with a dried serous exudate. Often at this point, keratin pearls could be seen deep within the graft. Within two to three days of the initial coverage, layers of keratin were formed which could be removed grossly. This provided an unambiguous criterion for neoepidermal confluence. The majority of the experiments reported here used 500,000 viable cells/cm^2 graft. This cell density resulted in a mean time to neoepidermal confluence of 12.6 days with a standard deviationof 1.7 days. Grafts with infection and without evidence of gross neoepidermal proliferation were not included in this figure. Grafts seeded with a smaller number of cells required longer to achieve neoepidermal confluence. In contrast, grafts seeded with cell

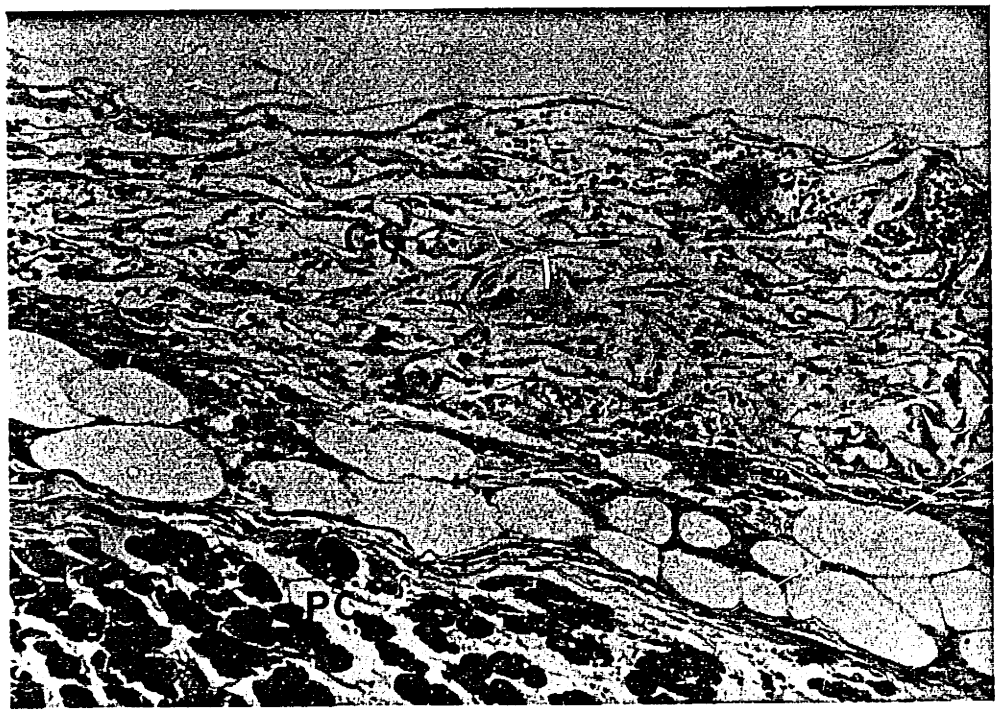

Figure 53. Stage 1, day 7. Graft (CG) has been infiltrated with mesenchymal cells, inflammatory cells and blood cells and is well adhered to the panniculus carnosus (PC). Animal No. 503-1, 300 X.

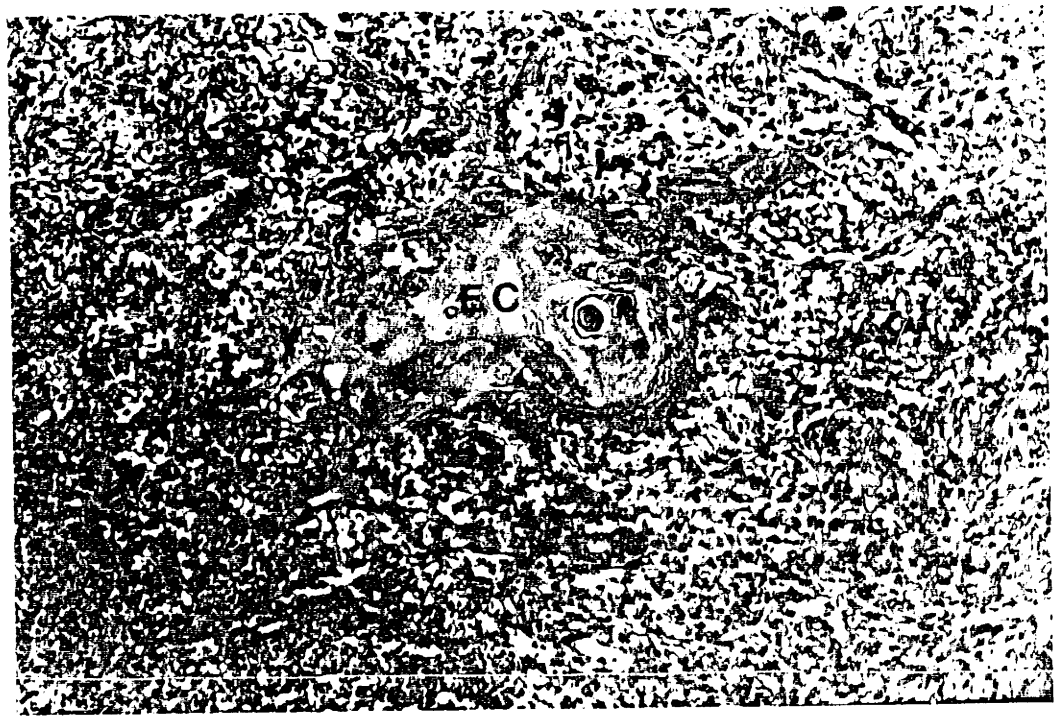

Figure 54. Stage 2, day 7. Graft has a much denser cellular infiltrate compared with Stage 1 grafts on day 7 (Figure 53). In the center is an epidermal cluster (EC) which has a small ball of keratin in the center. Animal No. 134-3, 300 X.

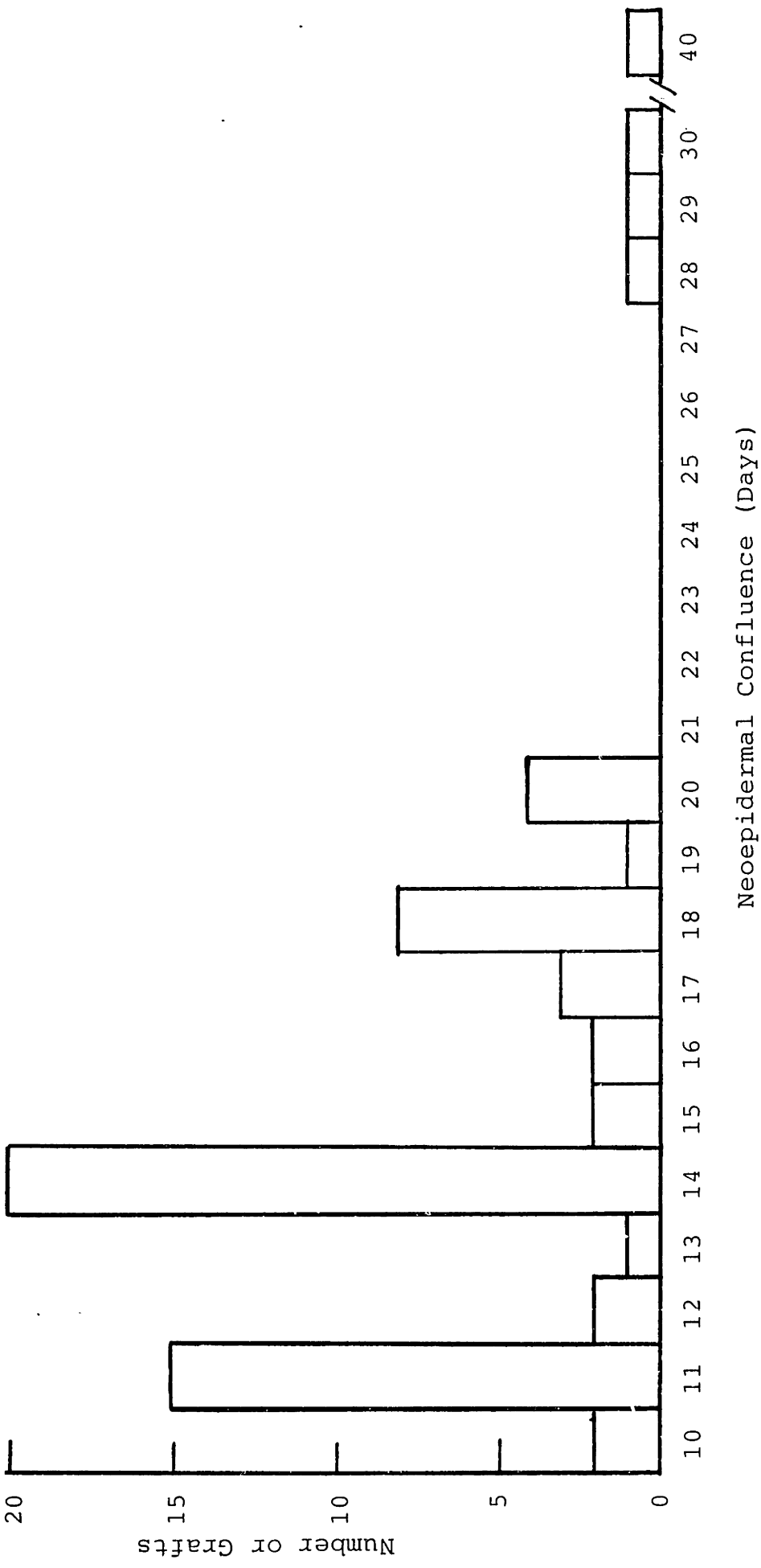

Figure 55. Histogram of the time at which neoepidermal confluence occurred. This time was defined as the time at which at least 75% of the graft was grossly covered with neoepidermis. Wounds were frequently inspected on days 11, 14, and 18 accounting for the higher numbers on these days.

densities in excess of 500,000 cells/cm^2 graft showed no decrease in the time to neoepidermal confluence (Figure 56). Linear regression of the data at 50,000, 200,000, and 500,000 cells/cm^2 graft gave a slope of -8.8 days per decade of cells seeded/cm^2 graft with a correlation coefficient $r = -0.78$.

From each square centimeter of skin biopsy, typically 2,000,000 viable epidermal cells could be isolated. This resulted in an expansion factor of 4:1 and 40:1 when 500,000 and 50,000 cells/cm^2 were used respectively.

Throughout the course of this research, important observations were made with regards to the expansion factor. The initial experiments used thick split-thickness skin biopsies (0.4 mm) which were stored in chilled saline for 48 hours prior to cell isolation. This resulted in a mean time for neoepidermal confluence of 11 days. In later experiments, facility with the dermatome resulted in thinner biopsies (0.2 mm). The thinner biopsies were easier to separate post-trypsinization than the thick biopsies. They also left a donor site which closed in four to five days rather than two weeks for the more deeply excised sites. These grafts, however, tended to have a delayed neoepidermal confluence requiring about 14 days or more. Later, grafts were seeded on the same day as the biopsy was taken. Even though these were thin biopsies, neoepidermal confluence times were comparable to the initial experiments.

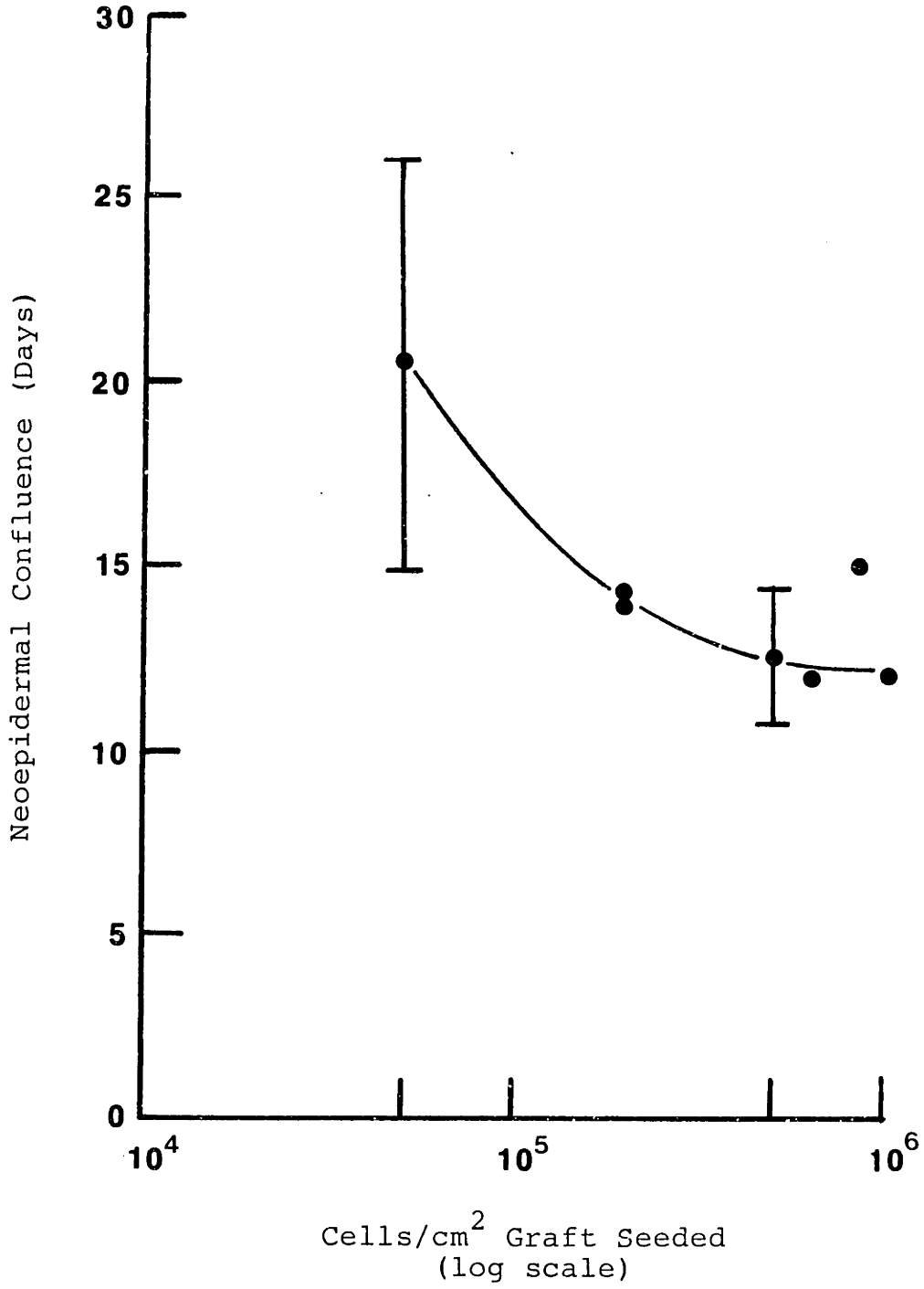

Figure 56. The effect of the number of cells seeded per square centimeter of graft on the time at which neoepidermal confluence was observed. Cell seeding densities above 500,000 cells/cm^2 graft did not increase the rate of neoepidermal confluence.

The time to neoepidermal confluence influenced the contraction kinetics. When seeded with 50,000 cells/cm^2 graft, the contraction pattern of the grafts was similar to that seen with Stage 1 (cell free) grafts, with the long-term wound area appearing like a linear scar. The re-expansion of these grafts was much less pronounced than grafts seeded with a greater number of cells (Figure 57).

Because significant contraction occurred by the 18th day with epidermal ingrowth from the edges, it was found that in the guinea pig model, seeding with larger number of cells (200,000 to 500,000 cells/cm^2 graft) gave clearer evidence of neoepidermal proliferation.

Associated with the larger number of cells were numerous keratin pearls which were grossly evident between days 11 and 25. By day 11, keratin pearls could be seen as small whitish spots within the graft. As the graft matured, these keratin pearls rose to the surface and were ejected from the graft. When 50,000 cells/cm^2 graft were seeded, very few keratin pearls were visible grossly. In all grafts to date, the keratin pearls have emerged to the surface and in no cases have dermal or epidermal cysts been observed.

Gravity Seeding of Grafts

In earlier sections, the efficacy of membranes seeded with epidermal cells has been shown. In considering the transfer of this technology to a clinical situation, it was realized that the centrifugation step was somewhat cumber-

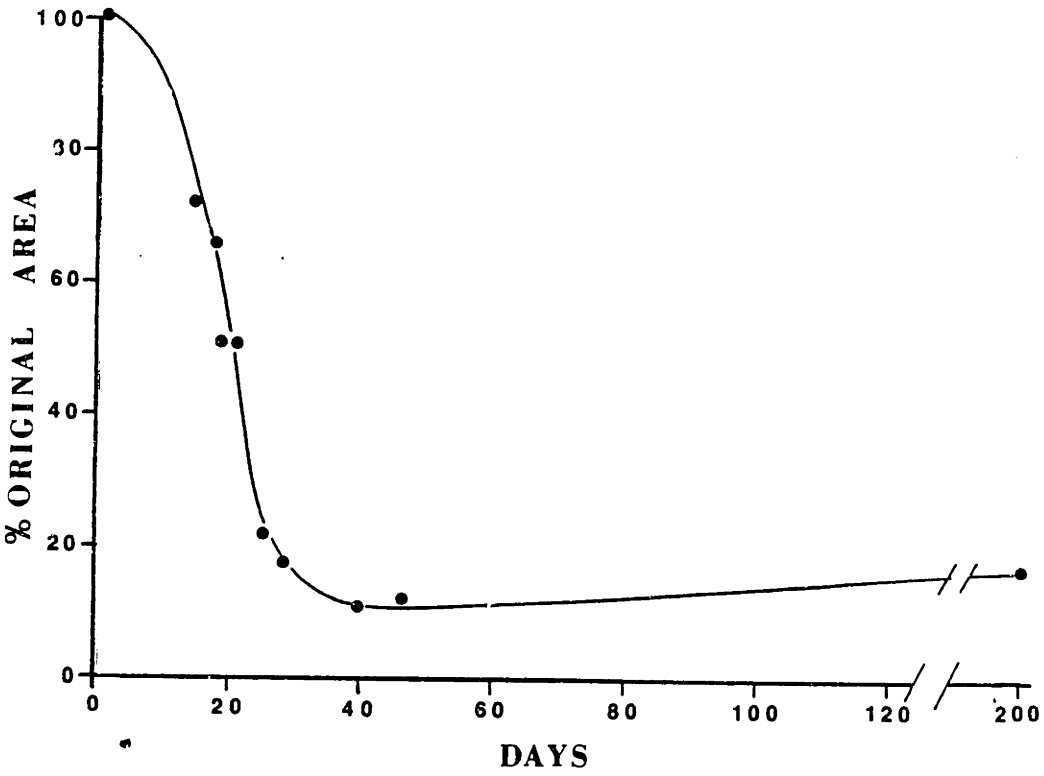

Figure 57. Contraction curve for a 1.5 x 3.0 cm graft seeded with 50,000 autologous epidermal cells/cm^2 graft. This graft contracted more than grafts seeded with 500,000 cells/cm^2 and showed little re-expansion.

some. Most standard centrifuges have holders which would limit the size of the membrane to about 3" by 5". To produce grafts larger than this would require either a larger redesigned holder or use of a larger centrifuge.

The results of the SEM of seeded membranes showed that even without centrifugation, epidermal cells would settle out on silicone. Observations of cells in TCM at 1 g showed that they had a downward velocity of the order of 1 mm per minute. Two membranes were seeded by allowing the graft and the cellular suspension to sit for 40 minutes (1 g) prior to grafting (161 series). The silicone was removed 14 days after grafting and a layer of necrotic material about 1 mm thick was found below the silicone (Figure 58). After the necrotic material had been carefully removed, a confluent layer of neoepidermis was found underneath. The necrotic material, when examined microscopically, showed a collagen-GAG matrix infiltrated with necrotic mesenchymal cells, capillaries, neoepidermis, and keratin pearls. The wound contracted faster than most 3 x 3 cm grafts and only expanded to 23% of its original area by day 187 (Figure 59).

Cell Suspension Media Used

The majority of Stage 2 grafts were prepared with DMEM with 10% fetal calf serum. Because of the immunologic reactions which might occur with the use of serum from a different species, other cell suspension media were used

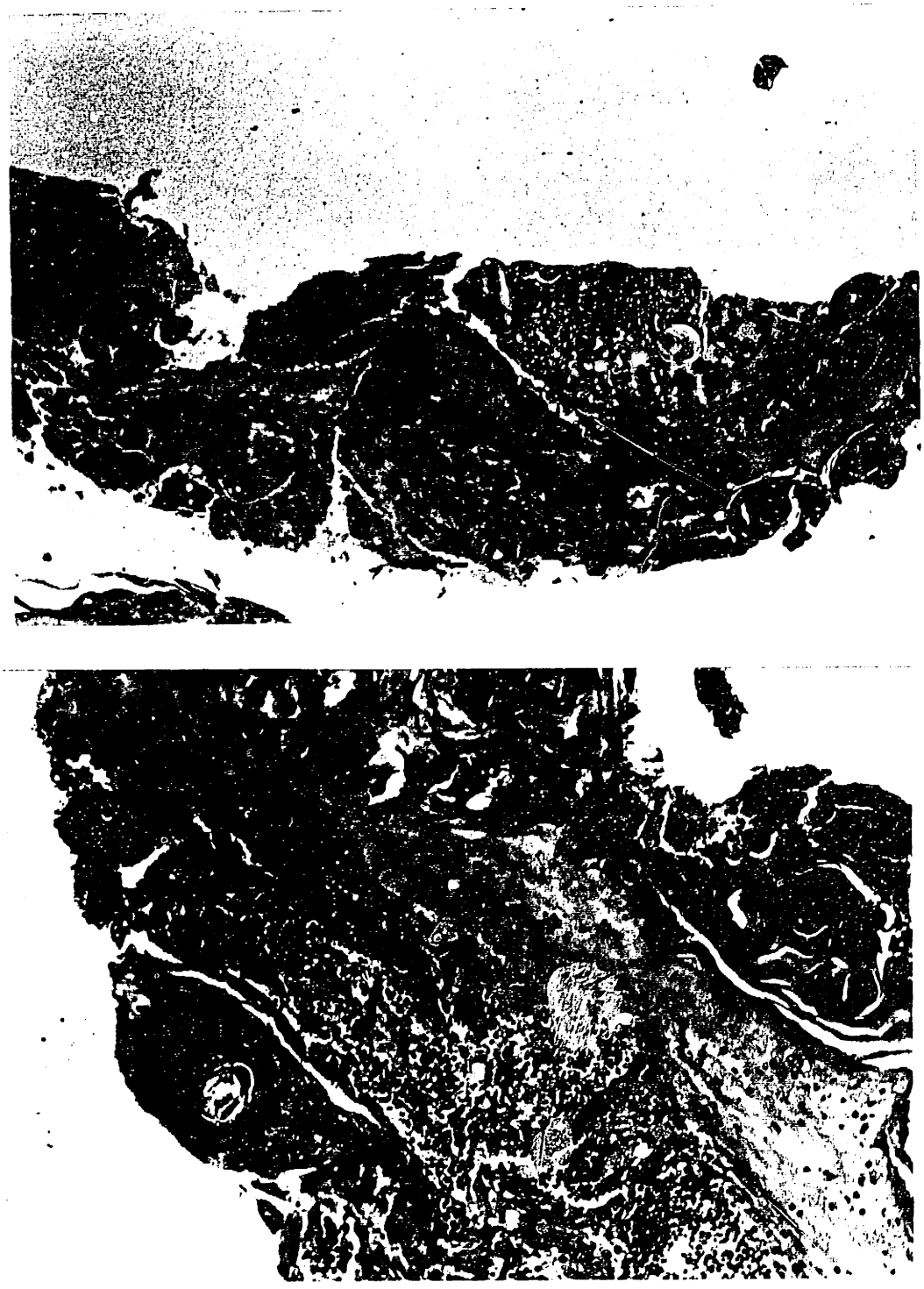

Figure 58. Low (75 X) and high (300 X) power view of the layer of necrotic debris found between the silicone layer and the neoepidermis on day 14. This graft was seeded with 500,000 cells/cm^2 without centrifugation (1 g). The vascular supply to the upper levels of the graft may have been cut off by the formation of a neoepidermis near the bottom of the collagen-GAG membrane. Animal No. 161-1.

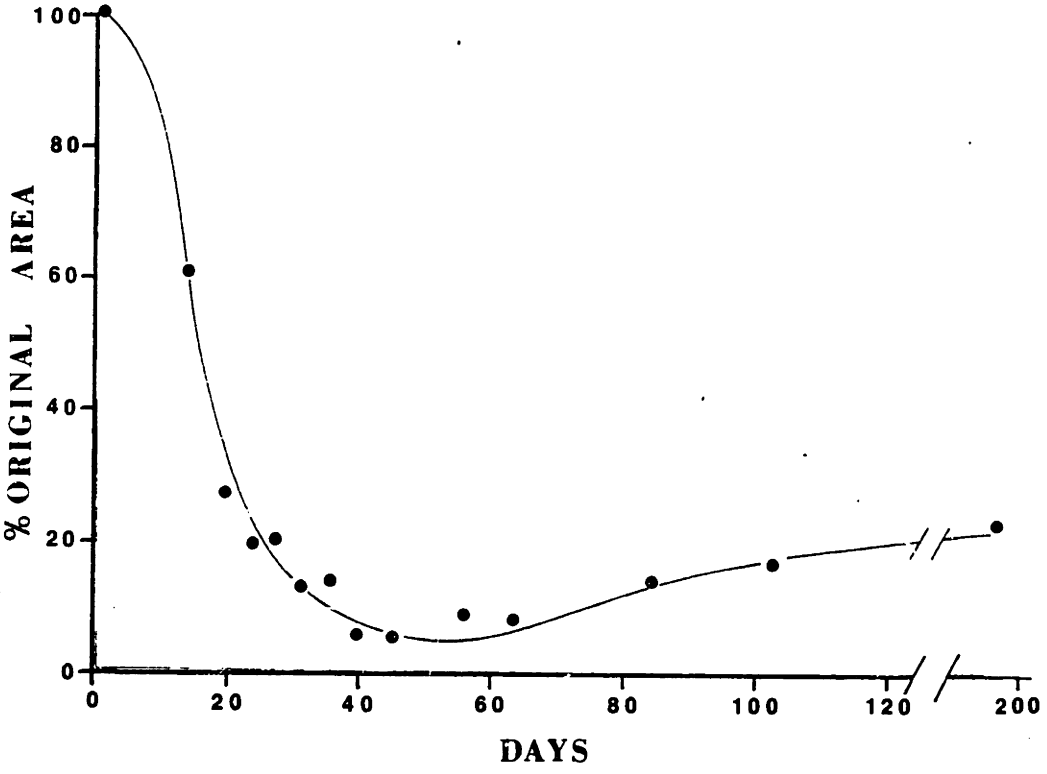

Figure 59. Contraction curve of a membrane seeded without centrifugation (1 g). Although a confluent neoepidermis was observed after day 13, the wounded area contracts rapidly with only a small amount of re-expansion. Animal No. 161-1.

in a few grafts. Grafts in which the suspension medium was DMEM with 10% human AB sera were in general associated with less neoepidermal proliferation. Of the 10 grafts in which AB serum was used, only two showed gross evidence of neoepidermal proliferation even though 8 were sacrificed after the 11th post operative day. Microscopically, there was evidence of areas of neoepidermal coverage with occasional keratin pearls by day 14; however, the proliferation was much less than typically seen in grafts where FCS was used in the medium.

When only a salt solution (PBS) was used as a suspending medium, the epidermal cells were found to clump after the dermal portion of the graft was vortexed. This clumping occurred with PBS both in the presence and absence of calcium and magnesium, and also occurred when 10% ACD was added to the PBS. None of the three animals grafted with membranes prepared with PBS showed any gross or microscopic evidence of neoepidermal proliferation.

The Effect of Fibroblasts

In a preliminary study, 200,000 fibroblasts/cm^2 graft were seeded into the collagen-GAG matrix in addition to 500,000 epidermal cells/cm^2 graft (138 series). Of the three animals grafted, one had neoepidermal confluence before day 14. The microscopic section of the graft at day 15 showed good neoepidermal coverage with numerous keratin pearls. The neodermis, however, was about half the normal thickness

of other Stage 2 grafts without seeded fibroblasts at a comparable time. This study suggested that the fibroblast may be important in the biodegradation of the collagen-GAG matrix (Figure 60).

Cryopreservation of Epidermal Cell

Eight grafts were prepared with cells which were cryopreserved in DMSO for a period of 4 to 190 days. Of these grafts, only one did not show gross evidence of neoepidermal proliferation by day 14. Cell viabilities measured by trypan blue post-freezing ranged from 69 to 78%, and all produced actively dividing cell cultures *in vitro*. Contraction patterns observed for the two long-term animals were similar to other 3 x 3 cm grafts seeded with cells isolated and seeded in the same day. Neoepidermal confluence occurred on the average on day 12 (Figure 61).

Grafts Seeded with Hair Follicles

After being seeded with 500,000 epidermal cells/cm^2 graft (15 min x 50 g), one graft was seeded with 24,000 hair follicles/cm^2 graft (20 min x 1 g). Over 88 days of observation, no hairs were observed grossly within the graft. The silicone was removed on day 14 with neoepidermal confluence. This graft followed a contraction pattern similar to standard Stage 2 grafts.

Grafts Seeded with Heterologous Cells

Thirty grafts were prepared with heterologous cells. These cells isolated from split-thickness skin grafts were given a variety of treatments before being seeded into the

Figure 60. Stage 2, day 15. Graft seeded with 500,000 epidermal cells/cm^2 followed by 300,000 fibroblasts/cm^2. Neodermis (ND) is thinner than normal. Numerous keratin pearls (KP). Animal No. 138-1, 150 X.

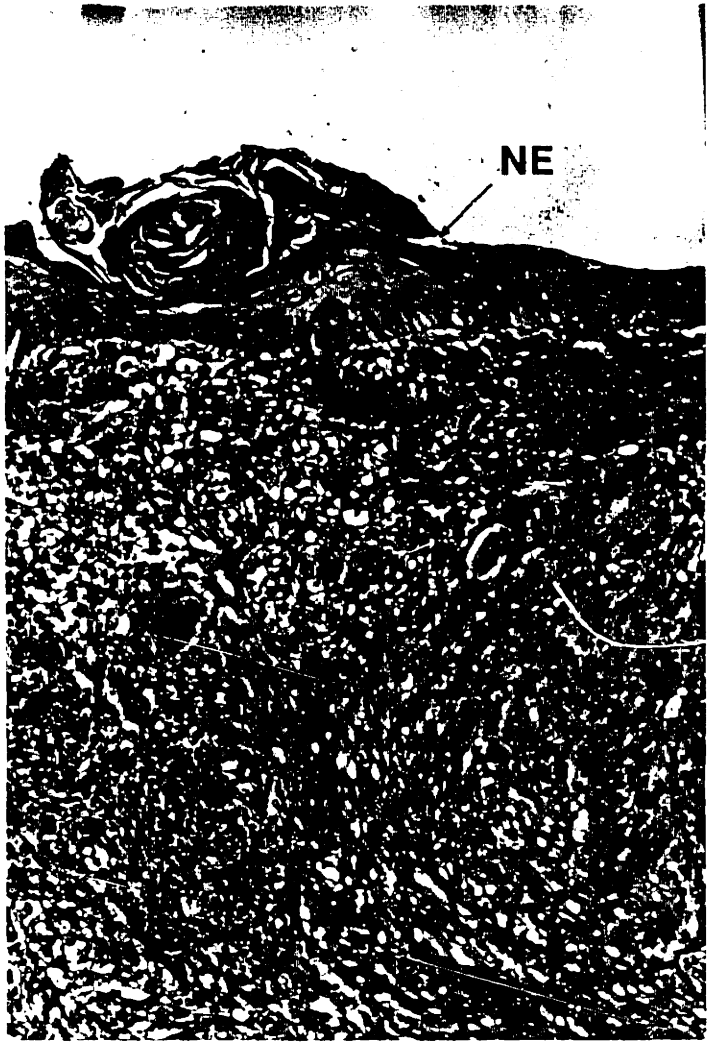

Figure 61. Stage 2, day 12. Graft seeded with 500,000 epidermal cells/cm^2 which were cryopreserved for 6 months in DMSO. Note thin confluent neoepidermis (NE). Animal No. 170-2, 300 X.

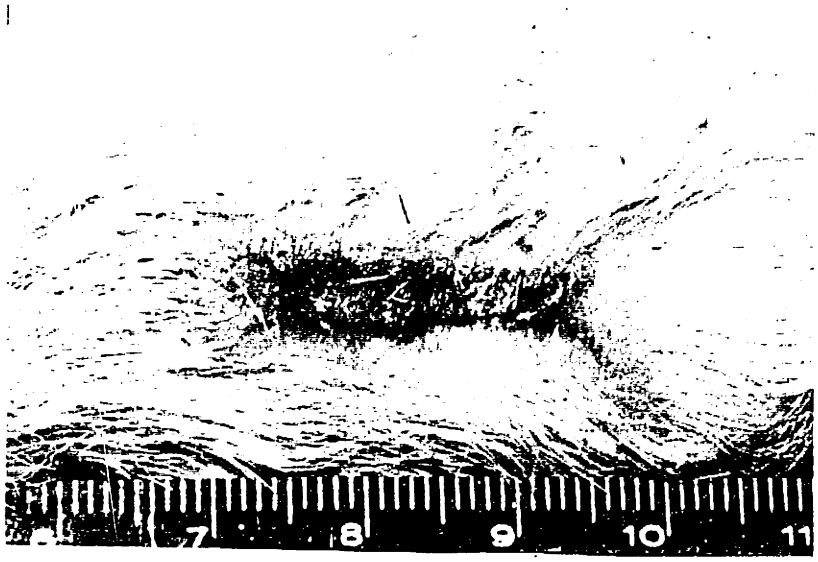

Figure 62. 1.5 x 3 cm artificial skin graft seeded with 500,000 heterologous epidermal cells/cm^2 14 days after grafting. A mature neoepidermal coverage is observed. No visible signs of rejection were observed during the 50 days of the experiment. Animal No. 300-4.

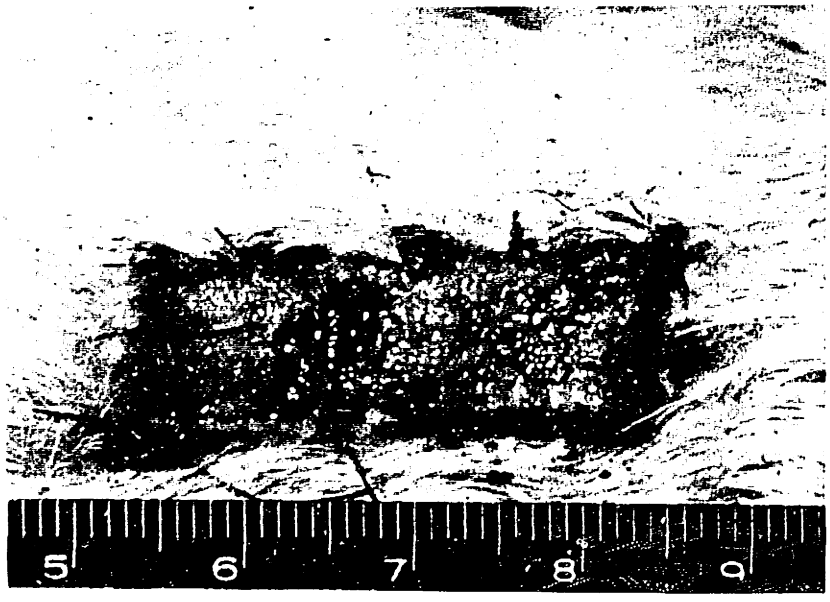

Figure 63. Rejection of full-thickness homograft 14 days after transplantation. A 1.5 x 3 cm graft from the same donor from which the heterologous cells were obtained. The homograft was grafted 19 days after the initial artificial skin graft.

HETEROLOGOUS SEEDED CELL EXPERIMENT

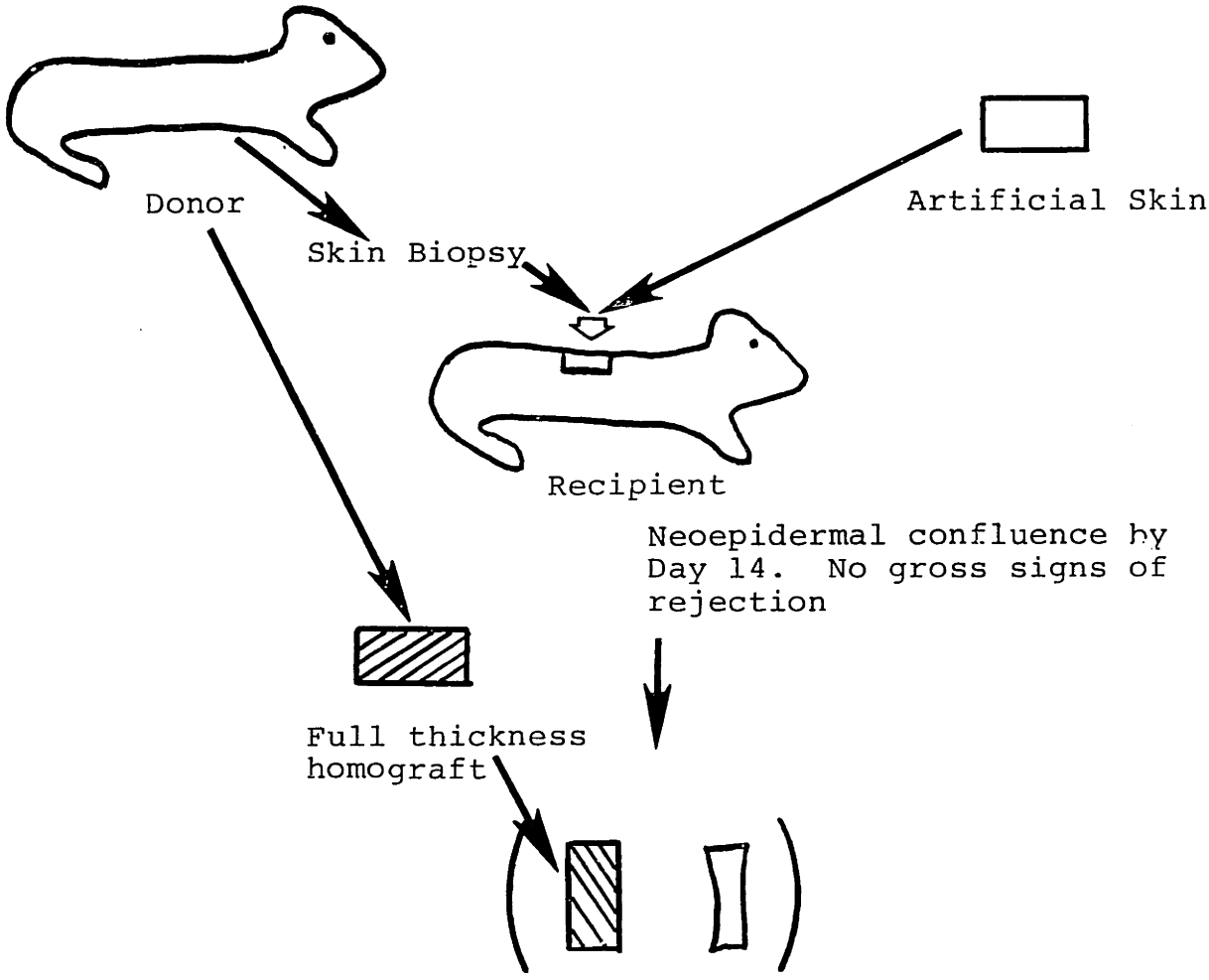

Recipient, Day 19

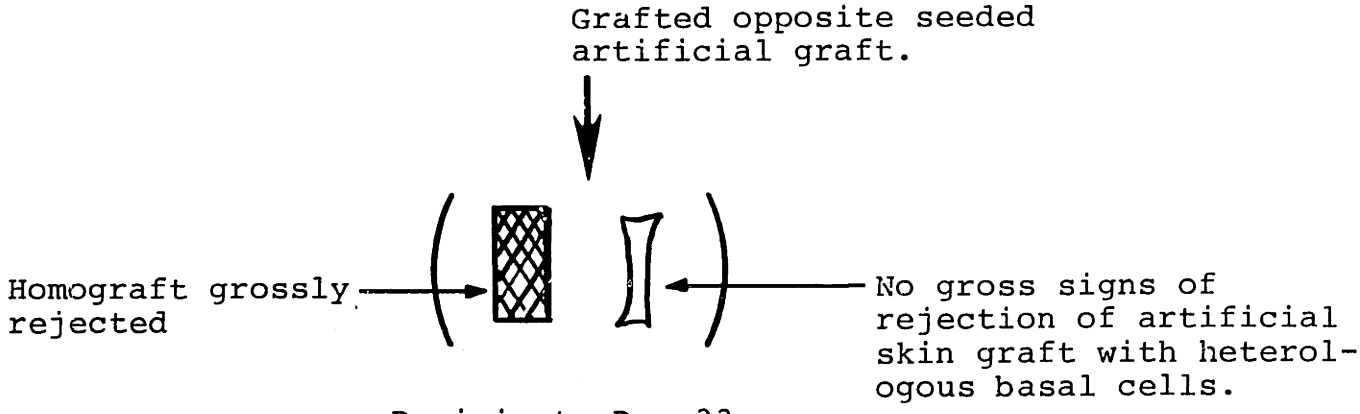

Recipient, Day 33

Figure 64

graft. These treatments included density sedimentation using Percoll (500 g for 30 min) or Ficoll-Hypaque (500 g for 20 min) gradients, cryopreservation of cells, and maintaining the cells in culture (see Materials and Methods). Using the above density gradients, it was possible to obtain an enrichment of basal cells in the pellet of gradient. This was easily demonstrated by the much greater incidence of epidermal colonies in cell culture from cells derived from the pellet compared to cells at other locations in the gradient.

Despite the many methods of cell preparation, none was shown to consistently produce grafts without evidence of rejection. Eleven of the grafts behaved similar to Stage 2 grafts and showed no gross evidence of rejection (Figure 62). Three of these animals were subsequently grafted with a homograft from the same animal that the heterologous cells were derived. In these cases, this homograft showed gross signs of rejection between 7 and 10 days after grafting (Figure 63,64). The rejection of the homograft showed the immunocopetence of the animal.

Most of the animals grafted with grafts seeded with heterologous cells showed gross clinical evidence of rejection. This usually occurred between day 12 and 14 and often followed the appearance of areas of neoepidermal confluence. The rejected seeded graft initially showed a serous exudate on top of the graft, and then appeared similar to a wound healing by secondary intent. If left

undisturbed, these grafts closed by contraction. All of the larger grafts (3 x 3 cm) showed gross evidence of rejection while about half of the 1.5 x 3.0 cm grafts showed evidence of rejection. Density gradient centrifugation, cell culturing, and cryopreservation of basal cells did not correlate with the acceptance of the seeded grafts.

Effects of Animal Treatments on Stage 2 Performance

Day Silicone Removed

The day on which the silicone was removed was a very important parameter in the use of Stage 2 grafts (Figure 65). Premature removal of the silicone was associated with infection and a lack of neoepidermal proliferation. In six Stage 2 grafts, the silicone was removed before day 9. All had delayed confluence of the neoepidermis and three developed wound infections. In contrast, if the silicone was left on after neoepidermal confluence occurred, a moist, whitish proteinaceous material accumulated between the silicone and the neoepidermis. This material was probably necrotic epidermal cells or wet keratin. It was felt that the space under the silicone would be a likely site for an infection to develop, and the silicone was promptly removed when this was observed. After the silicone was removed, the wounded area was observed to be moist. The moisture quickly evaporated leaving a dry smooth neoepidermal coverage. Over the next two to three days, the neoepidermis matured and flakes of dry keratin could be peeled from the wounded area.

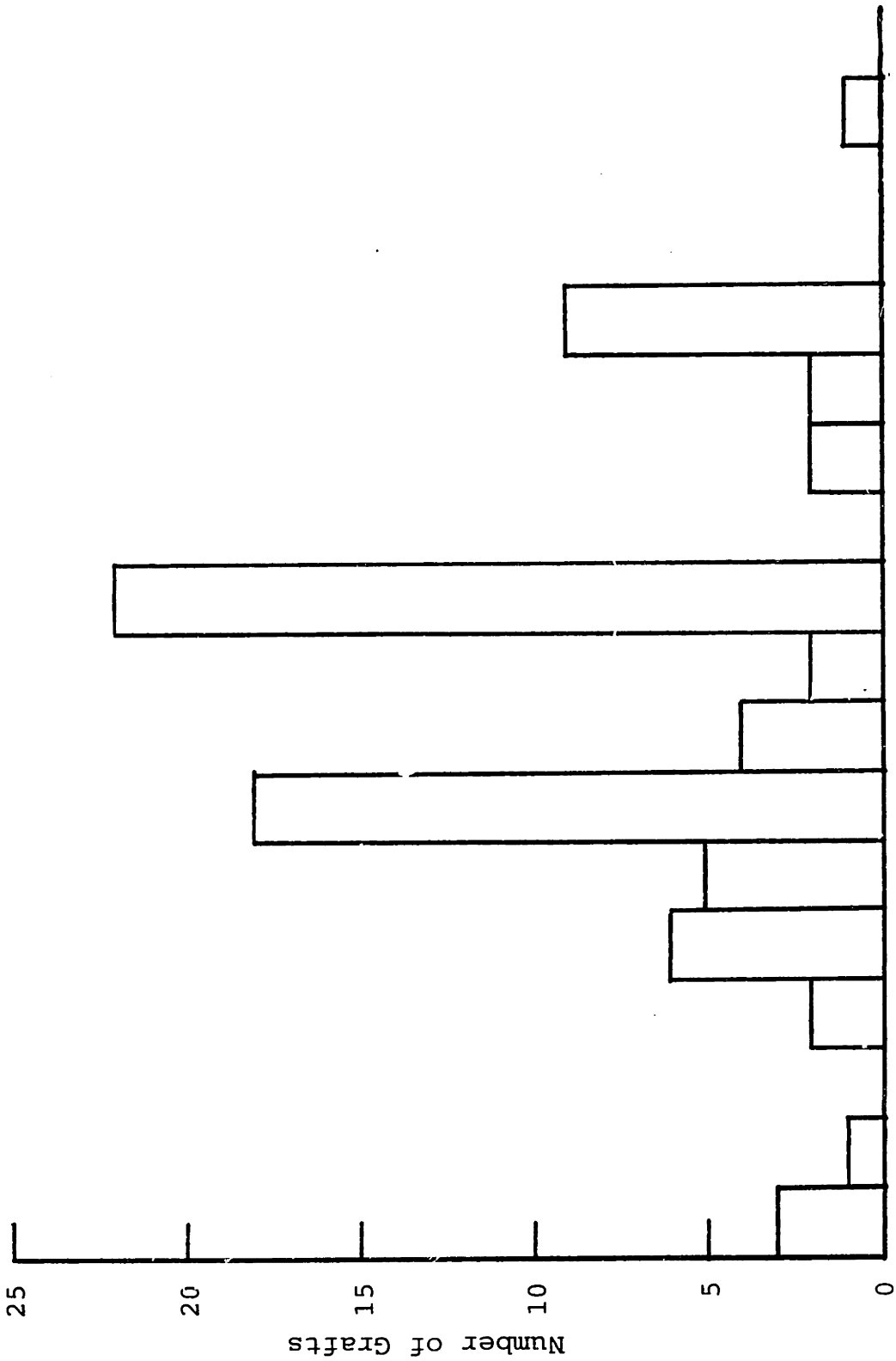

Figure 65. Histogram of the day at which the silicone layer was removed from Stage 2 grafts.

The most reliable indicator for readiness to remove the silicone layer was air spaces between the silicone and the collagen-GAG membrane. In many cases, a good portion of the silicone was lifted up off of the graft by day 11. Thus, when neoepidermal confluence had occurred, a close to zero peel force was required to remove the silicone from the wounded area. The neoepidermal and neodermal tissue was fragile early on, and was easily disrupted by the animals claws or surgical instruments. By keeping the animal in bandages until day 30 to 40, significant trauma to the grafted area was avoided.

Donor Sites

Donor sites (Figure 66) were treated with either a petroleum gauze or a cell free Stage 1 membrane. Both techniques had a low incidence of infection and allowed the wound to close by epidermal migration. Stage 1 membranes delayed the closure of donor sites compared with the petroleum gauze treatment. Figures 67 and 68 compared microscopically the appearance of matched donor sites on day 4. Epidermal cells arising from the hair follicles have closed the wound of the donor site treated with the petroleum gauze by day 4. In contrast, the lower part of the Stage 1 membrane has been vascularized, and the epidermal growth has been slowed. In this donor site, a biopsy at day 7 showed epidermal confluence at the donor site treated with the Stage 1 membrane. Long-term microscopic views of the donor site showed a thicker scarring zone for the petroleum gauze control compared with the site treated with Stage 1 (Figures 69 and 70). More detailed work in the future will be necessary to show that these results are significant.

The long-term donor sites appeared very similar to long-term Stage 2 grafts. Figure 71 shows a large donor site one year post grafting which has few hair follicles present and shows significant scarring. In one animal, a Stage 2 graft was placed juxtaposed to a donor site. Grossly it was impossible to distinguish a border between the donor site and Stage 2 graft after day 21 (Figure 72).

Figure 66. Donor site, day 0. This donor site was prepared using a 0.008" Goullian knife. At this level, many of the hair follicles have been removed. 75 X.

Figure 67. Donor site, day 4. This donor site was treated with a petroleum gauze. Epidermal cells from within the hair follicles have covered the wound with epidermis (E). 75 X.

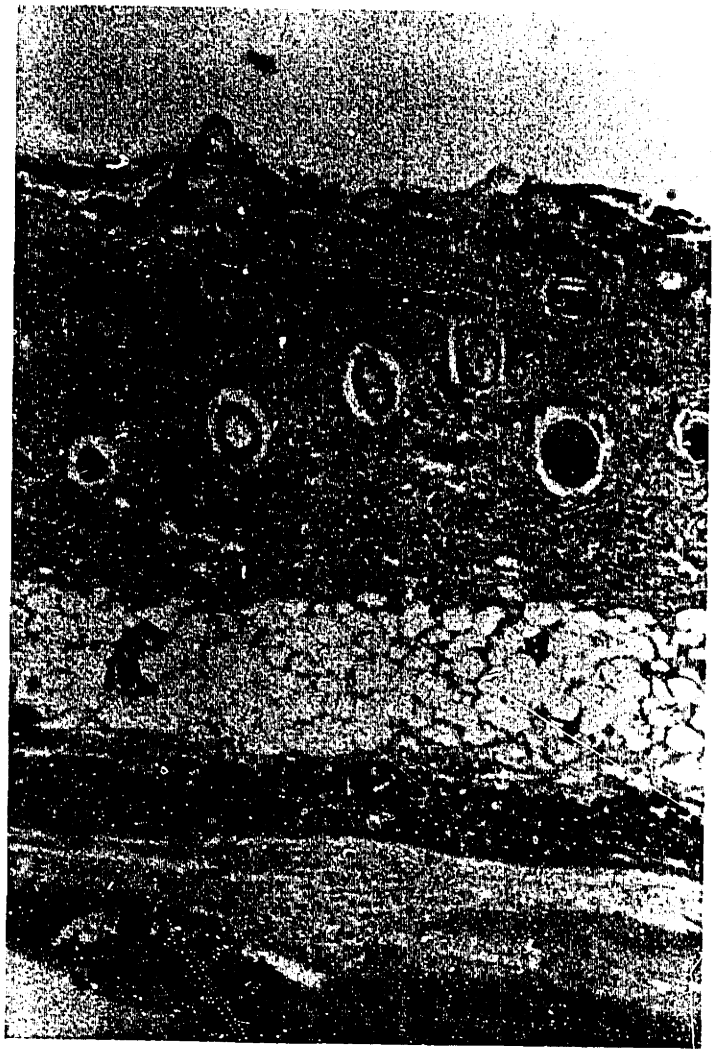

Figure 68. Donor site, day 4. This donor site was treated with a Stage 1 artificial skin. Epidermal coverage does not occur until day 7 to 10. 75 X.

Figure 69. Donor site, day 175. Originally treated with a petroleum gauze. The top third of the dermis shows a oriented collagen morphology characteristic of scar. 75 X.

Figure 70. Donor site, day 175. Treated originally with a Stage 1 artificial skin graft. Less scar tissue is seen in the upper part of the dermis than in Fig. 66, 75 X.

Figure 71. Long-term gross appearance of a donor site prepared with a Brown Electrodermatome (0.015"), day 348. Most of the hair follicles in this area have been lost. Animal No. 140-2.

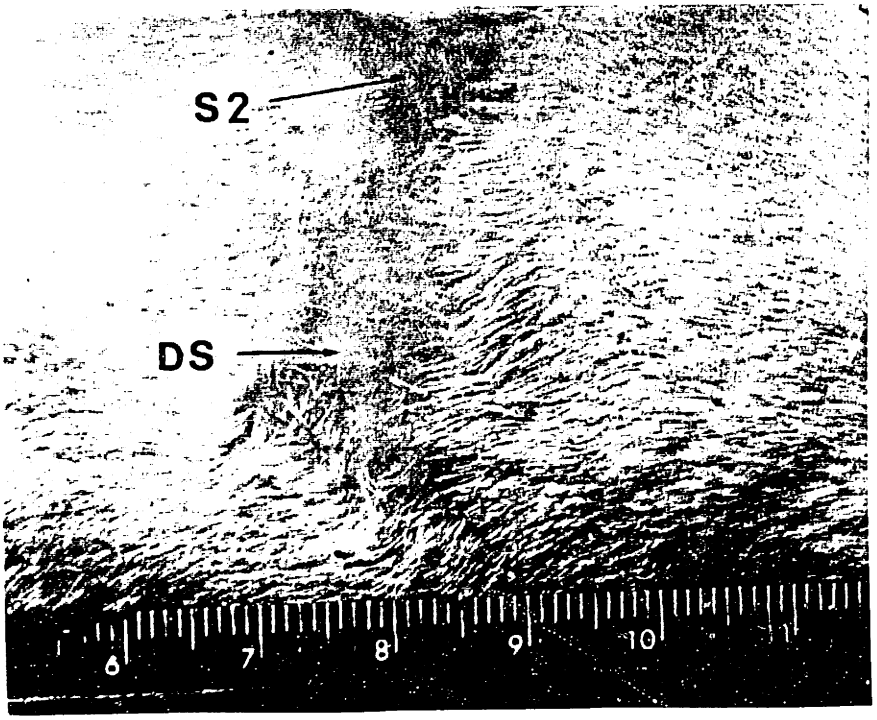

Figure 72. Long-term gross appearance of a Stage 2 graft (S2) juxtaposed to a donor site (DS). There is not a clear border between the areas, and they appear similar grossly. Animal No. 166-1R, day 152.

This result suggests a method to eliminate linear scars at edges of wounds.

Morbidity and Mortality of Animals Grafted

There were 144 Hartley Guinea Pigs which were grafted and reported in this thesis. They were divided into five groups: 1) ungrafted controls, 2) autograft controls, 3) Stage 1 membranes (cell free), 4) Stage 2 autologous cell, and 5) Stage 2 heterologous cell. Twenty five died throughout the course of the experiments, 15 within two weeks of grafting. Of these animals, the mortality rate was very dependent on graft size. Animals which received the largest grafts, 4 x 4 cm, had the highest mortality rate (46%). Animals with smaller grafts, 3 x 3 cm or 1.5 x 3 cm had a mortality rate of 6.8% during the first two weeks. The remainder of the animals died at various times throughout the experiment with no particular clustering. Since autopsies were not performed in most cases, the causes of the deaths were not proven. The chief cause of morbidity was wound infection. The infection rate for all of the animals grafted was 10.4%. Almost all of the infections were isolated into two groups of animals. The initial 18 animals grafted with Stage 2 membranes had a 50% infection rate. In these animals, it was found that removal of the silicone prior to the formation of a neo-epidermis was associated with a high incidence of infections. During these early studies, the bandaging techniques were also improved, which included the use of

Stage 2 Morbidity and Mortality

Time Period	Sep.- Dec. 1981	Jan.- April 1982	May- August 1982	Sept.- Dec. 1982	Jan.- April 82	Total
Stage 2 Autclogous	38	28	28	7	2	103
No. Infected	10	0	0	0	0	10
No. Deaths	10	5	3	3	1	22
Stage 2 Heterologous	4	7	14	2	1	28
No. Infected	2	0	2	1	1	6
No. Deaths	1	0	2	0	0	3

TABLE VI

sterile gauze and masks. The other group of animals with a high infection rate was the Stage 2 heterologous cell group (19%). Infections in these groups were often associated with an immunologic rejection of cells within the graft. Of the other 117 animals grafted, only two infections were observed (Table VI).

Analysis of Stage 2 Skin

Preliminary Mechanical Properties of Stage 2 Skin

Because of the small amount of Stage 2 skin generated, only a limited number of basic mechanical tests were made. Figure 73 shows representative stress-strain curves for the autograft, Stage 2, and normal skin. At low strains, the Stage 2 sample is stiffer than either the normal skin or autograft controls. The intact normal skin specimen has the highest tensile strength of 4700 p.s.i. and the longest elongation to break of 90%. In contrast, the Stage 2 and autograft samples shown here both have tensile strengths at breakage of about 1,000 to 2,000 p.s.i.

Figure 74 summarizes the tensile strength at breakage and the thickness data for the three Stage 2 and one autograft, each with its normal skin control. Normal skin is significantly stronger than Stage 2 skin samples taken 165 to 349 days post grafting ($p < 0.025$, t-test, two-tailed). Thickness measurements of normal skin, Stage 2, and autograft were within 10% of the respective normal skin control.

The positive second derivative associated with the stress-strain curve is a characteristic mechanical property

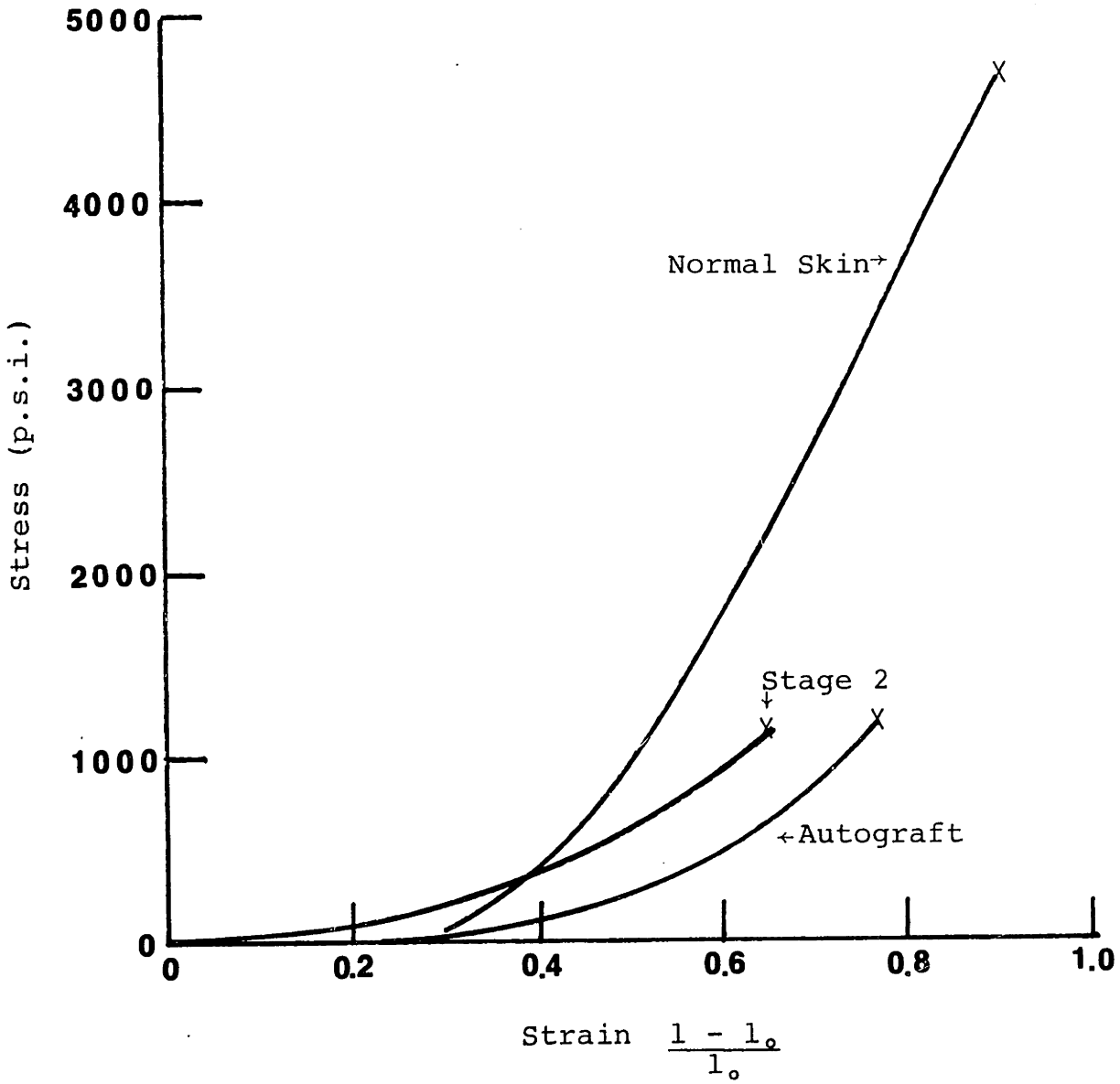

Figure 73. Representative stress-strain curves for normal guinea pig skin, Stage 2 skin and autograft.

MECHANICAL TEST RESULTS

Animal No.	Day Post Grafting	Ultimate Tensile Strength (p.s.i.) Normal Skin	Stage 2	Autograft
163-1	165	4400	1000	-
147-2	323	4600	-	1100
137-1	349	5700	2000	-
135-4	284	4400	2100	-
	Mean	4775	1690	
	Std. Dev.	620	630	

THICKNESS DATA

Animal No.	Day Post Grafting	Thickness (in.) Normal Skin	Stage 2	Autograft
163-1	165	0.060	0.062	-
147-2	323	0.063	-	0.060
137-1	349	0.047	0.047	-
135-4	284	0.040	0.036	-
	Mean	0.053	0.048	
	Std. Dev.	0.011	0.013	

Figure 74.

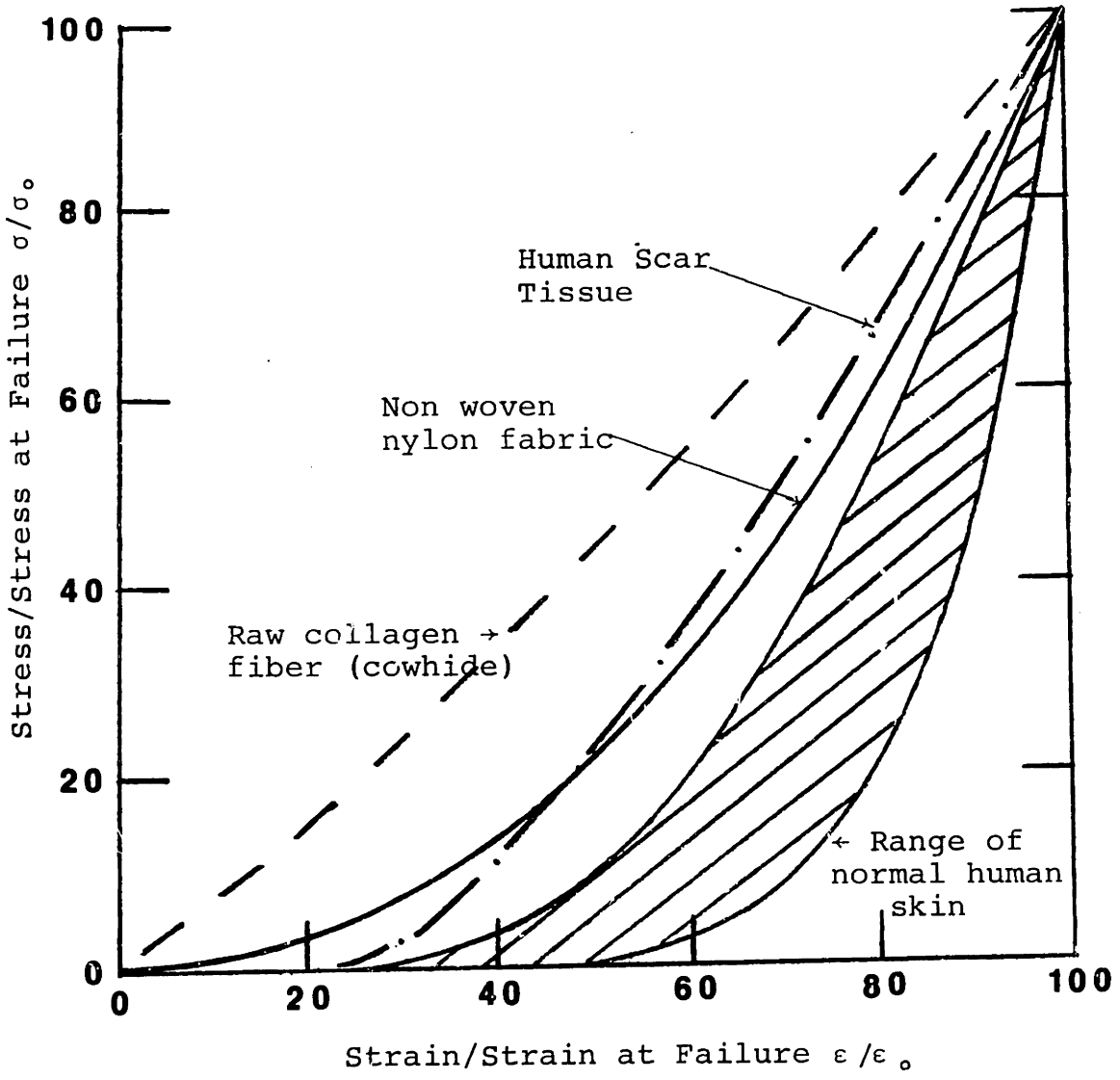

Figure 75. Normalized stress strain curves for human skin and other materials. Modified form Kenedi, R.M., Gibson, T., Daly, C.H.: Bio-Engineering Studies in the Human Skin II, in Biomechanics and Related Topics, Kenedi, R.M. (ed.), Pergamon, Oxford, 1965.

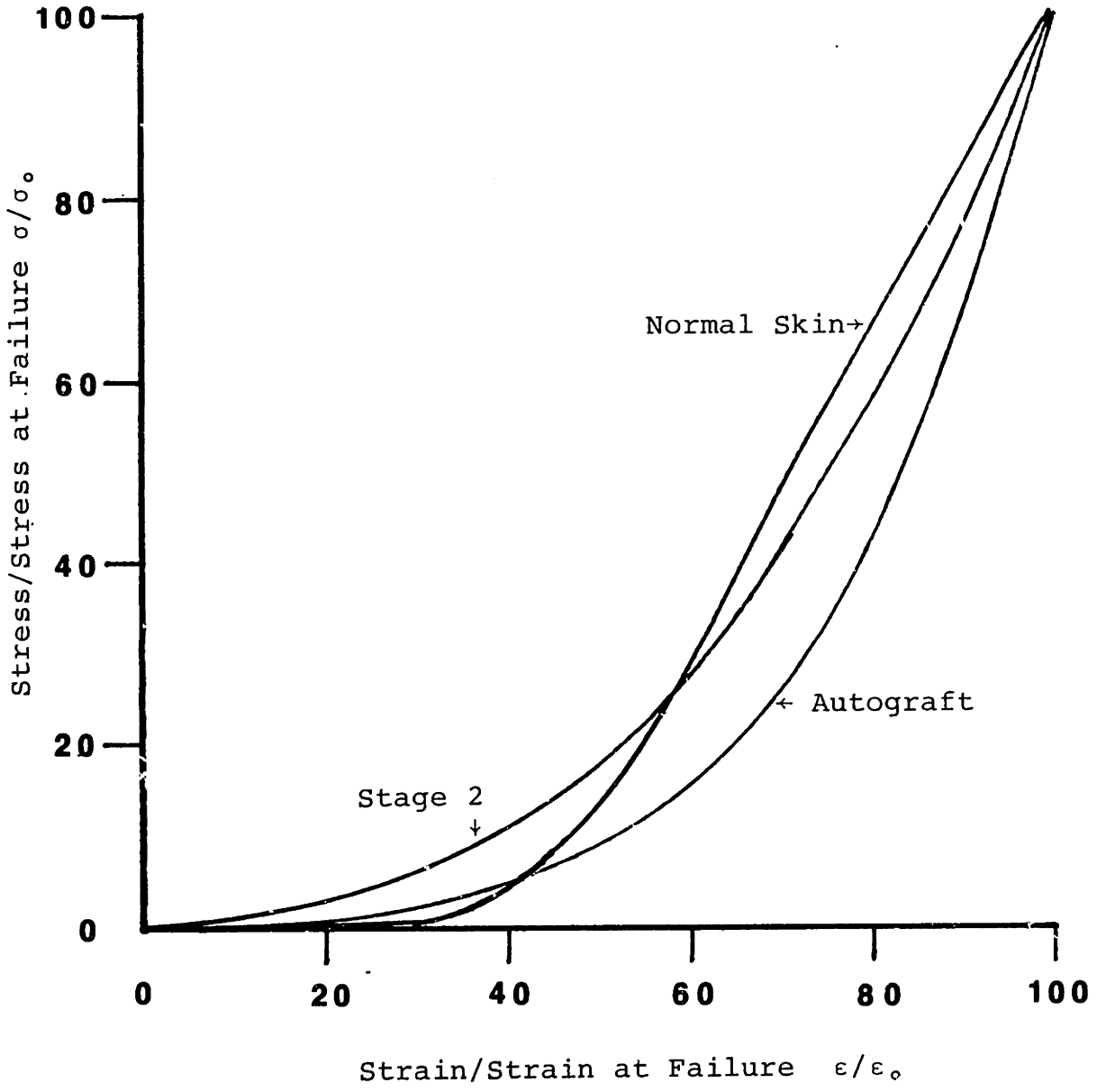

Figure 76. Normalized stress-strain curve for normal guinea pig skin, autograft, and Stage 2 skin.

of many biologic materials. Kenedi (10) states that various types of materials have characteristic upward sloping stress-strain curves (Figure 75). Shown in Figure 75 is a large area within the stress-strain curves of normal human skin fall. When the stress-strain curves for Stage 2, autograft and normal guinea pig skin are plotted in this form, most lie within the range for normal human skin (Figure 76). The exception to this is the Stage 2 sample which falls to the left of this area at low strains. Human scar tissue as reported by Kenedi (10) falls even further to the left of normal skin (Figure 75). The scars produced as a result of ungrafted wounds were not large enough to test mechanically using this method.

In Vivo Measurement of Skin Permeability

Measurements of permeability were made in vivo with Servo-Med Evaporimeter. Control values were measured over a section of normal skin on the opposite side of the back. Figure 77 displays the results of the evaporimetry measurements for various Stage 2 grafts. The Stage 2 measurements had a mean moisture flux of 4.5 $gm/m^2/hr$ compared to a control value of 4.7 $gm/m^2/hr$. The differences between the Stage 2 and control areas was not significant ($p > 0.5$, t-test, two-tailed). One 22 day Stage 2 graft had a water flux much greater than the control value (31.7 $gm/m^2/hr$), but within the physiologic range reported by Scheuplein and Blank (95).

Stage 2 Evaporimetry Results

Long-Term

Animal No.	Days Post Grafting	Water Flux Stage 2	Water Flux Normal Skin
135-4	273	3.3 gm/m^2/hr	3.2 gm/m^2/hr
135-8	272	5.2	3.0
137-1	245	4.8	6.9
140-2	244	4.6	5.5
	Mean	4.5	4.7
	Std. Dev.	0.8	1.9

Other Evaporimetry Results

Animal No.	Days Post Grafting	Type of Graft	Water Flux	Water Flux Normal Skin
147-1	140	Autograft	3.0 gm/m^2/hr	3.2 gm/m^2/hr
139-1	244	Stage 1	3.0	3.3
153-1	51	Stage 2	9.3	4.1
153-2	51	Stage 2	3.1	3.1
156-1	22	Stage 2	31.7	7.7

Figure 77. *In vivo* evaporimetry results.

Histology

Ungrafted Controls

Histology sections were prepared from long-term ungrafted full-thickness wounds. At day 200, there was a small area of linear scar which was composed mostly of fine compact collagen and fibroblasts. Capillaries observed within the scar tissue were more prevalent and perpendicular to the epidermis than in adjacent normal skin. Examination of the scar tissue under polarized light revealed increased birefringence indicating further maturation of the collagen fibers between 200 and 323 days. The direction of the collagen fibers in the mature scar seemed to be oriented parallel to the primary axis of contraction (Figures 78-81). The long-term specimens showed no significant inflammation or foreign bodies.

Autograft Controls

Histology specimens were prepared from long-term full-thickness autografts. Masson's trichrome stained sections (Figures 82,83), clearly demarcated where the autograft was originally placed. This demarcation was characterized by scar tissue which was similar to that seen in the ungrafted controls. The close packed collagen morphology seen in the area separating the normal skin from the autograft was also seen at the wound base and in the epidermal portion of the dermis of the autograft (Figures 84,85). In the center of the autograft, the collagen morphology appears similar to that of normal skin. The number of hair follicles present

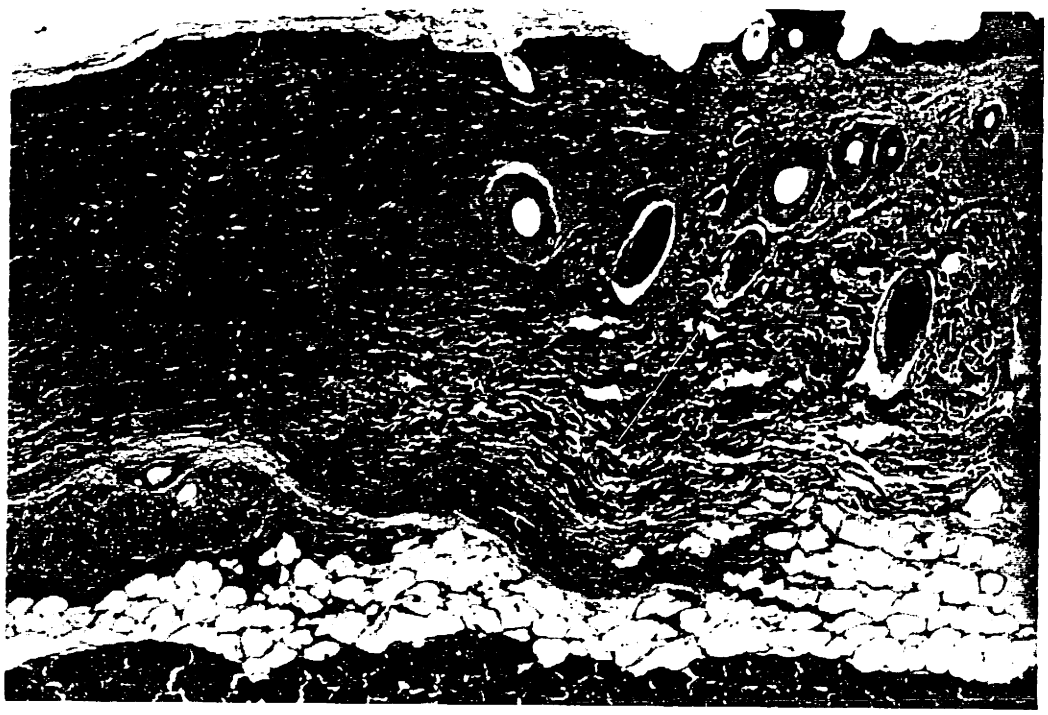

Figure 78. 200 day histology specimen of ungrafted 1.5 x 3 cm wound at the junction between scar (S) and normal dermis (D). Hematoxylin and eosin, 75 X. Animal No. 144-2.

Figure 79. View of above specimen through polarizing filters oriented at 90°. This shows the collagen fiber morphology of scar to be thin and oriented parallel to the epidermis as opposed to that of normal dermis which is thicker and wavey.

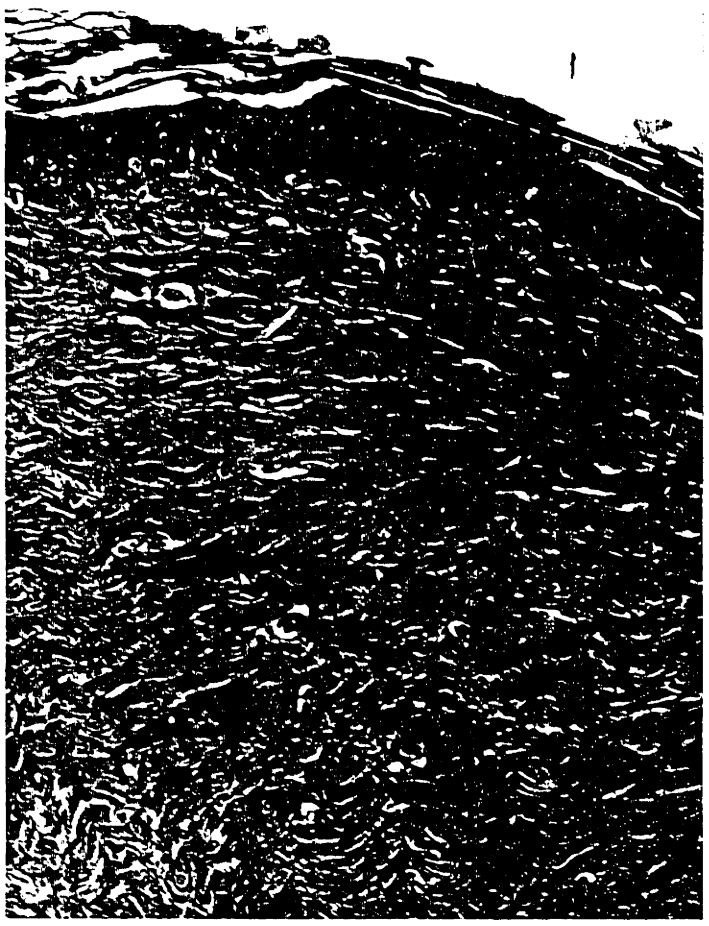

Figure 80. 323 day histology of scar generated from an ungrafted 1.5 x 3.0 cm wound. Hematoxylin and eosin, 300 X. Animal No. 144-3

Figure 81. Birefringent view of scar specimen seen in Figure 80. Note orientation of collagen fibers.

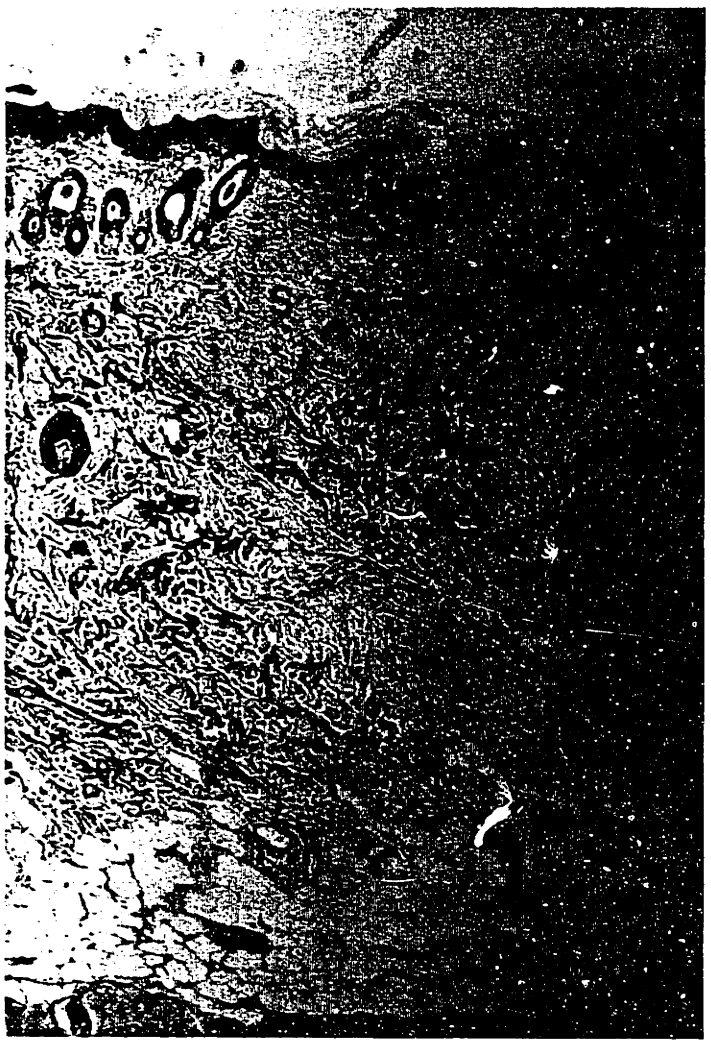

Figure 82. 200 day histology specimen of a 1.5 x 3 cm autograft (A) at the junction with normal dermis (D). Note the scar (S) at the junction. Masson's trichrome, 75 X. Animal No. 147-4

Figure 83. Birefringent view of autograft demonstrating the collagen morphology in normal dermis (D), autograft (A) and junction (S).

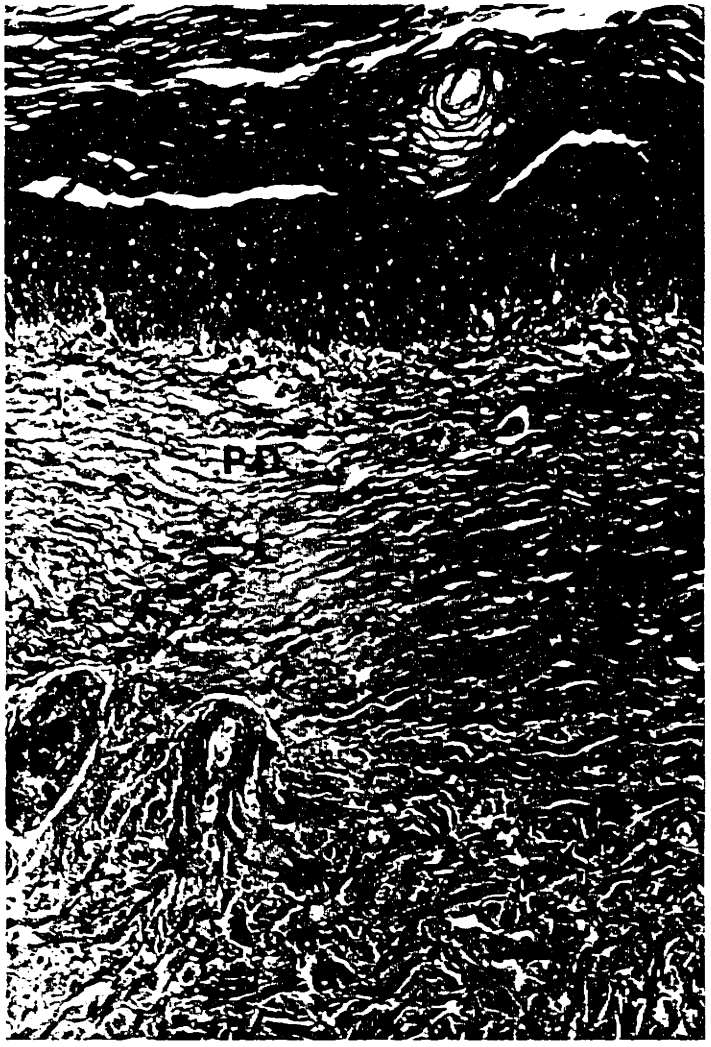

Figure 84. High power view (300 X) of epidermis and papillary dermis (PD). Note loss of hair follicles in this autograft. Hematoxylin and eosin. Animal No. 147-3, day 323.

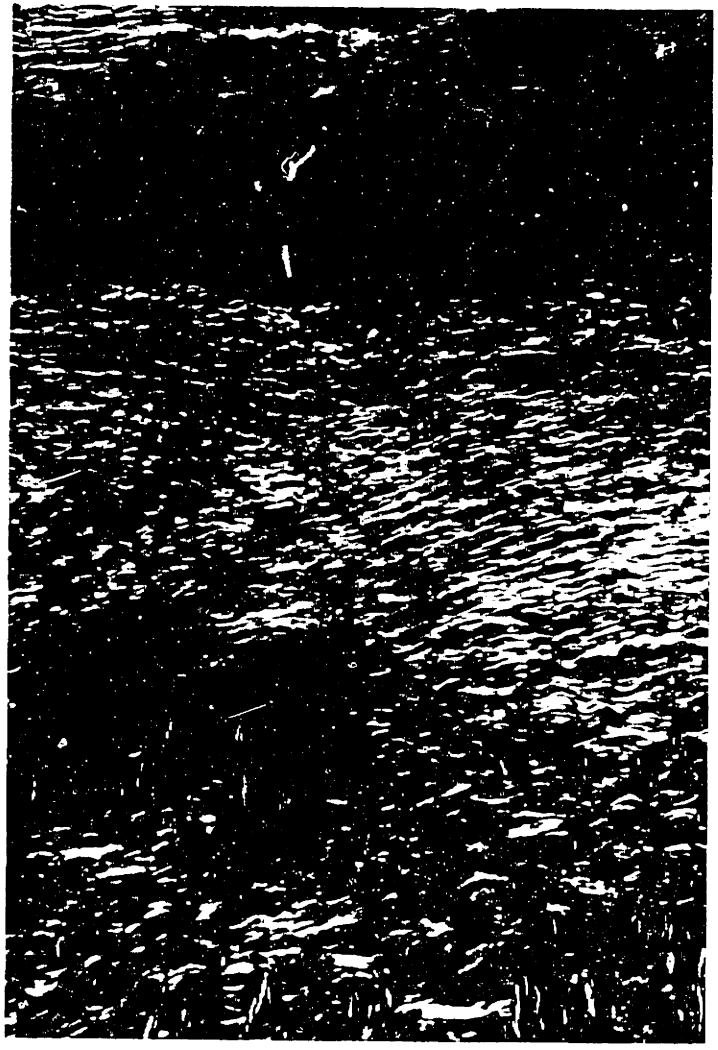

Figure 85. Birefringent view of autograft showing finer and more oriented collagen fibers in the papillary dermis.

in the autograft was variable, but was in general about an order of magnitude less than those seen in the adjacent normal skin. There was some evidence of contraction at the base of the autograft, where the normal skin had moved centripitally. The long-term specimens had no significant inflammation or foreigh bodies.

Stage 1 Controls

The results of early Stage 1 histology have been described in detail (51-57). Histology specimens from long-term Stage 1 implants were utilized as controls for the Stage 2 work. These specimens appeared very similar to the ungrafted controls in that the wounds had contracted and there was no inflammation, adenexa or foreign bodies. The collagen fiber morphology, however, appeared more wavy and less compact than in the ungrafted controls (Figures 86,87). This was particularly evident when viewed with polarized light or fluorescent microscopy. The collagen bundle orientation is primarily coincident with the direction of contraction and lines of stress.

Stage 2 Grafts

Within the first four days of application, Stage 2 grafts appeared similar to Stage 1 grafts. This included a polymorphonuclear leukocyte infiltration in the first 24 hours ascribed to the trauma of surgery. By day 4, the grafts were well attached at the base and were being invaded by mesenchymal cells from the woundbed. Red blood cells and a small number of inflammatory cells

Figure 86. 200 day histology of a Stage 1 graft juxtaposed to normal skin (D). Hematoxylin and eosin, 75 X, Animal No. 145-4.

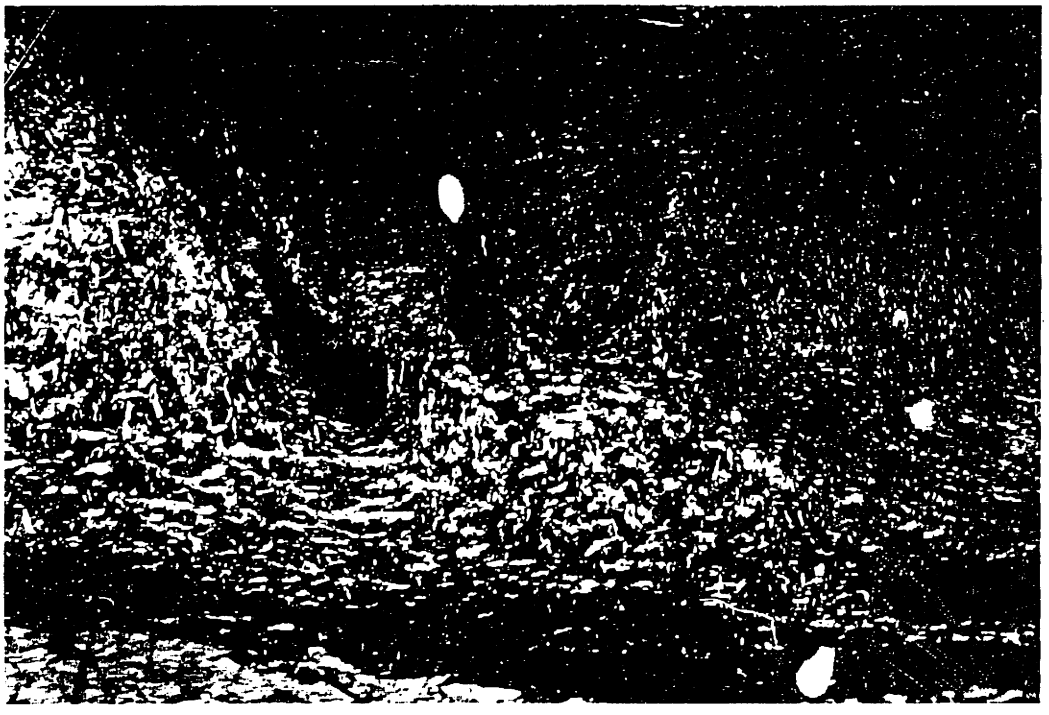

Figure 87. Birefringent view of the above specimen. Note that the collagen fiber morphology within the grafted area is more random than that seen in ungrafted controls (Figure 79).

including polys, lymphocytes, and monocytes were also present. By day 7, the grafts were very cellular with a predominance of mesenchymal cells as well as a mixture of inflammatory cells. The grafts at this point were hypervascular being filled with a rich bed of capillaries which appeared similar to that seen in early granulation tissue. The collagen-GAG matrix was starting to degrade at this point. As mentioned previously, the Stage 2 grafts had a more cellular infiltrate on day 7 than was typically seen with Stage 1 grafts (Figures 53,54). On day 7, some epithelial islands could be seen within the graft. These consisted of several epidermal cells clustered together. Some of these were just beginning to form keratin at the center of the islands (Figure 54).

By day 9-14, the epidermal cells near the silicone membrane had divided and formed a confluent layer of cells across the top of the graft separating the silicone from the underlying vascularized graft. Mature keratin seemed to be formed two to three days after the silicone was removed. The epidermal islands which formed deep in the graft divided to form clusters of cells some with a central core of keratin pearls. These keratin pearls have routinely been observed in the histologic sections and seem to rise to the top of the graft between the 14th and 28th post operative day (Figures 88,89). In no case were epidermal cysts observed in any of the histologic specimens. The collagen-GAG material was progressively degraded, and it

Figure 88. Day 22 histology of Stage 2 graft showing a vascularized neodermis (ND), a confluent neoepidermis, and a keratin pearl emerging from the neodermis into the neoepidermis. Animal No. 135-1, 150 X, hematoxylin and eosin.

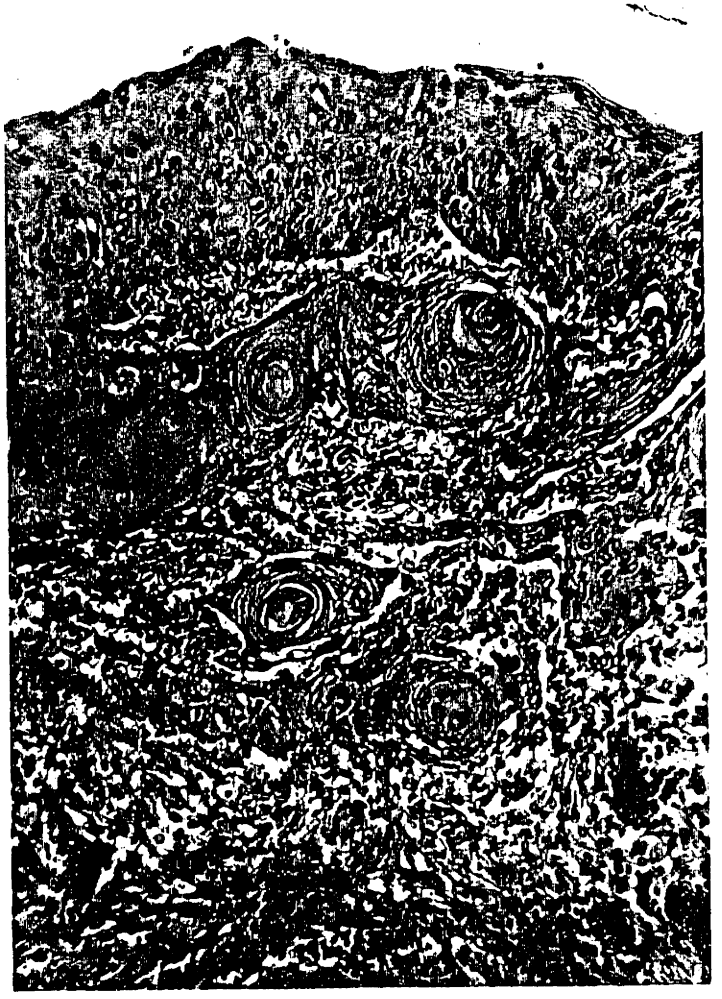

Figure 89. Day 18 histology of a seeded graft showing a confluent neoepidermis and numerous keratin pearls. Animal No. 142-3, 150 X, hematoxylin and eosin.

appeared that about half of it was degraded by day 14 to 21. As the graft matured, the inflammatory infiltrate decreased and became more chronic in nature. Multinucleated giant cells were observed as early as day 7, and were usually found around the collagen-GAG matrix or a foreign body such as a hair within the graft. The multinucleated giant cells seemed to reach a maximum at around 21 days, although they were present in some long-term animals where foreign bodies were present.

After three to four weeks, the cellularity and vascularity of the grafts began to decrease. It was possible to monitor the production and maturation of collagen because of its birefringent characteristics when examined under polarized light and its autofluorescence in stained sections when examined with the fluorescent microscope. Collagen synthesis began to take place, but this occurred slowly within the dermis. By day 84 (Figures 90,91), there was a maturing neodermis securely attached to the neoepidermis; however, the collagen in the neodermis was only slightly birefringent under polarized light. By 200 days, the collagen in the graft had matured significantly and was moderatley birefringent. Further maturation occurred between 200 and 500 days (Figures 92,93).

The collagen morphology of the long-term Stage 2 grafts was less compact and less oriented than the ungrafted controls. This was particularly evident when viewed under polarized light or with fluorescent

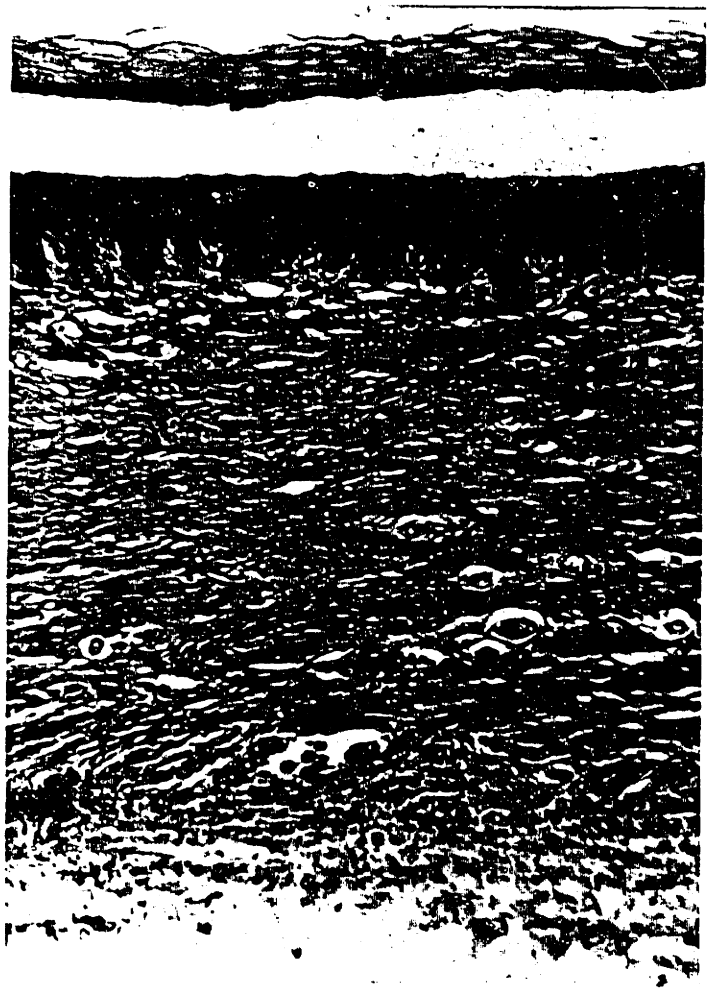

Figure 90. Day 84 histology showing a maturing neodermis and an irregular neodermal-neoepidermal junction. Animal No. 142-1, 150 X, hematoxylin and eosin.

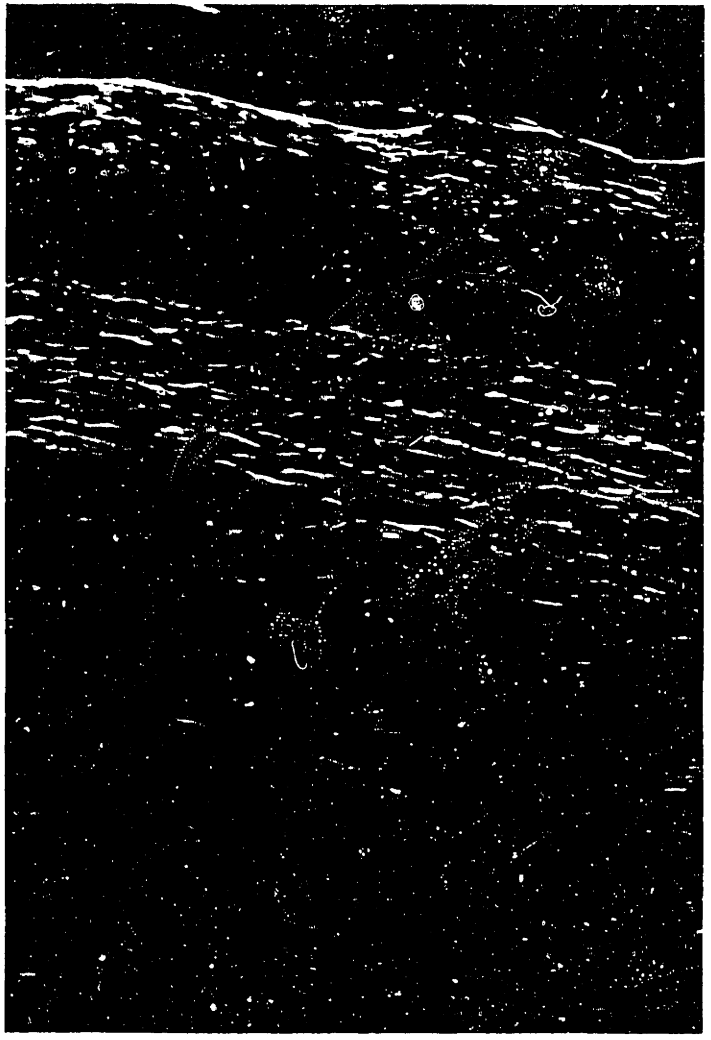

Figure 91. Higher power (300 X) view of day 84 Stage 2 histology. Very little of the graft at this point is birefringent.

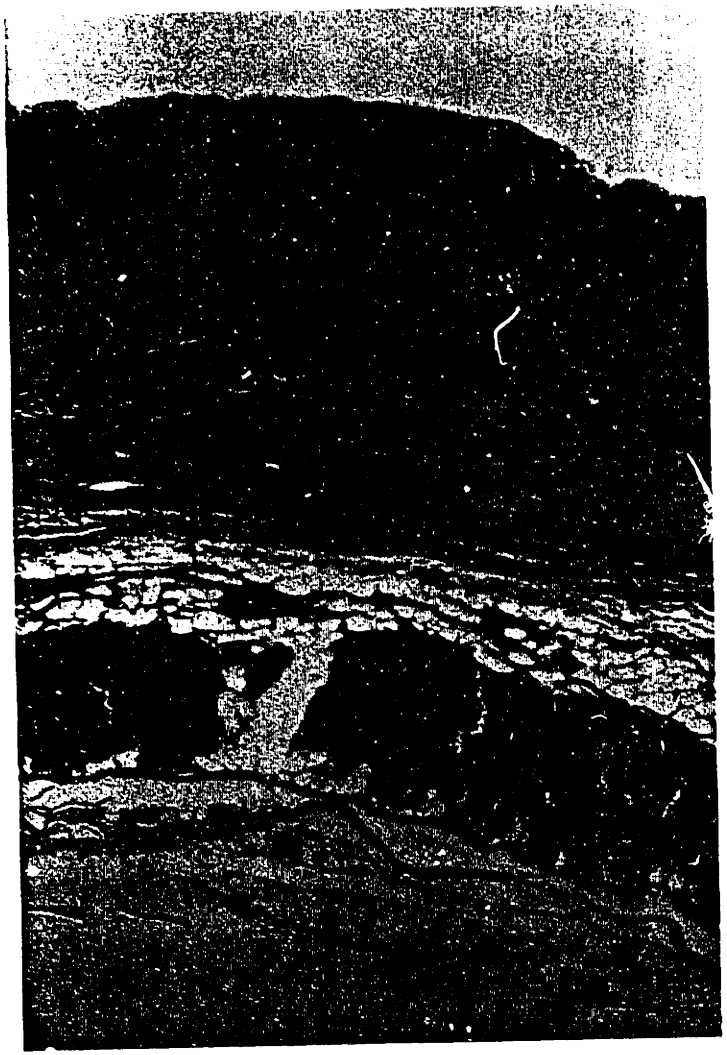

Figure 92. Long-term Stage 2 histology, 483 days. The neodermis is comparable in thickness to the normal dermis. Animal No. 140-2, hematoxylin and eosin, 75 X.

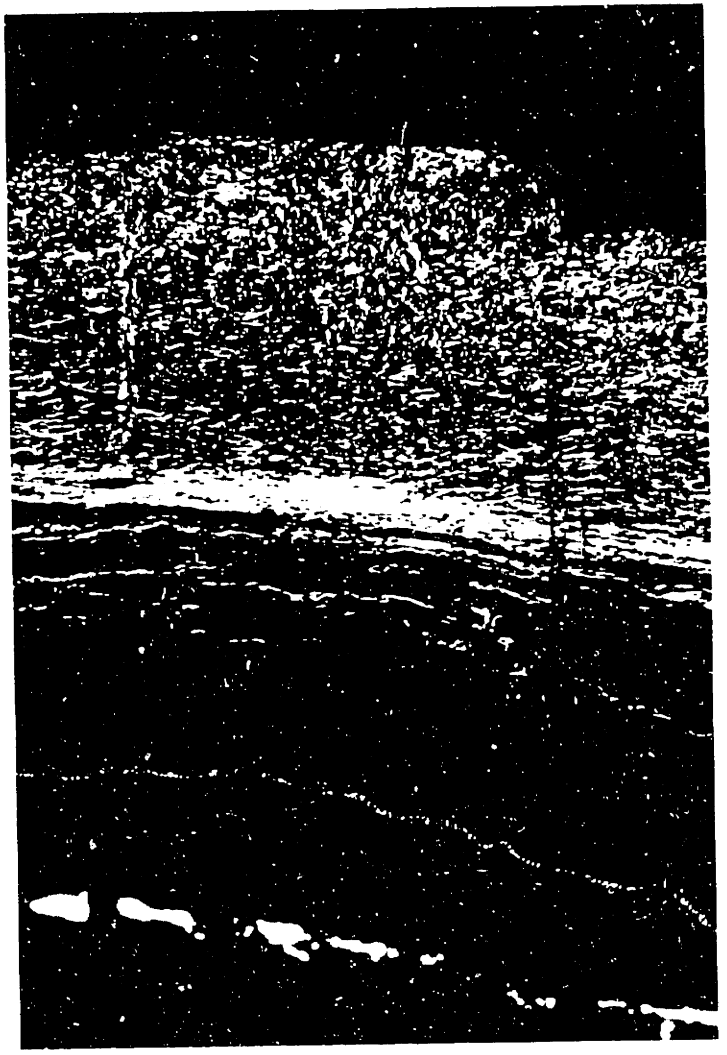

Figure 93. Birefringent view of long-term Stage 2 histology. Note morpholgy of collagen fibers. A dense oriented layer is seen just above the panniculus suggesting some scarring.

Figure 94. Long-term Stage 2 histology, 483 days. Animal No. 140-2, hematoxylin and eosin, 300 X.

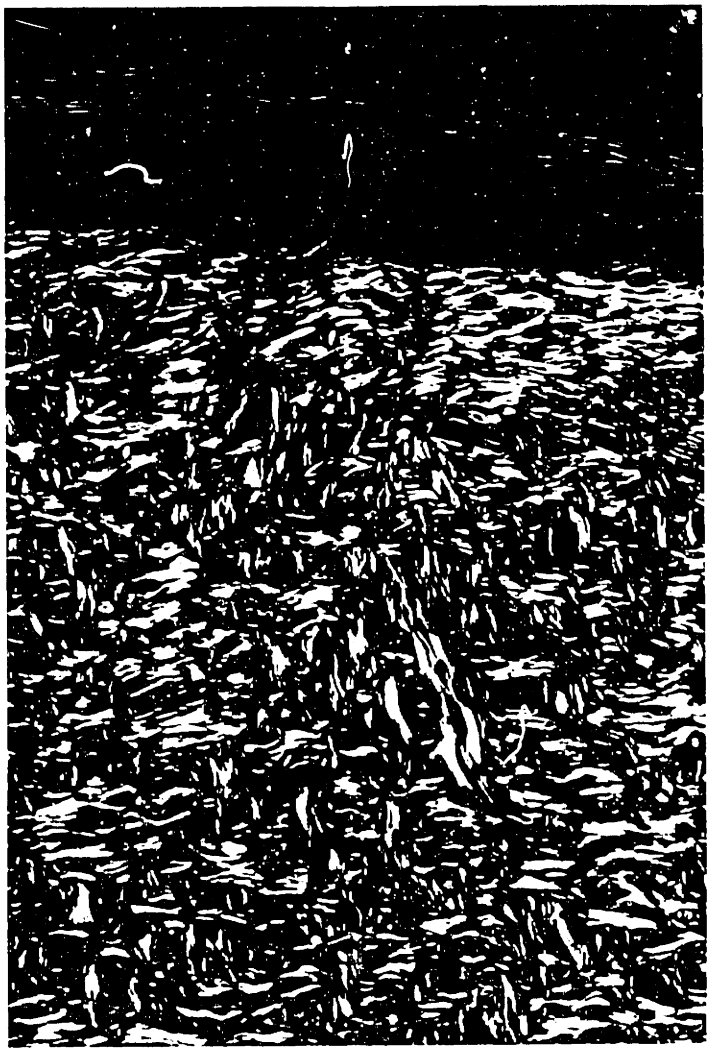

Figure 95. Birefringent view of long-term, Stage 2 histology. Note morphology of collagen fibers and compare with Figures 81, 85, and 96.

microscopy. However, the collagen fibers were more oriented and lacked the interlacing character of collagen fibers found in normal skin (Figure 96). Quantitative stereological measurements of the collagen fiber morphology were not made at this point; therefore, it was difficult to quantitate these differences.

Hair follicles were observed in many of the long-term samples. The origin of these follicles was not clear as serial histologic sections were not taken. Many of these hair follicles occurred in the center of the wounded area suggesting that they may not have originated from hair follicles at the border. These hair follicles and associated sebaceous glands appeared smaller and less well developed than normal hair follicles (Figure 97). These hair follicles could have originated from invagination of the neoepidermis, from the seeded cellular suspension, or because of artifacts from the surgery. The exact origin of these hair follicles will require further investigation.

Some of the collagen-GAG used in some of the later experiments appeared more coarse and was more basophilic when stained with hemotoxylen and eosin than that typically observed (Figure 96a). This material appeared to require longer times to biodegrade and provoked a greater influx of multinucleated giant cells. It is probable that either the collagen used or the manufacturing procedure followed in making these membranes was altered. In long-term animals both types of material gave similar results except for the

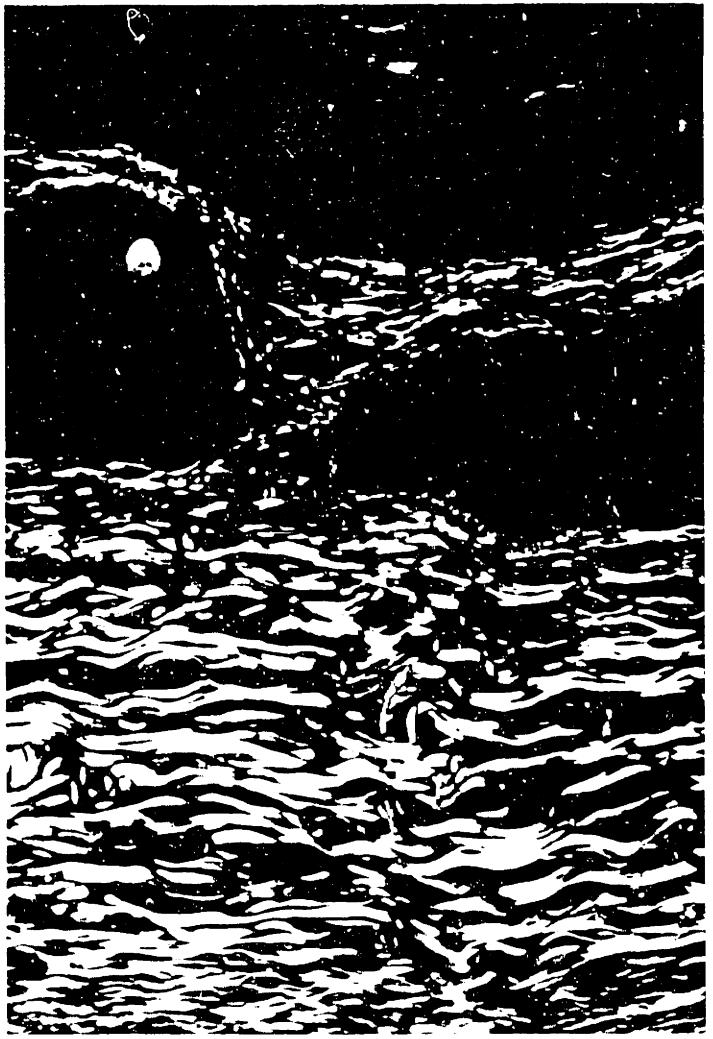

Figure 96. Birefringent view of normal skin. Animal No. 142-4, 300 X, hematoxylin and eosin. Note large collagen bundles which are wavey and interlace. Compare with Figures 81, 85, and 95.

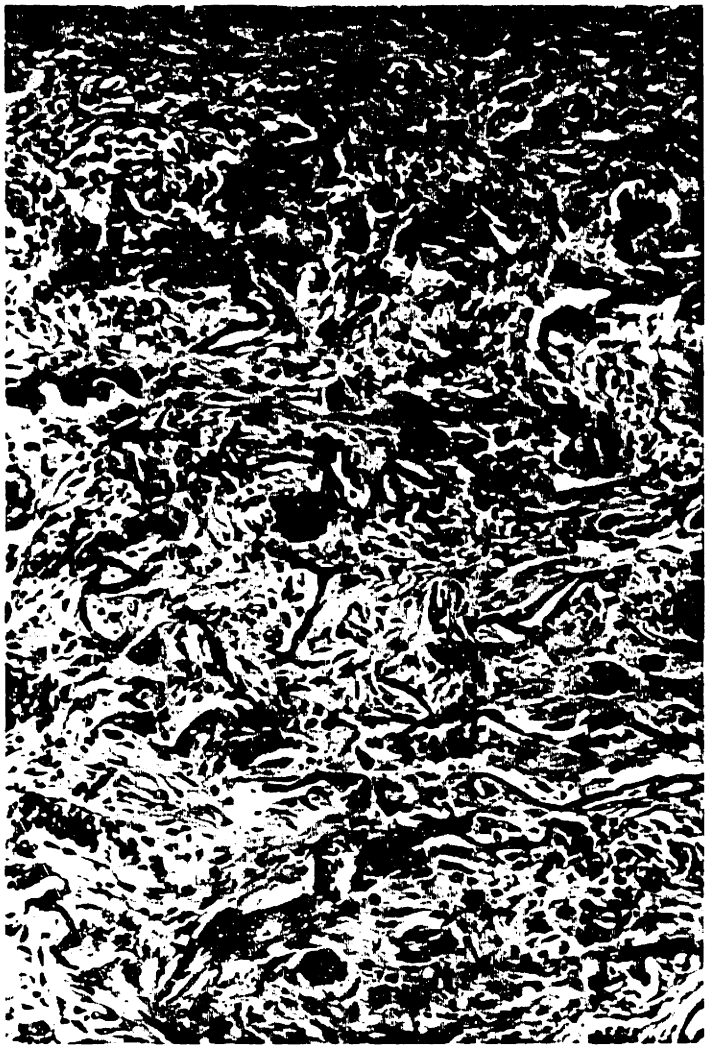

Figure 96a. Coarse collagen-GAG material seen in some of the grafts. This basophillic material was associated with multinucleated giant cells. Animal No. 166-3, Day 21, 300 X, hematoxylin and eosin.

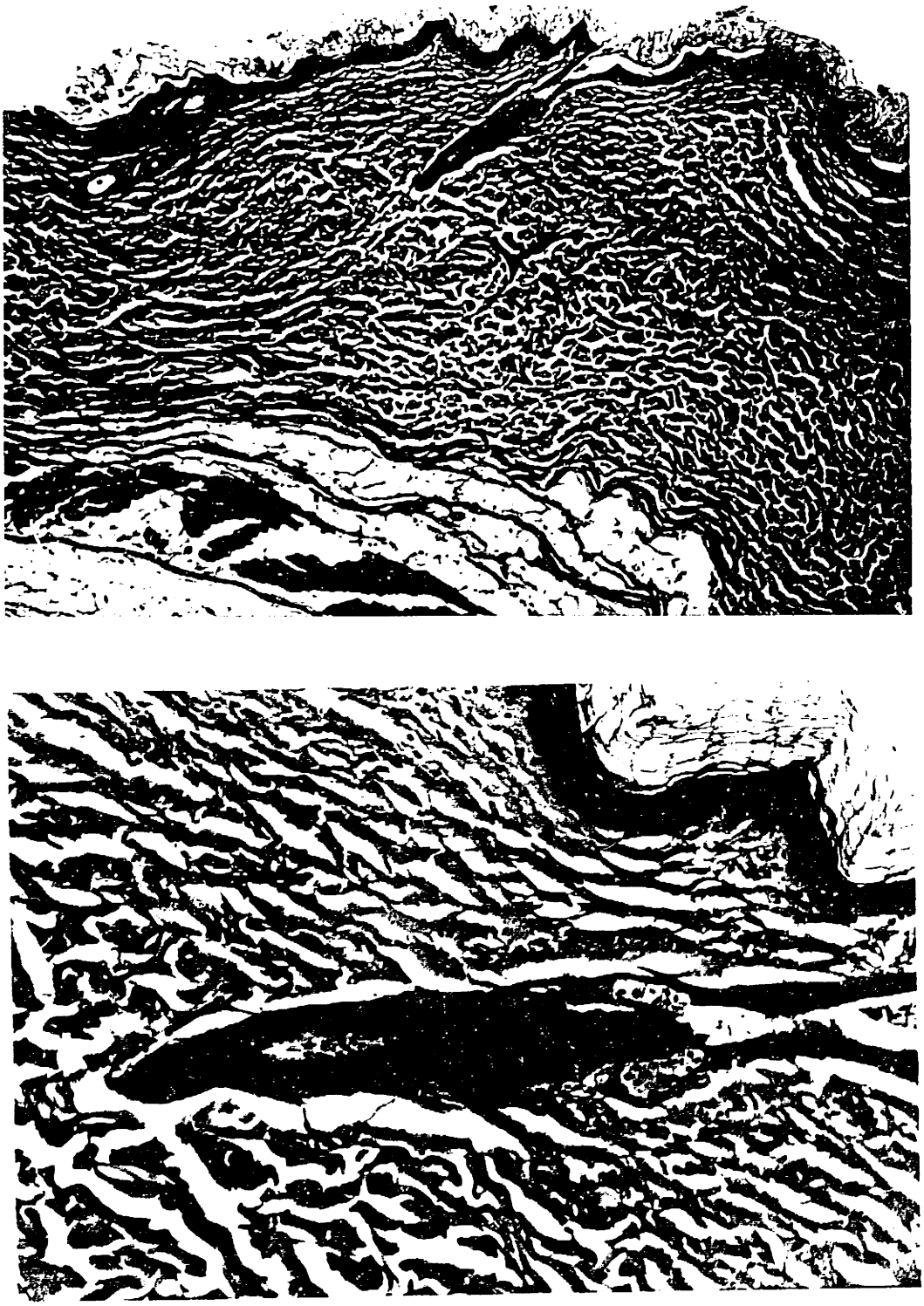

Figure 97. Low (75 X) and high (300 X) power view of a hair follicle in the center of a stage 2 graft. Sebaceous glands can also be seen in the low power view.

presence of more foreign bodies in the later material.

Special Stains

Several of the specimens were stained with special stains to define different aspects of microscopic anatomy. Masson's Trichrome stain proved to be useful in defining the collagen fiber morphology of the various grafts. With this stain, the junction between the autograft and normal dermis was clearly demarcated. It also provided a method to distinguish between the artificial skin grafts and normal skin early on due to color changes.

Bodian and Bieilkowsky stains were used to define nervous tissue in the long-term Stage 2 grafts. In the few samples stained, nervous tissue was not visualized within the graft or in normal dermis. Further work with these stains will be required to better understand the innervation of the artificial skin grafts.

Vorheoff's elastin stain was used on long-term samples of scar, normal dermis, and Stage 2 neodermis. This stained the collagen fibers a dark red, and elastin black. Elastin was found in all of these tissues, but in scar tissue fibers were very fine and closely associated with the collagen fibers. Most of the elastin seen in the dermis of normal skin and Stage 2 skin was seen in the papillary dermis. The elastin fibers in normal dermis were larger and more randomly oriented than those seen in Stage 2 neodermis (Figures 98 to 101).

Figure 98. Papillary dermis of normal skin stained with Verhoeff's elastin stain, 1200 X. Elastin fibers are stained black (ef). Epidermis (E). Animal No. 153-2, day 290.

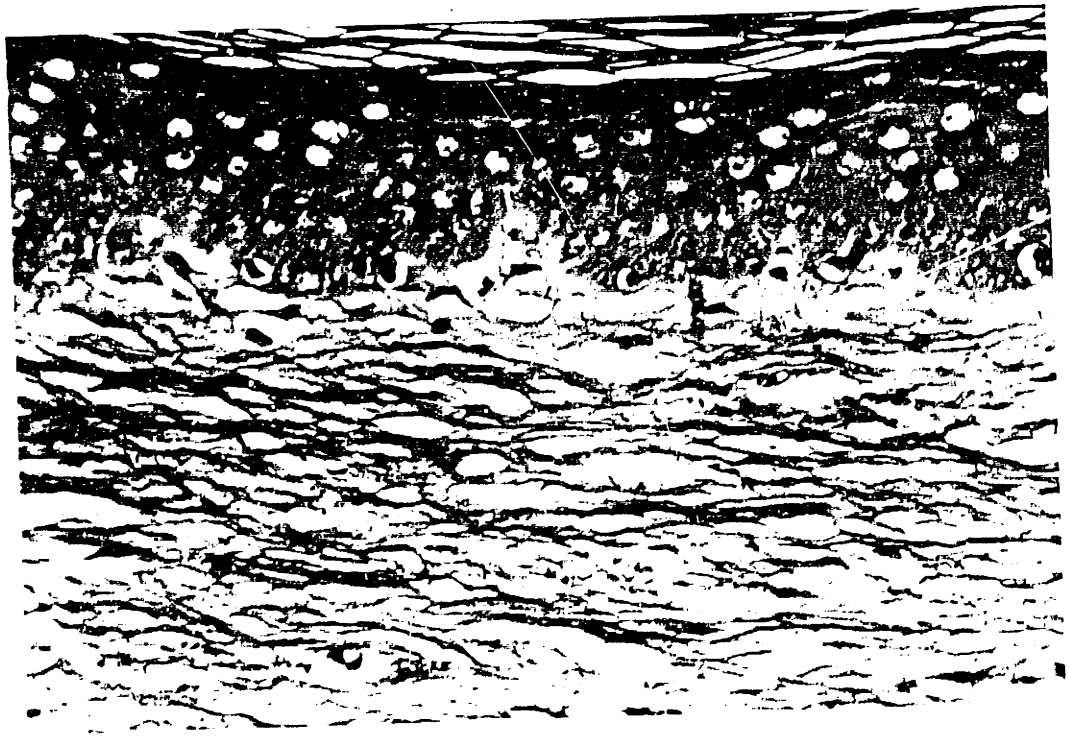

Figure 99. Epidermis and scar tissue stained with Verhoeff's elastin stain, 1200 X. Elastin fibers are thin and run in close contact with the collagen. Animal No. 144-1, day 379.

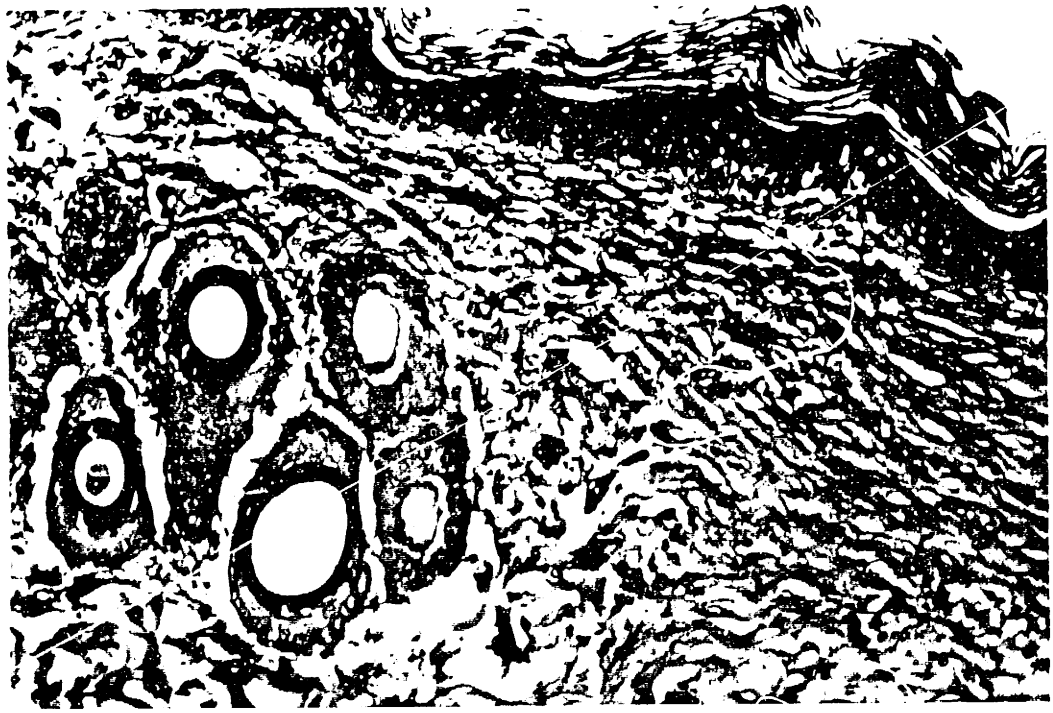

Figure 100. Junction of Stage 2 with normal skin stained with Verhoeff's elastin stain. Animal No. 153-2, day 290 300 X.

Figure 101. Stage 2 skin stained with Verhoeff's elastin stain. Elastin is stained black. Compare with Figures 98 and 99. Animal No. 153-2, day 290, 1200 X.

Frozen Cells

Grafts seeded with cryopreserved cells were not significantly different in histologic appearance than standard Stage 2 grafts.

Grafts Seeded with Hair Follicles

One Stage 2 graft seeded with hair follicles and held long-term. Although there were a few hairs present in the neodermis, the number and morphology of the hairs present was not different than many Stage 2 grafts not seeded with hair follicles. The histologic appearance of this long-term graft was similar to other long-term Stage 2 animals.

Heterologous Cells

Grafts seeded with heterologous cells appeared similar to grafts seeded with autologous cells during the first week. Over the next two weeks some of the grafts achieved clinical neoepidermal confluence and remained closed until sacrificed. Most of the grafts, however, showed some clinical evidence of rejection and were sacrificed between day 10 and 21. The first evidence of rejection was an increase amount of vascularity in the epidermal region beginning about day 10. This was followed by necrosis of the neoepidermis and surrounding tissue and an influx of round cells consisting primarily of lymphocytes. Evidence of necrosis and a round cell infiltrate was typically observed between day 10 and 21. Keratin pearls proved to be a valuable marker for assessing the antigenicity of the neoepidermal tissue. In grafts where the neoepidermis was

being rejected, the keratin perals appeared necrotic and were surrounded by round cells (Figure 102). In contrast, other grafts showed keratin pearls which were viable and did not have a round cell infiltrate (Figure 103). Since keratin pearls have not been observed in cell-free Stage 1 artificial skin grafts, they provided an unambigous marker for neoepidermal tissue. There were few correlations between the heterologous cell separation techniques and the results of the histology. The only grafts which achieved neoepidermal confluence without histologic evidence of rejection were 1.5 x 3.0 cm grafts. The larger grafts, 3.0 x 3.0 cm, all had histologic evidence of rejection when sacrificed between day 10 and 21.

Full-thickness homografts were rejected in all cases between the 7th and 10th post operative day. These homografts were taken from the same donor animals as were the heterologous epidermal cells seeded into the artificial skin. The artificial skin grafts seeded with heterologous cells showed no gross evidence of rejection in animals subsequently grafted with a homograft. Histologic examination of the rejected homografts revealed necrotic material full of inflammatory cells (Figures 104,105).

Pin Prick Test

The pin prick test on long-term Stage 2 animals (greater than 60 days) was positive. When pricked, the animals responded with a twitch of the skin, or a body movement away from the stimulus.

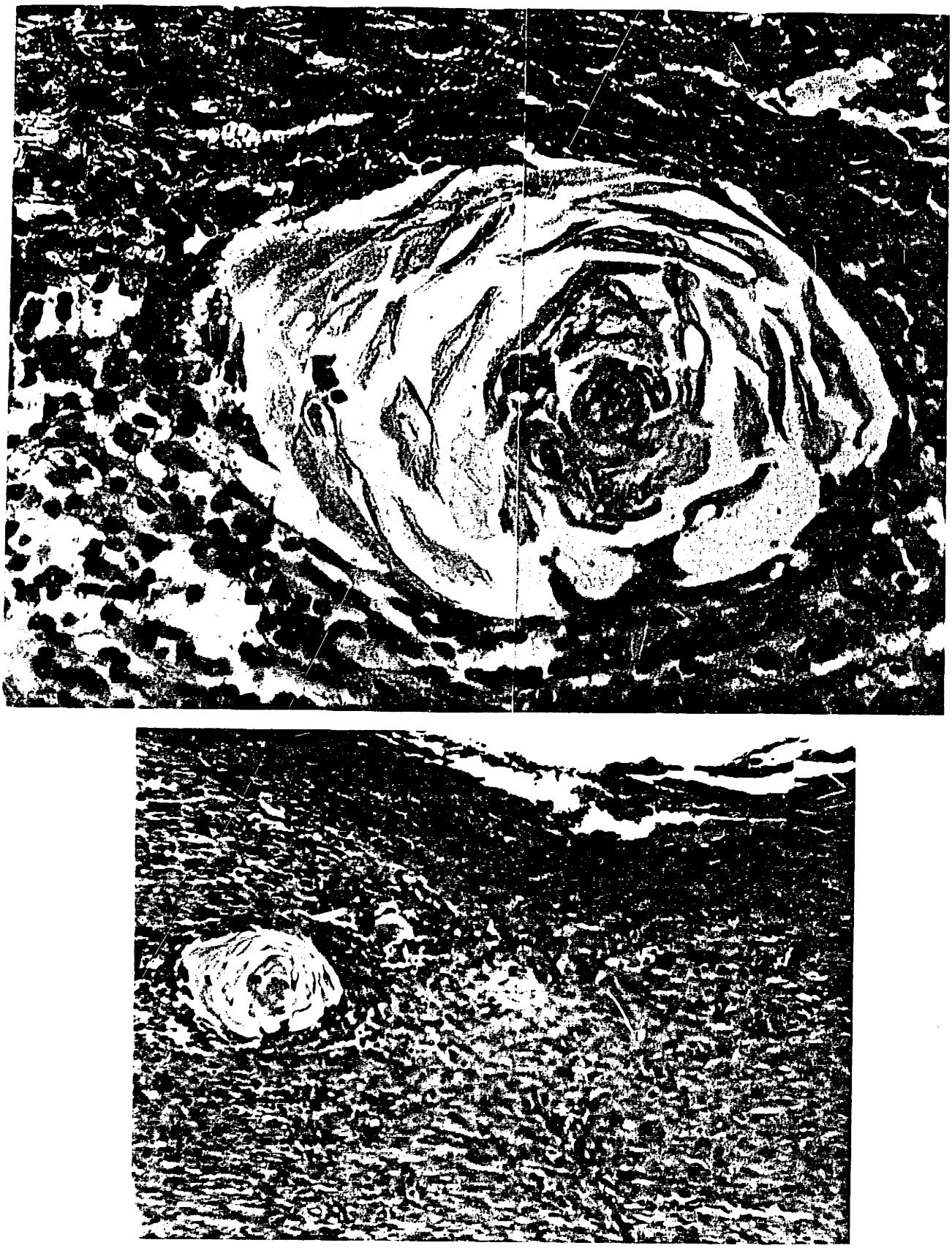

Figure 102. High (675) and low (150 X) magnification of a keratin pearl with a round cell infiltrate. Animal No. 300-2, day 15, hematoxylin and eosin.

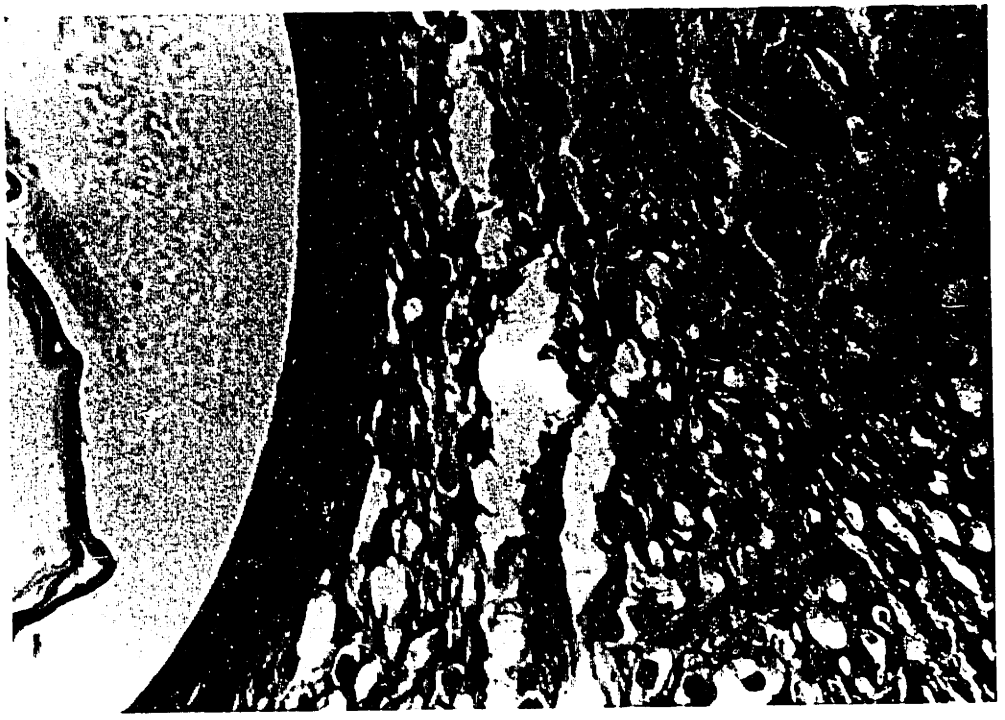

Figure 103. High (150 X) and low (675 X) magnification of a keratin pearl in a graft seeded with heterologous epidermal cells. Keratin pearls are evidence of heterologous cell proliferation since they are not seen in Stage 1 (unseeded) grafts. Round cell infiltrate is absent. Animal No. 302-3, day 21.

Figure 104. Graft seeded with heterologous epidermal cells, day 49. Lymphocytic infiltrate is absent. A complete epidermal coverage was present by day 14 (Figure 62). Animal No. 300-4, 150 X, hematoxylin and eosin.

Figure 105. Homograft rejection, day 14. A full-thickness homograft was excised from the same donor as the heterologous cells were derived. Animal No. 300-4, 150 X.

Type of Silicone Used

Three types of silicone were used as a moisture barrier for the collagen-GAG membrane: 1) Medical Grade Adhesive A, Knife Coated, 2) Preformed 0.007 in. Reinforced Silicone, and 3) Preformed 0.010 in. Non-Reinforced Silicone. The preformed sheets were glued to the collagen-GAG with 355 Medical Adhesive (see Materials and Methods).

The preformed non-reinforced silicone was preferred from the surgical standpoint. It draped easily over curved wounds and was amenable to suturing. The reinforced silicone was so strong that if a suture were pulled very tightly, it could break through the skin before it would break through the silicone. The reinforcing fiber also made the material stiff. Sutures frequently fractured the knife-coated material when applied, but were not observed to fracture the preformed sheets. The knife-coated material was difficult to suture as too much tension would fracture the silicone. The preformed non-reinforced material had a very long elongation to break, 300-400%, which enabled it to be subjected to large local deformations without breakage. All three types were satisfactory in maintaining the wound free from infection and allowing the growth of epidermis between the silicone and the collagen-GAG membrane.

Peel Strength Results

During the first four days of the peel strength experiment, fracture occurred at the interface between the collagen-GAG membrane and the woundbed. Measurable adhesion was

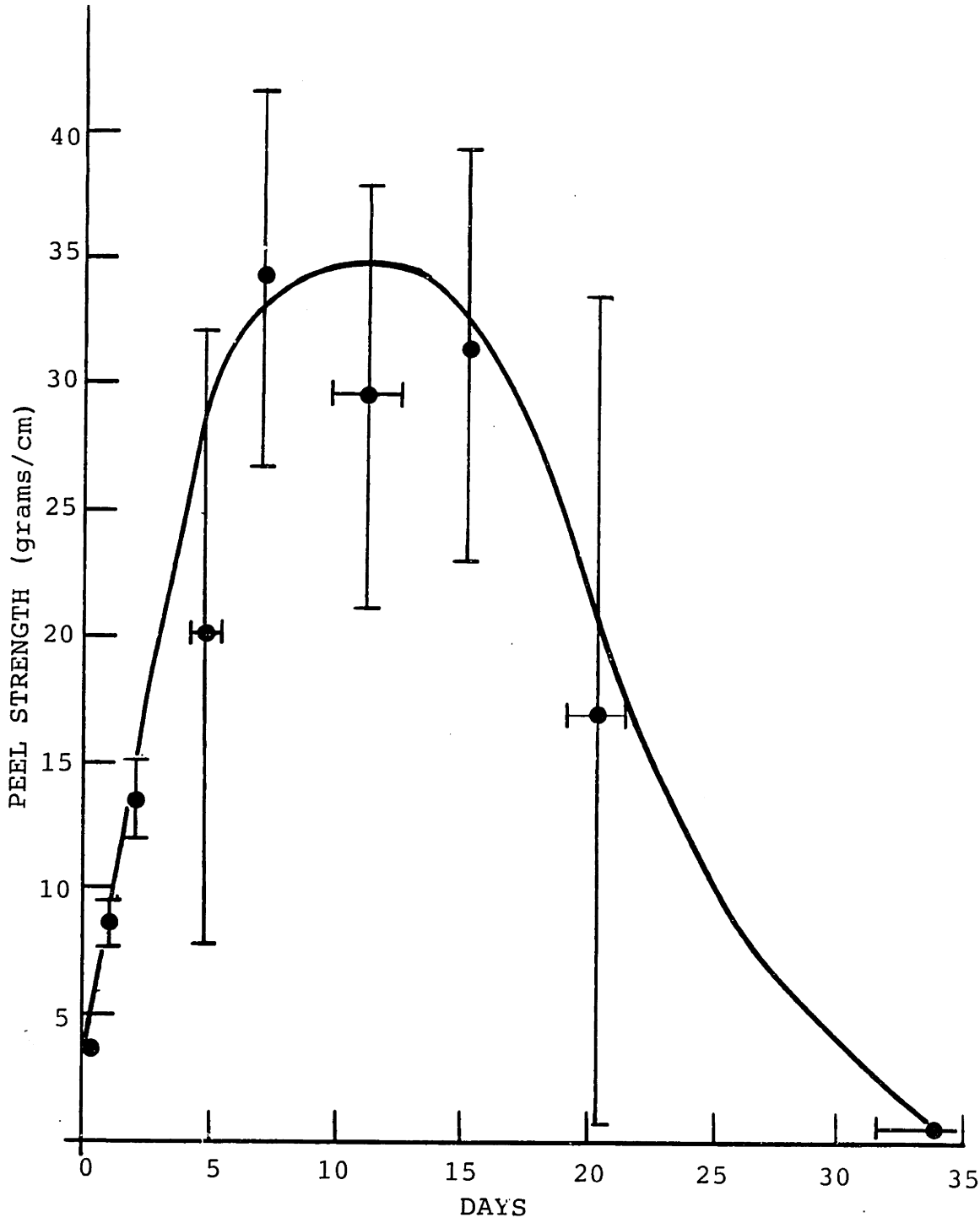

Figure 106. Peel Strength of 1.5 x 3.0 cm Stage 1 grafts. Horizontal bars were used when data from more than one day were used in calculating an average peel strength. The peel strength goes to zero on about day 34 for Stage 1 membranes. In contrast, Stage 2 membranes have a zero peel force about day 12.

observed soon after grafting with peel strengths of the range 2 to 5 g/cm being observed after 2 hours of grafting. By day 7, the fracture plane shifted between the collagen-GAG membrane and the silicone layer. After day 15, the peel strength began to decrease, being coincident with wound contraction and epidermal ingrowth. Figure 106 summarizes the results of 27 grafts in which the peel strength was measured over the last three years with standard Stage 1 membranes. In some cases, data from adjacent days were combined (as indicated by horizontal error bars) in order to have enough values to calculate a standard deviation. The value at 34 days represents the mean day at which the silicone rubber is ejected from a 1.5 x 3.0 cm Stage 1 graft. Because of the limited number of Stage 2 grafts, peel strength measurements were not made. However, when neoepidermal confluence occurred on about day 12, a close to zero force was required to move the silicone from the graft.

TABLE VII

UNGRAFTED CONTROLS

Animal No.	Wound Size	Wound Thickness	50% Original Area (days)	Infection	Outcome, Day
144-1	1.5x3	Full	11	N	S, 379
144-2	"	"	10	N	D, 189
144-3	"	"	11	N	S, 323
144-4	"	"	9	N	S, 200

S = Sacrificed

D = Died

Full = Full thickness wound (dermis + epidermis)

Y = Yes

N = No

TABLE VIII

AUTOGRAFT CONTROLS

Animal No.	Size of Graft	Thickness of Graft	Infection	Outcome, Day
147-1	1.5 x 3 cm	Full	N	S, 379
147-2	"	"	N	S, 323
147-3	"	"	N	S, 323
147-4	"	"	N	S, 200

S = Sacrificed

D = Died

N = No

Y = Yes

Full = Full thickness autograft (epidermis + dermis)

TABLE IX

STAGE 1 CONTROLS

Animal No.	Size of Graft (cm)	Type of Silicone	Type of Collagen-GAG	Graft Medium	50% Original Area (Day)	Infection	Outcome, Day
139-1	1.5 x 3	A	Std.	TCM	24	N	S, 427
139-2	"	"	"	TCM	-	N	S, 8
145-1	"	"	"	PBS	22	Y, 33	S, 46
145-2	"	"	"	PBS	25	N	S, 379
145-3	"	"	"	PBS	28	N	S, 200
145-4	"	"	"	PBS	26	N	S, 200

A = Medical Grade Silicone A

Std. = Standard Collagen-GAG membrane

S = Sacrificed

D = Died

Y = Yes

N = No

TABLE X

STAGE 2 GRAFT RESULTS

Key

Type of Silicone

A - Medical Grade Silicone A, knife coated

R - Reinforced preformed Silicone, 0.007 in.

NR - Non-reinforced preformed Silicone, 0.010"

Type of Collagen-GAG

Std. - Standard

1.6 - 1.6 times the standard Collagen-GAG density

Centrifuge Speed

g - acceleration of gravatational field (9.8 m/sec^2)

Type of cell culture media

TCM - DMEM with 10% FCS, penicillin, and streptomycin

PBS - Phosphate Buffered Saline

AB - DMEM with 10% Human AB serum, penicillin, and strep.

Infection

Y - Yes

N - No

Outcome

S - Sacrificed

D - Died

TABLE X (cont)

Animal No.	Size of Graft (cm)	Type of Silicone	Type of Collagen-GAG	% Cell Viability	No. cells seeded/ cm^2 graft	Hours between biopsy and graft	Centrifuge Speed	Type of cell culture media	Day Silicone Removed	Neoepidermal confluence (days)	50% Original Area (days)	Infection (type)	Biopsy (day)	Outcome, (day)
133-1	1.5x3	A	Std.	57	500,000	48	64 g	TCM	11	11	15	Y, poster.	N	S, 483
133-2	"	"	"	69	"	"	"	"	11	11	18	N	N	S, 483
133-3	"	"	"	57	"	"	"	"	11	28	26	Y	N	D, 296
134-1	1.5x3	"	1.6x	59	"	"	"	"	-	-	-	Y	N	S, 11
134-2	"	"	1.6x	41	"	"	"	"	-	-	-	Y	N	S, 7
134-3	"	"	1.6x	67	"	"	"	"	-	-	-	N	N	S, 7
135-1	"	"	Std.	61	"	"	"	"	9	-	13	Y, E. cloac.	N	S, 22
135-2	"	"	"	64	"	"	"	"	5	20	15	Y, S. aureus	N	D, 32
135-3	"	"	"	79	"	"	"	"	12	12	15,70	N	N	S, 512
135-4	"	"	"	54	"	"	"	"	9	11	15,70	N	N	D, 284
135-5	"	"	"	50	"	"	"	"	5	18	15	Y, E. cloac. S. aureus	N	D, 88
135-6	"	"	"	50	"	"	"	"	8	15	14	Y, E. cloac.	N	D, 88

TABLE X (cont)

Animal No.	Size of Graft (cm)	Type of Silicone	Type of Collagen-GAG	% Cell Viability	No. cells seeded/ cm^2 graft	Hours between biopsy and graft	Centrifuge Speed	Type of cell culture media	Day Silicone Removed	Neoepidermal confluence (days)	50% Original Area (days)	Infection (type)	Biopsy (day)	Outcome, (day)
135-7	1.5x3	A	Std.	46	500,000	48	64xg	TCM	10	19	19	N	N	D, 19
135-8	"	"	"	48	"	"	"	"	10	10	15,100	N	N	S, 511
135-9	"	"	"	52	"	"	"	"	11	11	17,75	N	N	S, 511
135-10	"	"	"	56	"	"	"	"	10	18	14	N	N	S, 455
136-1	1x2 isl.	"	"	64	"	"	"	"	-	-	-	N	N	S, 4
136-2	1x2 isl.	"	"	58	0	"	"	"	-	-	-	Y	N	S, 8
137-1	1.5x3	"	1.6X	47	500,000	"	"	"	11	11	15,200	N	N	S, 349
137-2	"	"	1.6X	52	"	"	"	"	9	14	19,115	N	N	S, 484
137-3	"	"	1.6X	70	"	"	"	"	11	13	22,75	N	N	S, 483
138-1	"	"	Std.	64	500,000[1] 300,000 fibroblt.	"	"	"	9	11	-	N	N	D, 15
138-2	"	"	"	67	"	"	"	"	11	20	22	N	N	S, 36
138-3	"	"	"	51	"	"	"	"	8	20	20	N	N	S, 36

TABLE X (cont)

Animal No.	Size of Graft (cm)	Type of Silicone	Type of Collagen-GAG	% Cell Viability	No. cells seeded/ cm^2 graft	Hours between biopsy and graft	Centrifuge Speed	Type of cell culture media	Day Silicone Removed	Neoepidermal confluence (days)	50% Original Area (days)	Infection (type)	Biopsy (day)	Outcome, (day)
140-1	4x4	A	Std.	60	680,000	48	64g	TCM	6	-	-	N	N	S, 14
140-2	"	"	"	54	630,000	"	"	"	10	12	17	N	N	S, 483
140-3	"	"	"	60	470,000	"	"	"	5	-	17	N	N	D, 23
141-1	1.5x3	"	"	73	100,000	"	"	"	-	-	-	N	N	S, 12
141-2	"	"	"	67	"	"	"	"	-/	-	-	N	N	D, 0
141-3	"	"	"	61	"	"	"	"	11	18	-	N	N	S, 20
141-4	"	"	"	64	50,000	"	"	"	18	18	20	N	N	
141-5	"	"	"	58	"	"	"	"	18	18	18	N	N	S, 442
141-6	"	"	"	45	360,000	"	"	"	11	14	18	N	N	S, 32
141-7	"	"	"	56	500,000	"	"	"	14	14	14	N	N	S, 32
142-1	4x4	"	"	58	870,000	"	"	"	14	15	18	N	N	S, 84
142-2	"	"	"	54	690,000	"	"	"	14	-	18	N	N	S, 21
142-3	:	:	:	55	720,000	"	"	"	-	-	-	N	N	D, 17

TABLE X (cont)

Animal No.	Size of Graft (cm)	Type of Silicone	Type of Collagen-GAG	% Cell Viability	No. cells seeded/ cm^2 graft	Hours between biopsy and graft	Centrifuge Speed	Type of cell culture media	Day Silicone Removed	Neoepidermal confluence (days)	50% Original Area (days)	Infection (type)	Biopsy (day)	Outcome, (day)
142-4	4x4	A	Std.	47	650,000	48	64g	TCM	14	40	16	Y, S. aureus	N	S, 84
143-1	2x4	"	"	69	500,000	"	"	"	12	-	19	N	N	S, 21
146-1	1.5x3	"	"	63	"	"	"	"	11	14	18	N	N	S, 21
146-2	"	"	"	56	"	"	"	"	12	14	18	N	N	S, 46
146-3	"	"	"	58	"	"	"	"	-	-	-	N	N	D, 4
146-4	"	"	"	54	"	"	"	"	14	18	18	N	N	S, 21
146-5	"	"	"	43	"	"	"	"	11	18	18	N	N	S, 33
146-6	"	"	"	48	"	"	"	"	11	-	-	N	N	S, 15
148-1	4x4	"	"	65	50,000	"	"	"	21	29	35	N	60,89	S, 295
148-2	"	"	"	47	500,000	"	"	"	-	-	-	N	N	D, 7
148-3	"	"	"	50	"	"	"	"	-	-	-	N	N	D, 4
149-1	"	"	"	42	"	"	"	"	14	14	16	N	N	S, 295
149-2	"	"	"	53	"	"	"	"	16	-	-	N	N	S, 21

TABLE X (cont)

Animal No.	Size of Graft (cm)	Type of Silicone	Type of Collagen-GAG	% Cell Viability	No. cells seeded/ cm^2 graft	Hours between biopsy and graft	Centrifuge Speed	Type of cell culture media	Day Silicone Removed	Neoepidermal confluence (days)	50% Original Area (days)	Infection (type)	Biopsy (day)	Outcome, (day)
149-3	1.5x3	A	Std.	53	500,000	48	64g	TCM	-	-	-	N	N	D, 4
149-4	"	"	"	40	"	"	"	"	18	-	-	N	N	S, 18
149-5	"	"	"	41	"	"	"	"	16	16	18	N	N	S, 118
149-6	"	"	"	36	"	"	"	"	18	20	21	N	N	S, 351
150-1	3x3	"	"	40	100,000	"	"	"	14	-	-	N	N	S, 18
150-2	"	"	"	48	200,000	"	"	"	14	"	"	N	N	S, 18
150-3	"	"	"	40	300,000	"	"	"	18	-	-	N	N	S, 32
151-1	"	"	"	53	500,000	"	"	AB	-	-	-	N	N	S, 7
151-2	"	"	"	26	"	"	"	AB	11		16	N	N	S, 11
151-3	"	"	"	43	"	"	"	AB	11	-	-	N	N	D, 13
152-1	"	"	"	--[2]	"	"	"	PBS	-	-	-	N	N	S, 7
152-2	"	"	"	--[2]	"	"	"	PBS	-	17	-	N	N	S, 21
152-3	"	"	"	--[2]	"	"	"	PBS	-	-	-	N	N	S, 14

TABLE X (cont)

Animal No.	Size of Graft (cm)	Type of Silicone	Type of Collagen-GAG	% Cell Viability	No. cells seeded/ cm^2 graft	Hours between biopsy and graft	Centrifuge Speed	Type of cell culture media	Day Silicone Removed	Neoepidermal confluence (days)	50% Original Area (days)	Infection (type)	Biopsy (day)	Outcome, (day)
153-1	3x3	A	Std.	71	500,000	5	64g	TCM	9	10	13,80	N	N	S, 290
153-2	"	"	"	82	"	5	"	"	14	14	18,100	N	N	S, 290
153-3	"	"	"	71	"	5	"	"	14	14	18	N	N	S, 38
154-1	"	"	"	58	"	48	"	"	14	-	-	N	N	S, 14
154-2	"	"	"	46	"	"	"	"	18	40	25	N	N	S, 287
154-3	"	"	"	37	"	"	"	"	18	-	-	N	N	S, 22
155-1	"	"	"	46	"	"	"	AB	-	-	-	N	N	S, 14
155-2	"	"	"	41	"	"	"	AB	18	-	-	N	N	S, 22
155-3	"	"	"	40	"	"	"	AB	18	-	-	N	N	S, 21
156-1	"	R	"	81	"	4	"	AB	13	18	15	N	N	S, 102
156-2	"	R	"	69	"	4½	"	AB	11	-	-	N	N	S, 13
156-3	"	R	"	70	"	6	"	AB	13	-	-	N	N	S, 13
156-4	"	R	"	53	"	6	"	AB	14	15	-	N	14	S. 16

TABLE X (cont)

Animal No.	Size of Graft (cm)	Type of Silicone	Type of Collagen-GAG	% Cell Viability	No. cells seeded/ cm^2 graft	Hours between biopsy and graft	Centrifuge Speed	Type of cell culture media	Day Silicone Removed	Neoepidermal confluence (days)	50% Original Area (days)	Infection (type)	Biopsy (day)	Outcome, (day)
157-1	3x3	R	Std.	75	500,000	6½	64g	TCM	11	16	–	N	N	S, 20
157-2	3x3	R	"	83	"	7	"	"	11	14	15	N	14	S, 262
158-1	3x3	R	"	83	50,000	7	"	"	17	17	17	N	N	S, 187
158-2	"	A	"	51	50,000	6	"	"	–	–	–	N	N	D, 2
159-1	"	R	"	75	100,000	6	"	"	–	–	–	N	N	D, 2
159-2	"	A	"	77	100,000	7	"	"	17	30	17	N	N	S, 187
160-1	"	R	"	57	200,000	5	"	"	14	14	16	N	N	S, 187
160-2	"	A	"	82	200,000	7	"	"	14	14	–	N	N	S, 17
161-1	"	R	"	80	500,000	6	1g	"	14[3]	14	17	N	N	S, 187
161-2	"	A	"	83	500,000	5	1g	"	14[3]	14	16	N	14,43	S, 187
162-1	3x1.5	R	"	66	500,000[4]	7	64g	"	12	14	12	N	N	S, 162
162-2L	"	R	"	80	500,000[5]	7	"	"	–	–	–	N	N	D, 1
162-2R	"	R	"	71	500,000[4]	7	"	"	–	–	–	N	N	D, 1

TABLE X (cont)

Animal No.	Size of Graft (cm)	Type of Silicone	Type of Collagen-GAG	% Cell Viability	No. cells seeded/ cm^2 graft	Hours between biopsy and graft	Centrifuge Speed	Type of cell culture media	Day Silicone Removed	Neoepidermal confluence (days)	50% Original Area (days)	Infection (type)	Biopsy (day)	Outcome, (day)
166-1R	3x1.5	R	Std.	70	$500,000^{4}$	7	64g	TCM	14	14	21	N	N	S, 152
166-1L	"	"	"	49	$500,000^{5}$	7	"	"	14	14	21	N	N	S, 152
166-2R	"	"	"	62	$500,000^{4}$	7	"	"	14	14	-	N	N	S, 14
166-2L	"	"	"	71	$500,000^{5}$	7	"	"	14	14	-	N	N	S, 14
166-3R	"	"	"	82	$500,000^{4}$	7	"	"	14	17	-	N	N	S, 21
166-3L	"	"	"	77	$500,000^{5}$	7	"	"	14	14	-	N	N	S, 21
168-1	3 x 3	"	"	69	$500,000^{6}$	5	"	"	14	14	16	N	N	S, 88
168-2	"	"	"	72	$500,000^{6}$	6	"	"	-	-	-	N	N	D, 3
169-1	4 x 4	NR	"	97	500,000	4	"	"	-	-	-	N	N	D, 3
169-2	"	"	"	84	500,000	5	"	"	11	11	24	N	N	
169-3	"	"	"	91	500,000	6	"	"	-	-	-	N	N	D, 3

GRAFTS SEEDED WITH CRYOPRESERVED CELLS

TABLE X (cont)

Animal No.	Size of graft (cm)	Type of Silicone	% Viability	No. days frozen	Day Silicone Removed	Neoepidermal confluence (days)	50% Original Area	Infection (type)	Biopsy, (day)	Outcome, (day)
163-1	3x3	NR	77	4	11	11	18	N	21	S, 165
163-2	"	NR	69	4	11	11	16	N	N	S, 165
165-1	"	R	77	4	11	14	-	N	N	S, 16
165-2	"	R	78	4	10	-	-	N	N	S, 16
167-1	"	R	72	43	14	14	-	N	N	S, 19
167-2	"	R	76	43	11	11	-	N	N	S, 19
171-1	"	R	71	190	11	11	-	N	N	S, 12
171-2	"	R	72	190	-	-	-	N	N	D, 0

All grafts were prepared using the standard collagen-GAG membrane seeded with 500,000 viable cells/cm graft. Cells were cryopreserved with DMSO.

TABLE XI

GRAFTS SEEDED WITH HETEROLOGOUS CELLS

All membranes listed below used standard collagen-GAG membranes seeded with 500,000 viable cells/cm^2 graft. Cells were suspended in TCM and centrifuged into the graft at 64g for 15 min.

Animal No.	Size of Graft (cm)	Type of Silicone	Hours between biopsy and graft	Day Silicone Removed	Neoepidermal confluence (days)	50% Original Area (days)	Infection	Full-thickness homograft (days following grafting of seeded membrane	Homograft rejection (days)	Biopsy (day)	Outcome, (day)	Gross neoepidermal rejection, (days)	% Viable Cells
300-1	1.5x3	A	48	13	18	14	N	19	Y,9	49	D, 52	N	67
300-2	"	"	"	11	12	14	Y	-	-	-	S, 15	Y, 15	67
300-3	"	"	"	12	-	-	Y	-	-	-	S, 15	Y, 13	67
300-4	"	"	"	11	11	15	N	19	Y,9	49	S, 61	N	67
301-1	"	"	408^7	14	-	14	N	-	-	-	S, 17	N	87
301-2	"	"	408^7	14	-	16	N	-	-	-	S, 17	Y, 13	87
302-1	2 x 4	"	48	10	-	-	N	-	-	-	S, 10	-	65
302-2	"	"	"	10	21	14	N	-	-	-	S, 21	Y, 14	65
302-3	"	"	"	12	14	21	N	-	-	-	S, 21	N	65

TABLE XI (cont)

Animal No.	Size of Graft (cm)	Type of Silicone	Hours between biopsy and graft	Day Silicone Removed	Neoepidermal confluence (days)	50% Original Area (days)	Infection	Full-thickness homograft (days following grafting of seeded membrane	Homograft rejection (days)	Biopsy (day)	Outcome, (day)	Gross neoepidermal rejection, (days)	Type of gradient	% Viable Cells
303-1	2 x 4	A	48	12	-	-	N	-	-	-	S, 12	N	-	54
303-2	"	"	"	12	21	14	N	-	-	-	S, 21	Y, 15	-	54
304-1	3 x 3	R	5	11	11	18	N	-	-	14,22	S, 205	Y	-	76
306-1	1.5x3	R	8	14	14	14	N	19	Y, 7	19	S, 152	N	FP	66
306-2	"	R	8	11	14	-	N	-	-	-	S, 14	N	FI	79
306-3	"	R	9	14	14	15	N	-	-	-	S, 19	Y, 15	FP	71
307-1L	"	NR	96[8]	-	-	-	N	-	-	-	D, 5	N	-	69
[9]307-1R	"	NR	96[8]	-	-	-	N	-	-	-	D, 5	N	-	69
308-1	3 x 3	R	96[8]	11	-	-	N	-	-	-	S, 16	N	-	77
308-2	"	R	96[8]	-	-	-	N	-	-	-	D, 7	-	-	78
[θ]309-1	"	R	96[8]	14	-	-	Y	-	-	-	S, 16	Y, 16	FP	53
[θ]309-2	"	R	96[8]	16	-	15	N	-	-	-	S, 49	N	FP	49

TABLE XI (cont)

Animal No.	Size of Graft (cm)	Type of Silicone	Hours between biopsy and graft	Day Silicone Removed	Neoepidermal confluence (days)	50% Original Area (days)	Infection	Full-thickness homograft (days following grafting of seeded membrane	Homograft rejection (days)	Biopsy (day)	Outcome, (day)	Gross neoepidermal rejection, (days)	Type of gradient	% Viable Cells
310-1	3 x 3	R	6 Δ	14	-	-	N	-	-	-	S, 17	Y,14	FP	70
310-2	"	R	6 Δ	14	-	-	Y	-	-	-	S, 14	Y,14	FP	70
310-3	"	R	6 Δ	14	-	-	N	-	-	-	S, 17	Y,14	FP	62
310-4	"	R	6 Δ	14	-	-	N	-	-	-	S, 14	Y,14	FP	71
310-5	"	R	6 Δ	14	-	-	N	-	-	15	S, 21	Y,14	FP	77
310-6	"	R	6 Δ	14	-	-	N	-	-	-	S, 21	-	FP	82
311-1	"	R	6	11	-	-	Y	-	-	-	S, 11		PP	95
312-1	"	R	6	11	11	-	N	-	-	-	S, 14	Y,14	PP	95
313-1	1.5x3	R	¶24 days	14	14	13	N	-	-	14			-	86

TABLE XI (cont)

GRAFTS SEEDED WITH HETEROLOGOUS CELLS

Key: Similar to that of Stage 2 Table

7. Cells isolated on day of biopsy and stored in cell culture.
8. Cells isolated on day of biopsy and cryopreserved with DMSO.
9. Autologous cells.

Δ. 200,000 cells/cm^2 graft seeded.

θ. 100,000 cells/cm^2 graft seeded.

¶. In cell culture for 24 days.

DISCUSSION

Current Methods of Skin Replacement

Over the years, several attempts have been made to provide a functional replacement for skin. These attempts have spanned many disciplines and have each contributed to the current knowledge of design principles for a skin replacement. These different approaches to the replacement of skin will be divided into five categories for the sake of discussion (Figure 107).

Since two of the major functions of skin are to maintain a barrier to water and bacteria between the body and the environment, many attempts have been made to produce barriers out of synthetic polymers to serve as a skin replacement (97-103). This approach has the advantage that these membranes would be manufacturable in large quantities and would be relatively easy to apply. Despite intensive research efforts (97-103), these membranes have not gained acceptance for the clinical treatment of full-thickness wounds. Most of these synthetic polymers are inert and nonreactive with the biologic host and are not biodegradable. Lack of adhesion to the woundbed, accumulation of exudate, a high incidence of infection, and a low capacity to induce vascularization and epithelialization have been problems which have plagued many of these polymeric membranes.

The second approach to the replacement of skin, the autograft, has been discussed extensively in this thesis. The autograft is the most effective treatment of open

Method	Limitations
1. Polymeric Membranes	Low adherance, exudation, no degradation
2. Autograft	Short supply, scarring at donor site
3. Homograft and Xenograft	Immunologic rejection, lack of sterility, uncertain supply
4. Cell and Organ Culture	Time delay required to prepare skin, requires development of technology
5. Bioreplaceable templates	Availability, requires development of technology

Figure 107. Current approaches to the replacement of skin.

wounds available today. Using well established surgical techniques, autcgrafts can close large wounds rapidly leaving minimal scarring. The major problem with the autograft is its short supply. This occurs when the area to be covered is larger than the available donor sites. Because of this problem, surgeons have been able to expand the area covered by a given area of autograft by meshing it (104). The mesh graft typically expands the area covered from 1.5 to 5 times the area of the donor site. After the wound is covered by the mesh graft, epidermis from the mesh graft grows out to fill in the voids. Because the dermis is not able to expand in this fashion, scar tissue develops between the meshes resulting in the permanent cross-hatched pattern commonly seen on burn victims. A second problem which occurs with autografts is scarring of donor sites which can cause significant areas of disfigurement.

The third approach to the replacement of skin is the use of skin from another human or animal source. The most obvious problem with this approach is immunologic rejection which occurs if these homografts or xenografts are not changed frequently. Although immunosuppressive therapy has been successful in delaying the rejection of homografts (5), this thereapy also mutes the response which the recipient can mount to an infection. As advances in immunology continue to occur, it is conceivable that improved therapeutic regimes of immunosuppressive drugs will be developed which will selectively delay the rejection of the homograft

without suppressing other aspects of the immune system. It is also possible that various treatments of skin will reduce its antigenicity. Oliver et al (105-112) has treated full-thickness sections of skin with enzymes to remove all but the fibrous components of the dermis. When grafted onto open wounds of recipients, he found that this fibrous matrix was vascularized, showed little contraction, and was not rejected. Using radioactive hydroxyproline, he found that the turnover of these collagen grafts had a half life of about 60 days. When these grafts were cross-linked in a solution of 0.01%, glutaraldehyde at pH 7.2 for 16 hours (15° C), the half-life of these grafts was extended to greater than 170 days. This work has been important in demonstrating the effects of processing variables such as enzymatic digestion and cross-linking on vascularization and collagen turnover in these dermal collagen allografts.

A fourth approach to the problem is the use of cell and organ culture techniques to grow large areas of skin suitable to a particular patient. O'Connor et al (63) have grown epidermal sheets from skin biopsies and have grafted these onto experimental animals and a limited number of patients. Although this group has been successful in growing large areas of skin in culture, the results from the preliminary clinical trials have raised questions about the ability of these sheets to adhere to the wound and to expand peripherally. Bell et al (64) have grown epidermal sheets on a collagen lattice and have been successful in

grafting these onto experimental animals, although clinical trials have not been performed to date. Both of these approaches are interesting from the point of view of cell biology; however, they both require a time delay of the order of two weeks to grow the sheets *in vitro*. Therefore, they do not provide an immediate solution to the burn victim.

The fifth approach to the replacement of skin is what has been reported in this thesis. This method utilizes a biodegradable template on which the wound tissue can construct a neodermis and neoepidermis. This approach is an alternative to the common notion among many biomaterials scientists that the implant should not react with the tissues adjacent to it. In contrast, it recognizes the long-term needs of a skin replacement to heal when wounded and be able to undergo remodeling. This approach also provides a prompt closure of the wounds of the burn victim by using a membrane which can be potentially manufactured in large quantities. It addresses the immunologic problems caused by homografts or xenografts by being based on collagen, a material which is only slightly antigenic (113).

By seeding the manufactured membranes with epidermal cells, it was shown here that large wounds could synthesize an epidermis and eject the silicone layer within two weeks of grafting (Figure 34). Simultaneously, a neodermis was synthesized as the collagen-GAG matrix was enzymatically degraded. The maturation of the collagen fibers in the

neodermis occurred over at least 500 days. This maturation process was demonstrated in histologic specimens by thicker collagen fibers which were wavey and interlaced. The gross appearance of the skin formed 200 days after grafting 1.5 x 3.0 cm Stage 2 membranes showed that the wound area was about 70% of the original. This area was much greater than that observed with ungrafted wounds (23%) and wounds grafted with unseeded membranes (27% $p < 0.005$), but significantly less than that seen in the full-thickness autograft (121% $p < 0.005$).

Anatomic Location of Cells Within Graft

The SEM analysis of the seeded grafts showed that the distribution of the cells within the graft could be altered by varying the parameters of the centrifugation process. Initially, it was not clear what the optimal distribution of epidermal cells within the graft should be. Locating the epidermal cells at the interface of the silicone and collagen-GAG membrane would place them in the correct anatomic location, but would remove them from the nutrient supply of the woundbed. If the majority of the epidermal cells were located close to the woundbed (furthest from the silicone), adequate nutrition would be assured but the cells would be furthest from their ideal location.

The results of the experiments reported here clearly indicated that the correct anatomic location of the cells was the limiting design parameter for the formation of a neoepidermis. Figure 108 shows schematically tow initial

cell distributions within the graft and the location of epidermal cells two weeks post grafting. In the first case, cells were seeded into the graft for 15 minutes at 64 g and the cells near the silicone formed a confluent neoepidermis. This indicated that the nutrition of the epidermal cells was adequate in all areas of the graft either due to diffusion or the supply of cell nutrients in the cell culture media. Cells which were seeded in other locations of the graft formed keratin pearls which eventually rose to the surface. By contrast, in the graft where the majority of cells were located near the woundbed, the confluent neoepidermis formed within the graft. This probably cut off the blood supply to the areas of the graft above the epidermis resulting in necrosis of this part of the graft. Yannas (52) has proposed a dimensionless number S to describe the transfer of nutrients from the woundbed to a location in the graft at steady state:

$$S = \frac{r\ell^2}{Dc_o}$$

where r is the rate of utilization of a critical nutrient by the cell, expressed in mole/cm^3/sec, ℓ is the distance along the membrane thickness direction over which the nutrient is transported by diffusion alone, D is the diffusivity (cm^2/sec) of the nutrient in water, and C_o is the nutrient concentration at the surface of the woundbed. With Stage 2 membranes, there is an additional store of nutrients in the cell suspension media which must be

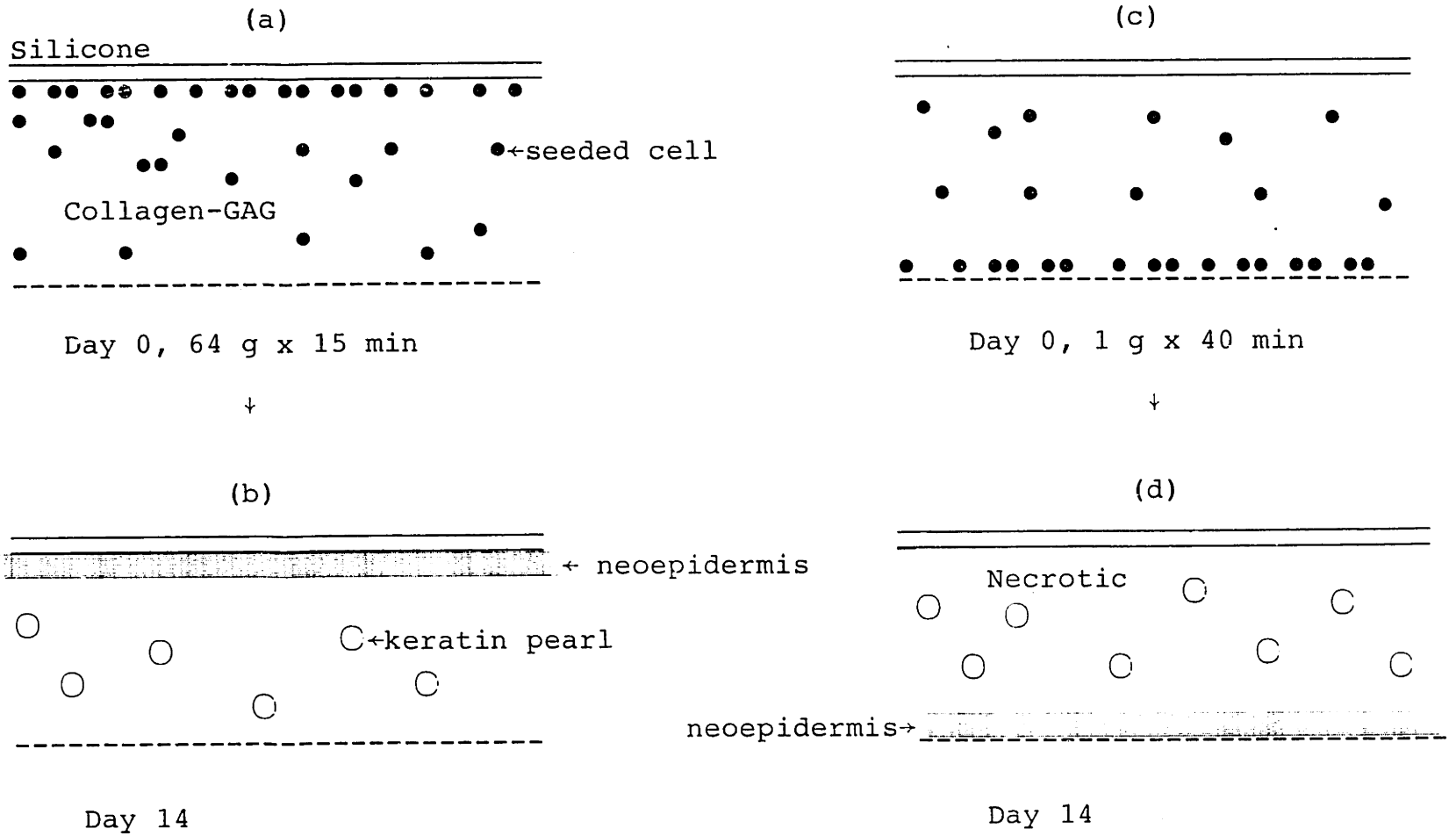

Figure 108. The effect of anatomical location on the performance of Stage 2 membranes. By seeding the cells by centrifugation (a), most of the cells end up near the silicone membrane to form a confluent neoepidermis (b). Cells deeper in the graft form keratin pearls which rise to the surface. By not centrifuging the cell suspension (c), the neoepidermis forms deep within the graft (d)

utilized before this steady state condition applies. This equation would predict that there is a critical distance ℓ_c where nutrient transport becomes limiting. Cells beyond ℓ_c would be required to have addtional sources of nutrients such as from capillaries invading the collagen-GAG membrane before growth could occur. These experiments suggested that single epidermal cells were unable to migrate the silicone surface of the membrane after the Stage 2 membranes were grafted onto the animal.

Disfigurement Model

The long-term disfigurement caused by open wounds can be modeled as the resultant of two components: scarring and the extent of contraction. Scarring will be defined here by the classic histologic criteria described in Table II. Contraction is defined as the change in wound area as a function of time. Depending on the type of injury and the method of treatment, the relative amount of scarring and contraction can be separately altered. For example, a linear surgical skin incision properly sutured, results in an area of disfigurement which has the histologic appearance of scar, but without significant contraction. In contrast, a flexor contracture such as Dupytren's contracture (104) can result from contraction of fascia and skin without significant scarring. In general, in injuries such as full-thickness skin loss, both scarring and contraction are present.

Control of Wound Contraction

The data from several investigators over the last 12 years (27-29, 115-117) suggest that the mechanism of wound contraction might best be modeled as resulting from the action of myofibroblasts. These cells commonly occur in granulating woundbeds and share pharmacological reactivity, ultrastructural appearance, and immunologic cross-reactivity with smooth muscle cells. McGrath and Hundahl have recently reported the spatial and temporal distribution of myofibroblasts in granulating circular (4.3 cm diameter) pig wounds (115). The percentage of myofibroblasts in a given location was calculated by dividing the number of fibroblasts with smooth muscle cell attributes, as seen with transmission electron microscope, by the total number of fibroblasts in the specimen. They reported a rapid rise in the percentage of myofibroblasts visualized in granulating wounds over the first two weeks followed by a gradual decline. The rate of percentage reduction in wound area was highest (-2.9%/day) between days 10 and 21, this time being coincident with the maximum percentage of myofibroblasts visualized (76%). Wound closure occurred by day 56 and by day 84, the population of myofibroblast visualized had gone to zero. The wounds expanded from an average of 24% of original area on day 84 to about 40% of original area on day 98.

Most of the myofibroblasts seen (115) were near inflammatory foci within the granulating woundbed. This led

McGrath (116) to hypothesize that contraction may be mediated by the effect of prostaglandins on myofibroblasts. A reduction of prostaglandin synthesis was postulated to reduce wound contraction by two mechanisms: 1) the reduction of inflammation and 2) the reduction of myofibroblast smooth muscle cell activity. Aspirin is well known to block cyclooxygenase, the enzyme which converts arachidonic acid to prostaglandins. However, there were no statistically significant differences in the rates of contraction amoung animals treated with aspirin and control animals (116). In addition, administration of glucocorticoids to these animals delayed, but did not eliminate contraction (116). Glucocorticoids are known to block the synthesis of prostaglandins at a step in the biosynthetic pathway prior to where aspirin blocks and also block the synthesis of leukotrienes.

Phillips and Peacock (24) were able to delay but not eliminate contraction by the application of a topical smooth muscle contraction inhibitor, Trocinate. Because contraction was not eliminated, it is possible that the local concentration of the smooth muscle inhibitor was insufficient, as topically applied in these experiments (24), to completely inhibit the myofibroblasts. These agents cannot be used systemically due to their high toxicity. It is also possible that other elements in the granulating woundbed contributed to contraction in addition to myofibroblasts. Harris et al (128) have demonstrated

the traction of fibroblasts when grown in culture on distensible sheets of silicone. Bell et al (129) have shown that fibroblasts can cause contraction of a collagen lattice in vitro. These experiments (128,129) demonstrate the ability of fibroblasts to contract and raise the possibility that fibroblasts may play a role in wound contraction.

Although the exact mechanism of wound contraction has not been worked out, the myofibroblast theory provides a good working hypothesis to explain much of the wound contraction literature. Wound contraction is well known to be inhibited by skin grafts, with full-thickness skin grafts being superior to split-thickness grafts (117). Thickness, however, is not the only factor in reducing contraction since thin full-thickness autografts are as effective in preventing wound contraction as thicker full-thickness grafts (117-120). Rudolph (117) has studied the distribution of myofibroblasts in 2.0 by 4.0 cm rat skin grafts. He found the majority of the myofibroblasts in the woundbed (i.e. between the panniculus carnosus and the skin graft). The minimum area of skin grafts occurred at 14 days for full-thickness grafts (85% original) and at 28 days for 0.15 in. split-thickness skin grafts (65%). Ungrafted wounds had a D_{50} of 9 days, were closed and contracted to about 10% of the original area by day 21. The percentage of myofibroblasts was calculated by dividing the number of fibroblasts with smooth muscle attributes by the number of fibroblasts in a given transmission electron microscopy

specimen. The percentage of myofibroblasts visualized reached a peak in all cases of about 50% at 14 days. The disappearance of myofibroblasts occurred by days 28 and 35 for full-thickness and split-thickness grafts respectively, but not until day 70 for ungrafted controls. The effective thickness of the Stage 2 artificial skin grafts was shown to be an important parameter in wound contraction. Stage 2 membranes not seeded by centrifugation (1 g x 20 min) resulted in a thinner neodermis and faster kinetics (Figure 59) than grafts seeded by centrifugation (64 g x 15 min). These grafts behaved similar to pure epidermal grafts described by Billingham in that the contraction kinetics were similar to those observed in ungrafted controls (15, 16, 114).

The work by Rudolph strongly suggests that something present in skin grafts inhibits the appearance of myofibroblasts and wound contraction. This inhibitory substance could either be present in the epidermis, dermis, or both. The literature indicates that the major inhibitory factor must reside in the dermis since pure epidermal grafts are well known not to inhibit wound contraction. Of the components in the dermis, the work by Oliver (105-112) suggests that much of the contraction inhibitory properties of skin grafts is attributable to the fibrous components of the dermis.

Oliver et al have been successful in reducing contraction by grafting only the fibrous components of the dermis (105-112); the cellular components being removed by

enzymatic digestion. These dermal collagen allografts were most successful in treating full-thickness skin defects when used in conjunction with thin split-thickness skin grafts. These experiments consisted of first implanting a dermal collagen allograft subcutaneously in rats. At two weeks, a 1.5 x 2.0 cm area of skin was excised from the top of the vascularized dermal matrix and a skin graft (split-thickness or full-thickness) was sutured in place. Oliver reported that these composite grafts maintained 60-100% of their original area (108).

The two most common components of the fibrous dermal matrix are collagen and glycosaminoglycans (GAGs). Since Stage 1 artificial skin grafts developed by Yannas and Burke (51-55) contain these two components, one would predict that alterations in the physicochemical variables of this artificial matrix may alter the distribution of myofibroblasts in the graft and the contraction kinetics. Recently, various of the physicochemical variables of the Stage 1 membranes have been altered, and the rate of contraction monitored. These variables included the concentration of collagen-GAG solution prior to freeze-drying (56), the presence of GAG (57), and the degree of cross-linking (56,57). As an index of contraction, the day at which the wounds reached 50% of the original area (D_{50}) was used. Keeping the porosity of the membranes relatively constant, it was found that changes in the physicochemical variables which delayed the <u>in vitro</u> degradation of the

graft (126) also delayed D_{50} (Table XII). For example, cross-linking of the collagen matrix in 0.25% glutaraldehyde at pH 3 increased the degradation time in an *in vitro* collagenase solution, and also delayed D_{50} (56, 57, 126). The presence of GAG also delayed the *in vitro* collagenase degradation of the graft and shifted the contraction curve to a longer time scale (57, 126).

Yannas (52) proposed that the biodegradation rate of an artificial skin graft, t_b, should be roughly equal to the time of healing, t_h.

$$\frac{t_b}{t_h} \cong 1$$

It was estimated that the time of healing of 1.5 x 3.0 cm guinea pig wounds was on the order of 25 days (52). Although the biodegradation rate of these membranes has not been measured directly, it is proposed that an index of the biodegradation can be obtained from the contraction kinetics of artificial skin membranes. This is consistent with the work done by Chen (56), Flynn (57), and Wilson (126) where the *in vitro* degradation times were related to the contraction kinetics. The thickness of artificial skin membranes, Stage 1 and Stage 2, have consistently been within 25% of the thickness of the adjacent wound when examined histologically. Since

$$\text{Area of graft} = \frac{\text{Volume of Graft,}}{\text{Thickness}}$$

the decrease in area associated with wound contraction must

EFFECTS OF PHYSICOCHEMICAL VARIABLES ON CONTRACTION OF STAGE 1 MEMBRANES: CROSSLINKING AND PRESENCE OF GAG

Presence of GAG (8% wt.)	Crosslinked in 0.25% Glutaraldehyde	D_{50}	Slope %/day	Ref.
Yes	Yes	25	-3.6	This work
Yes	No	15	-5.1	(56)
No	Yes	16	-5.5	(57)
No	No	12	-5.9	(57)

TABLE XII. Physicochemical variables of Stage 1 membranes

be due to a decrease in wound volume. It is proposed that this change in volume be related to the amount of biodegradation of the graft. This hypothesis is consistent with histologic examination of the artificial skin grafts as a function of time which indicated that the collagen-GAG membrane was degraded over the course of wound contraction. As an index of t_b, it is proposed that the time at which the graft reaches 50% of the original area D_{50} be used.

In light of the Stage 2 experiments it seems appropriate to modify the original design criteria of Yannas (52). The new design criteria would try to match the time constant of biodegradation to the time constant of synthesis of neodermis.

$$\frac{t_b}{t_s} \cong 1$$

In this modified equation, t_s is the time constant of synthesis of the neodermis. As with the contracting artificial skin grafts, the re-expansion occurred with the grafts maintaining a constant thickness. This implies an increase in the graft volume which is most likely due to synthesis of connective tissue. The synthesis of connective tissue within the graft occurs during both the contraction and re-expansion phase of the contraction curve. Therefore, it might be expected that t_s would have a time constant of the order of 60 to 100 days since most of the re-expansion has occurred by 120 days. If this hypothesis is correct, changes in the physicochemical variables of the graft which would extend the biodegradation rate would prolong D_{50} and reduce the contraction seen in

Stage 2 grafts. In the ideal case, if t_s was exactly matched to t_b, it might be expected that wound contraction could be minimized.

Snowden (130), divided the percent original area curve into three regions. Region I was labeled as a latent or lag phase during which the wound maintained a constant area. Region II is a phase during which the wound contracts at a constant rate, and Region III is a phase where the contracted wound maintains a constant contracted area. Based upon the results of this research, it would seem appropriate to redefine Region III as a phase of re-expansion when artificial skin grafts are used. In the vast majority of reports on wound contraction in the literature, wounds have been studied for only a few weeks. This time is usually insufficient to study any re-expansion which might have occurred. Indeed, if the myofibroblast theory is correct, one would expect some re-expansion of wounds when the myofibroblasts stop acting due to the tension present normally in skin (Figure 109).

In longer studies of autografts such as those done by Rudolph (117), re-expansion was observed. One difficulty in studying the re-expansion phenomena is the fact that most wound contraction experiments have been done on growing animals. The guinea pigs used in these experiments approximately doubled in weight over a 200 day period of observation. To estimate the contribution of growth to wound re-expansion, it was assumed that all locations of the skin increased in in area at the same rate. The anterior-posterior distance

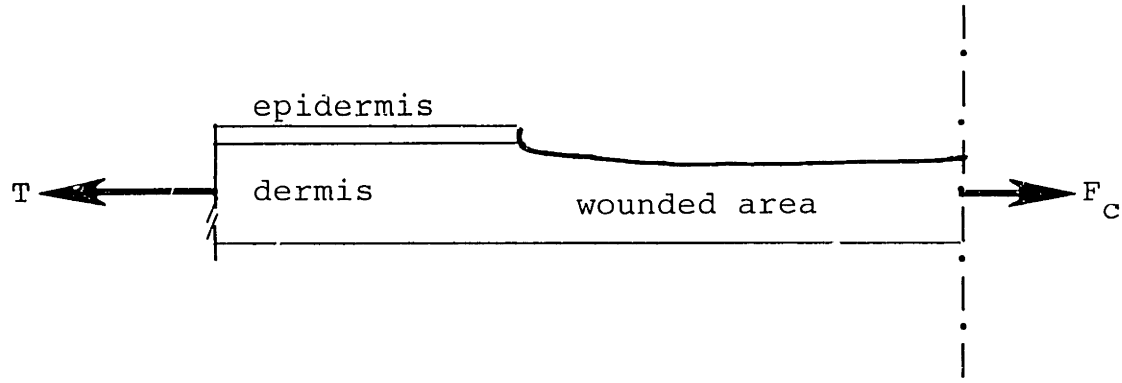

Figure 109. Free body diagram of contracting woundbed. The force of contraction F_c changes during various stages of wound contraction and may be related to the number of myofibroblasts present in the wounded tissue. This force is balanced by the tension T in the intact skin which is a function of its strain. If the force of contraction goes to zero, some re-expansion of the wound area might be expected to occur. Shear forces were considered negligible in the guinea pig model due to the mobile panniculus carnosus.

of the autograft provided a good control value since this dimension did not contract, and it was observed to expand over 200 days of observation by 18%. If growth also accounted for an 18% increase in the medial lateral direction, the area of the graft would have increased by a factor of 1.4 in 200 days. Figure 110 shows that for both the ungrafted and autograft controls, the ratio of the area at 200 days and the minimum area was 1.6 days. This ratio is only slightly greater than the estimate made of re-expansion due to growth. Growth possibly accounts for all of the wound expansion in these two cases.

In constrast, both Stage 1 and Stage 2 grafts showed ratios of 3.4 and 2.9 respectively. It seems unlikely that growth of the animal could have accounted for all of the re-expansion which was observed. Re-expansion in Stage 1 grafts had not been previously reported. However, a perusal of older Stage 1 data (51, 56) confirmed the observations of re-expansion made with Stage 1 membranes reported here. Although the mechanism of re-expansion may be different in Stage 1 and Stage 2 grafts, it is possible that this large re-expansion is due to some property of the collagen-GAG membrane. Birefringent histologic examination of a Stage 2 graft (day 84) showed only small amounts of mature collagen synthesis. The immature nature of the neodermis between 60 and 100 days may have resulted in a low modulus of elasticity of the neodermis. The myofibroblast theory would predict that after the contractile forces had dissipated, the primary

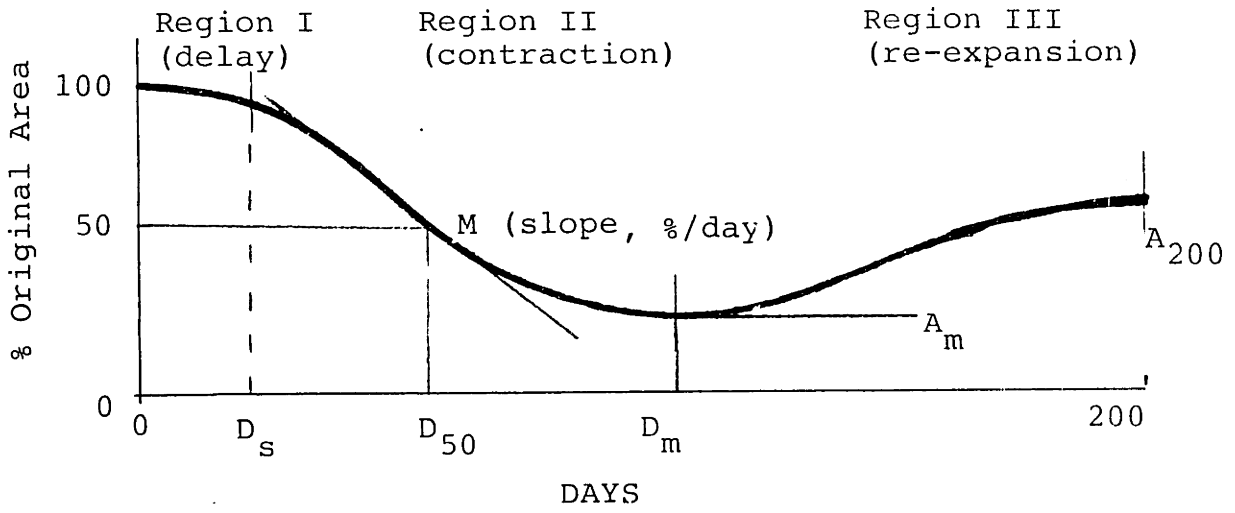

D_s - Number of days before contraction starts

D_{50} - Day at which graft reaches 50% original area

D_m - Day at which graft reaches minimum area

A_m - Minimum area of graft (% of original)

A_{200} - Area of graft at 200 days (% of original)

Type of Graft	D_s	Slope	D_{50}	D_m	A_m	A_{200}	A_{200}/A_m
Ungrafted	4	-7.2	10	32	14	23	1.6
Stage 1	11	-3.6	25	62	8	27	3.4
Stage 2	8	-3.7	17	52	25	72	2.9
Autograft	-	-0.98	-	26	78	121	1.6

Figure 110. Summary of contraction parameters of ungrafted wounds, Stage 1 and Stage 2 artificial skin grafts, and autograft controls. An idealized contraction curve is shown. All values shown are averages, N = 4.

forces on the neodermis would be tensile forces from the surrounding skin which would tend to expand the graft (Figure 109). Whether the neodermis demonstrated plasticity or creep when subjected to these tensile forces will require further investigation.

The seeding of artificial skin grafts with epidermal cells enabled large wounds to synthesize a neoepidermis within two weeks. Coverage of the wounded area with epidermis occurred by three mechanisms: 1) contraction of the surrounding dermis into the grafted area, 2) epidermal cell sheet migration from the edges of the wound into the space between the silicone and the collagen-GAG membrane, and 3) epidermal coverage due to multiplication of seeded cells.

In the 1.5 x 3.0 cm guinea pig model described here, the displacements in the medial-lateral direction greatly exceeded the displacements in the anterior-posterior direction (Figures 24, 26, 28, and 30). Histologic examination of intact skin specimens adjacent to the wounded areas showed that the primary orientation of the collagen fibers in intact skin adjacent to the wound perimenter was in the medial-lateral direction. This was consistent with past observations of surgeons that the direction of wound contraction occurs parallel to Langer's lines (104). Langer's lines mark the principal axis of collagen fiber orientation in a given anatomic location.

Because of the anisotropy of the wound contraction, it is possible to model the contraction process and coverage with

epidermis as a one dimensional process occuring along the medial-lateral axis (Figure 111).

Let V_c = Velocity of normal dermis relative to the center of the wound

V_e = Velocity of normal epidermis from the edges relative to the center of the wound

$V_e - V_c$ = Velocity of epidermal migration relative to the advancing edge of the dermis

Snowden (130) has analyzed contraction data of open wounds from a number of species from reports in the literature and concluded that after an initial delay, the migration of the wound edges occurs at a constant rate. Assuming a linear migration of wound edges, the velocities for 1.5 x 3.0 cm grafts and ungrafted controls are reported in Figure 111. The Stage 1 grafts had a V_c of 0.34 and a V_e of 0.38, whereas, the ungrafted controls had a V_c of 0.52 and a V_e of 0.60. The V_c accounted for the majority of the inward migration with the contribution of the epidermis advancing in front of the dermal edge ($V_e - V_c$) being small in both cases.

The major contribution to the epidermal coverage of the 1.5 x 3.0 cm Stage 2 grafts at two weeks was due to the seeded cells rather than cell migration from the wound perimeter. By day 14, Stage 2 grafts had contracted to about 80% of their original area and were usually completely covered by neoepidermis. Most of the contraction observed in Stage 2 grafts occurred after day 14 when these grafts were covered with a keratinizing neoepidermis. The keratinization could be seen grossly as dry flakes of material sloughing off the

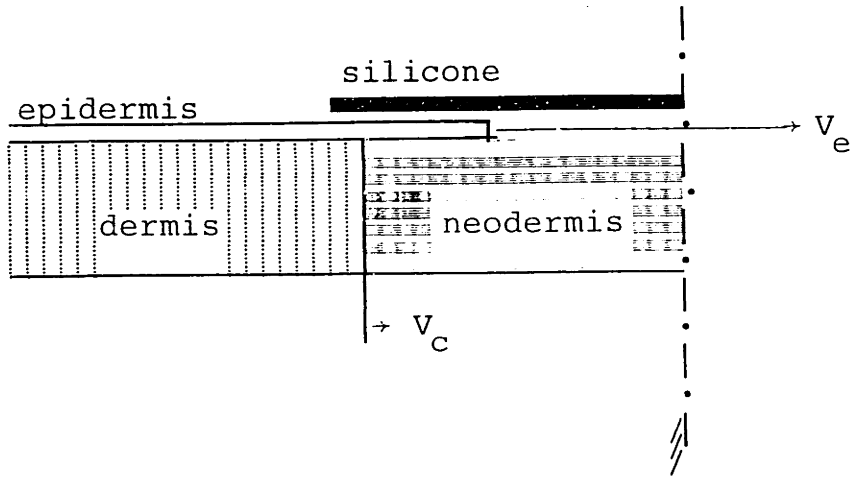

VELOCITIES OF WOUND EDGES

	V_c mm/day	V_e mm/day	$V_e - V_c$ mm/day
Ungrafted	0.54	0.71	0.27
Stage 1	0.27	0.31	0.04
Stage 2	0.28	*	*
Autograft	0.07	*	*

* - Not Measured

Figure 111. Velocities in a contracting artificial skin graft. Wounds are closed by two mechanisms 1) contraction of skin towards the center of the wound and 2) growth of epidermis over the open area. In Stage 2 wounds, there are a major contribution of epidermal coverage due to the seeded epidermal cells. For ungrafted controls, the neodermis would be replaced with granulation tissue and the silicone would not be present.

neoepidermis. An order of magnitude estimate of the number of cells needed to cover a square centimeter of graft was made by assuming that the epidermal cells had characteristic dimensions of 10 μm. The neoepidermis when viewed histologically was about 10 cells thick by day 12, therefore, about 10^7 cells would be required to cover a square centimeter of graft. Because the grafts were not well vascularized before day 4 and epidermal clusters were not seen until day 7, it will be assumed that all of the cell division occurred between day 4 and day 12. Given a cell seeding density of 500,000 cells/cm^2 graft and assuming an exponential growth of cells, this would predict a doubling time of 1.9 days/cell division.

$$e^{\frac{8 \text{ days}}{\tau}} = \frac{10^7 \text{ cells/cm}^2 \text{ neoepidermis}}{5 \times 10^5 \text{ cells/cm}^2 \text{ seeded}} = 20$$

$$\tau = \frac{8 \text{ days}}{\ln 20} = 2.7 \text{ days}$$

$$t_d = 0.693\ \tau = 1.9 \text{ days}$$

This is in reasonable agreement with the linear regression of the confluence times when the number of seeded cells varied between 50,000 and 500,000 cells/cm^2 graft (Figure 56). The slope of this regression was -8.8 days per decade of cells seeded. This analysis would predict a doubling time of 2.7 days (8.8x(log 2/log 10)). These numbers are slightly longer than the cell cycle length reported in the literature for rapidly proliferating epidermal cells around hair follicles in the human scalp of 1.5 days (8).

The larger Stage 2 grafts, 3 x 3 cm and 4 x 4 cm were shown to have similar percent of original area vs time curves (Figure 29). The change in area in these larger grafts was accounted for by centripital movement of all of the wound edges. Since contraction occurred bidirectionally, it was not appropriate to model the contraction of these larger wounds as a one-dimensional process. These results suggest that after a wound reaches a critical size that bidirectional contraction takes place.

Parameters Affecting Scarring

The collagen fiber morphology was judged by four criteria: 1) waviness of fibers, 2)orientation of fiber axis, 3)thickness of fibers, and 4) amount of birefringence present. Collagen fiber morphology in mature Stage 1 and Stage 2 grafts appeared more wavy, thicker, and less oriented parallel to the epidermis than that seen in mature scar. Within a given mature Stage 2 graft, variation in the collagen fiber morphology was observed from one part of the graft to another giving some areas of the graft an appearance which was more scar-like than others. It is possible that either local factors such as the presence of a foreign body or local differences in the time required for vascularization of a given area ultimately resulted in local scarring. The local structure of the collagen-GAG membrane may also influence the degree of scarring which occurs.

The parameters affecting scarring were much more difficult to assess than those affecting contraction. The major difficulty in interpreting the results was that there was no uniform method for quantifying the degree of scarring present in a given histologic specimen. Quantitative stereologic methods applied to collagen and elastin fiber morphology may result in a quantitative classification of scarring. The other problem encountered in assessing the degree of scarring was the long time periods which were required for mature scar to develop. Surgical Texts (104) state that maturation of scars takes place over a two year period. Our experience

with Stage 2 grafts is consistent with this time period in that changes in collagen fiber morphology were seen throughout the duration of this study (512 days). These long time periods required for the maturation of the collagen fibers resulted in a time delay between the time when the contraction data was available to when the data on scarring became available.

The full-thickness autografts preserved part of their collagen fiber morphology in the center of the grafts. Scar tissue occurred along the lines of excision and in parts of the papillary dermis. The scarring which occurred along the lines of excision may have been secondary to the inflammatory process or local necrosis. The mechanism of scarring at the papillary dermis may be explained by the delay in vascularization of this part of the graft resulting in necrosis. This delay in vascularization could also account for necrosis of the majority of the hair follicles and sebaceous glands in the autografts. A qualitative long-term evaluation of the classic criteria of scar applied to artificial skin grafts and autograft controls is reported in Table XIII.

TABLE XIII

Long-term Evaluation of Scarring in Artificial Skin

Classic Histologic Criteria

Tissue	Collagen Bundle Morphology (H & E)	Presence of Elastin (Verhoeff's)	Presence of Adenexa (H&E)	Direction of Capillaries (H&E)
Normal Skin	Thick, wavy fibers	Thick, wavy fibers	Hair follicles Sebaceous glands	Perpendicular and Parallel to Epidermis
Autograft	Normal morphology in center, scar-like morphology along wound edges, base and papillary dermis	Normal morphology	1/10th normal amount	Normal morphology
Stage 2	Medium sized wavy fibers, interlace. Scar-like morphology at wound base	Medium sized wavey wavey fibers mainly parallel to collagen	Occasional hair follicle or sebaceous gland (? artifacts)	Mostly perpendicular, some parallel to epidermis
Stage 1	Similar to Stage 2	Similar to Stage 2	No	Perpindicular to epidermis
Ungrafted	Thin, straight, close packed fibers parallel to epidermis	Thin fibers in close association with collagen fibers	No	Perpindicular to epidermis

H&E - Hematoxylin and Eosin

Function of Stage 2 Grafts

The long-term properties of the skin produced as a result of Stage 2 application were important in evaluating the function of Stage 2 grafts. The long-term grafts interfaced well with the adjacent skin and were soft and pliable. The ultimate tensile strengths of the Stage 2 grafts seemed to increase as a function of time resulting in an ultimate tensile strength of about 45% of normal skin at 300 days. As normal skin develops, changes in mechanical properties have also been reported. Vogel (123) measured the mechanical properties of rat skin as a function of time in growing rats from one week to twenty four months old. He found that it required about four months from birth for the tensile strength and the modulus of elasticity of the rat skin to reach a value comparable with that of a mature rat. Vogel (123) reported tensile strengths of 120 p.s.i. at one week and 2,200 p.s.i. at twenty four months. This study suggests the possible importance of ontogenesis on the development of mechanical properties of normal skin.

The application of Stage 2 artificial skin membranes brings about a partial regeneration of skin. Further mechanical tests would be required to compare the maturation rate of mechanical properties of Stage 2 skin with the time period over which the mechanical properties of normal guinea pig skin develop.

The permeability of Stage 2 grafts is an essential function which must be satisfied. Both histologic

specimens and in vivo evaporimetry indicated that the stratum corneum which formed on top of the neoepidermis is of normal microscopic appearance with a physiologic water flux by day 50. The permeability measurements suggested that the amount of water transport across the neoepidermis decreases slowly as the stratum corneum matures over the first few weeks.

The mature neodermis of Stage 2 grafts contained thick, wavey collagen and elastin fibers with rare adenexa. The lack of adenexa was one of the deficits of the skin which was produced, and therefore, the Stage 2 skin must lack the properties which the adenexa add to the skin such as thermal insulation provided by hair, moisturizing ability provided by sebaceous glands, and thermoregulation by sweat glands. Preliminary efforts to seed the membranes with hair follicles were not successful, but further work in this area would be valuable. The presence of melanocytes in Stage 2 grafts was not investigated. This was due, in part, to the fact that the guinea pig strain used was albino. Further experiments on different species will be required to demonstrate the ability to implant melanocytes into Stage 2 grafts.

One of the most interesting properties of the Stage 2 grafts was their ability to segregate into epidermal and dermal layers. The mechanism of keratin pearl migration to the top of the graft was not investigated, but at least two mechanisms could be proposed. One would be that the

host recognizes the keratin pearls as foreign bodies and ejects them like any other foreign body. The other possibility is that the dermal precursors and epidermal cells are able to sort out in a manner analogous to chimera experiments done in embryos (127). An understanding of these mechanisms would be important in assessing the regenerative capacity of skin when the appropriate matrix and cellular components are provided.

Both Stage 2 grafts and autografts alter the contraction kinetics and scarring seen in ungrafted wounds. This is analogous to a thermodynamic process which can be carried out either reversibly or irreversibly. The contraction of an open wound and the formation of scar can be thought of as a spontaneous irreversible process. In contrast, the use of an autograft can be thought of as almost a completely reversible process since little scarring or contraction occurs. Stage 2 membranes, therefore, could be considered as a partially reversible process since many elements of skin are regenerated. Figure 112 illustrates this concept.

Applicability to Human Subjects

With slight modifications of this technology developed for Stage 2 grafts used with guinea pigs, it would be possible to prepare larger grafts suitable for clinical trials. Using this technology, it would be hoped that surgeons could close large wound areas in a single operative procedure. After a small split-thickness skin biopsy had been

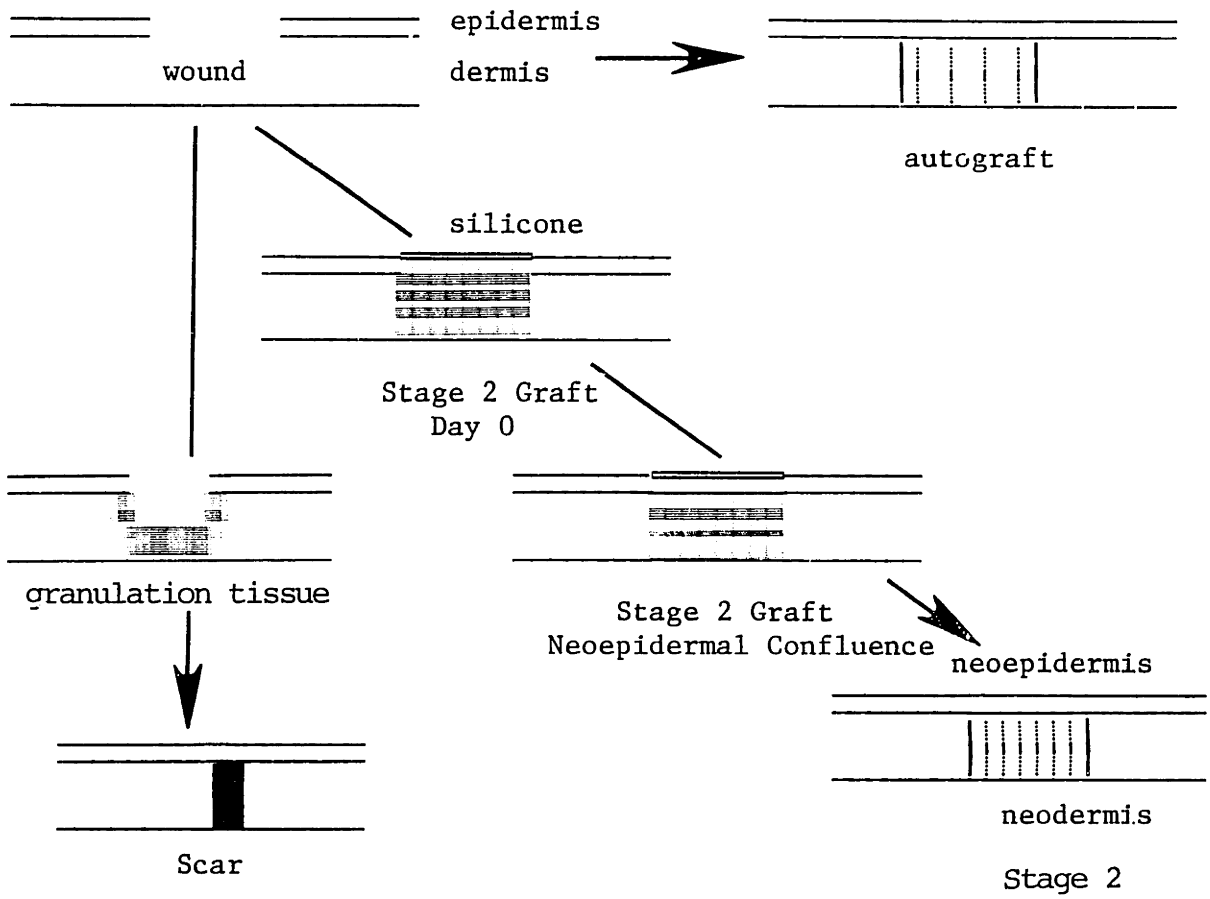

Figure 112. An open wound left untreated proceeds in an irreversible manner through the formation of granulation tissue, wound contraction, and the formation of scar. By treating the wound with an autograft or Stage 2 membrane, this course of events can be altered to give a less contracted and less scarred result.

obtained from the patient, seeded grafts could be prepared in a nearby laboratory during the time in which the surgeon excises the dead tissue from the wounds.

The major technical difficulties to overcome would be the time of cell isolation and seeding procedure, and the availability of a centrifuge system suitable for large grafts. The current cell isolation and seeding procedure requires about 100 minutes. This time could probably be significantly reduced for human trials. Since human skin has many less hair follicles than guinea pig skin, the separation of the dermis from the epidermis should be easier because of the reduced number of fibrous elements holding the two layers together. This may reduce the time which the skin must be exposed to trypsin. The first centrifugation step was used only to reduce the volume of cell suspension media. By using a larger centrifuge cup, this step could be eliminated. These changes along with the use of automated cell counting technology could possibly reduce the time of the cell isolation and seeding procedure to about one hour.

Another problem to be considered before clinical trials would begin would be the type of cell suspension medium to be used. Ten percent fetal calf serum (FCS) has been the most successful adjunct to DMEM in the guinea pig studies. However, because of the potential immunologic complications of the use of FCS in humans, other cell suspension media such as DMEM with 10% human AB serum may be

more appropriate.

The potential use of heterologous epidermal cells and cryopreservation would extend significantly the application of Stage 2 grafts. The technical difficulties of preparing the grafts under time pressures and the availability of large centrifugation systems would be potentially solved if these membranes could be prepared in central locations with heterologous cells and shipped to hospitals as needed. This would also reduce the anesthesia time by not requiring the surgeon to obtain skin biopsies from the patient. The interest in the use of heterologous epidermal cells has grown very rapidly in the last two years (75-84). The results reported here would suggest that with additional investigations of the immunology of the epidermal constituents and of biophysical methods of separation that heterologous cells may be used without undergoing immunologic rejection.

Applicability to Other Organ Systems

The results of applying a seeded bilayer membrane to skin deficits suggest the possibility that this type of technology may be useful in other organ systems. Scarring and contraction which are present in other organ injuries may be factors which block the regenerative capacity of these tissues. The work of Mulliken et al (124) has shown that using the appropriate matrix, i.e. demineralized bone, that congenital bone defects in the face could be corrected.

It is possible that extending the use of bioreplaceable templates to other organ systems which have been damaged to disease, trauma, or congenital defects will result in improved function of these organ systems.

APPENDIX

Cell Isolation and Seeding Protocol

Solutions:

A. Phosphate Buffered Saline without Calcium or Magnesium (PBS)

B. Tissue Culture Medium (TCM), Dulbecco's Modified Eagle's Medium with 10% heat inactivated fetal calf serum and 100 IU/ml penicillin, and 100 µg/ml Streptomycin.

C. Trypsin 2.5%, (1:250, GIBCO)

D. Trypan Blue (0.4%, GIBCO)

1. Rinse skin biopsy in PBS.
2. Incubate in 2.5% Trypsin for 40 minutes at 37° C with the dermal portion of the graft facing down.
3. Separate epidermis and dermis with forceps.
4. Place dermal portion in a 50 ml conical tube (Falcon,2098, Becton Dickenson) containig 25 ml of TCM.
5. Vortex for 60 seconds (Vortex Genie, Model K-550-G, Scientific Products at a setting of 10).
6. Filter cell suspension through sterile gauze.
7. Add 0.5 ml trypan blue to 0.5 ml of cell suspension.
8. After 15 minutes, count cells in hemocytometer. Those which exclude the dye are viable cells.
9. Spin the remainder of the cellular suspension at 500 g for 10 minutes, and adjust the volume of TCM so that the cell density is 1.7×10^6 viable cells per ml.
10. Equilibrate Stage 1 graft in TCM for 30 minutes.
11. Place graft in centrifuge cup with Silicone side down.

12. Add cellular suspension on top of the collagen-GAG membrane. For a 1.5 x 3.0 cm graft with 500,000 cells/cm^2 graft, add 1.3 ml of the cell suspension.
13. Spin for 15 minutes at 50 g.
14. Remove excess TCM with pipette.

BIBLIOGRAPHY

1. Montgomery, B.J.: J. Am. Med. Assoc. 243:345, 1979.
2. Holden, C.: Science 181:735, 1973.
3. Burke, J.F., Bondoc, C.C., Quinby, W.C.: J. Trauma 14:389, 1974.
4. Burke, J.F., Bondoc, C.C., Quinby, W.C.: Surg. Clin. North Am. 56:477, 1976.
5. Burke, J.F., Quinby, W.C., Bondoc, C.C., Cosimi, A.B., Russell, P.S., Szyfelbein, S.K.: Ann. Surg. 182:183, 1975.
6. Bloom, W., Fawcett, D.W.: A Textbook on Histology, Tenth Edition, Saunders, Philadelphia, p. 563, 1975.
7. Langman, J.: Medical Embryology, Third Edition, Williams and Wilkins Co., Baltimore, 1975.
8. Dermatology in General Medicine, Fitzpatrick, T.B. (ed), McGraw Hill, New York, 1979.
9. Muthiah, P.L., Ramanathan, N., Nayudamma, Y.: Biorheology 4:185, 1967.
10. Kenedi, R.M., Gibson, T., Daly, C.H.: "Bio-Engineering Studies of the Human Skin II", In: Biomechanics and Related Topics, Kenedi, R.M. (ed.), Pergamon, Oxford, p. 147, 1965.
11. Breasted, J.H.: The Edwin Smith Surgical Papyrus, Vol. 1, University of Chicago Press, Chicago, p. 83, 1930.

12. Weller, E.M.: "Regeneration", In: Biologic Basis of Wound Healing, Manaker, L. (ed), Harper and Row, Maryland, p. 291, 1975.

13. Borgens, R.B.: Science 217:747, 1982.

14. Abercrombie, M., Flint, M.H., James, D.W.: J. Embryol. Exp. Morphol. 2:264, 1954.

15. Billingham, R.E., Medawar, P.B.: J. Anat. 89:114, 1955.

16. Billingham, R.E., Russell, P.S.: Ann. Surg. 144:961, 1956.

17. Grillo, H.C., Watts, G.T., Gross, J.: Ann. Surg. 148: 145, 1956.

18. Straile, W.E.: J. Exp. Zool. 140:405, 1959.

19. Straile, W.E.: J. Exp. Zool. 141:119, 1959.

20. Reynolds, B.L., Leveque, T.F., Codington, J.B., Mansberger, A.R., Buxton, R.W.: Am. Surg. 25:540, 1959.

21. James, D.W., Newcombe, J.F.: J. Anat. 95:247, 1961.

22. Luccioli, G.M., Kahn, D.S., Robertson, R.H.: Ann. Surg. 160:1020, 1964.

23. Higton, D.I.R., James, D.W.: Br. J. Surg. 51:462, 1964.

24. Phillips, J.L., Peacock, E.E.: Proc. Soc. Exp. Biol. Med. 117:534, 1964.

25. Zahir, M.: Br. J. Surg. 51:456, 1964.

26. Sawhney, C.P., Monga, H.L.: Br. J. Plast. Surg. 23: 318, 1970.

27. Majno, G., Gabbiani, G., Hirschel, B.J., Ryan, G.B., Statkov, P.R.: Science 173:548, 1971.

28. Montandon, D., Gabbiani, G., Ryan, G., Majno, G.: Plast. Reconst. Surg. 52:291, 1973.

29. Madden, J.W.: Plast. Reconst. Surg. 52:291, 1973.

30. Ryan, G.B., Cliff, W.J., Gabbiani, G., Irle, C., Statkov, P.R., Majno, G.: Lab. Invest. 29:197, 1973.

31. Morton, D., Madden, J.W., Peacock, Jr. E.E.: Surg. Forum 23:511, 1972.

32. Knapp, T.R., Daniels, J.R., Kaplin, E.N.: Am. J. Pathol. 80:47, 1977.

33. Bhangoo, K.S., Quinlivan, J.K., Connelly, J.R.: Plast. Reconst. Surg. 57:308, 1976.

34. Brody, G.S., Peng, S.T.J., Landel, R.F.: Plast. Reconst. Surg. 65:673, 1981.

35. Bazin, S., Delauney, A., Nicoletis, C., Delbet, J.M.P.: Path. Biol. 18:1071, 1970.

36. Kischer, C.W., Shetlar, M.R.: Conn. Tissue Res. 2: 205, 1974.

37. Shuttlesworth, C.A., Forrest, L., Jackson, D.: BBA 229:681, 1975.

38. Bailey, A.J., Sims, T.J., Le Lous, M., Bazin, S.: Biochem. Biophys. Res. Comm. 66:1160, 1975.

39. Bailey, A.J., Bazin, S., Sims, T.J., Le Lous, M., Nicoletis, C., Delauney, A.: BBA 405:412, 1975.

40. Seyer, J.M., Hutcheson, E.T., Kang, A.H.: J. Clin. Invest. 59:241, 1977.

41. Isemura, M., Takahashi, K., Ikenaka, T.: J. Biochem. 80:653, 1976.

42. Forrest, L., Jackson, D.S.: BBA 229:681, 1971.

43. Forrest, L., Shuttlesworth, C.A., Jackson, D.S., Mechanic, G.: Biochem. Biophys. Comm. 46:1776, 1972.

44. Jackson, D.S., Ayad, S., Mechanic, G.: BBA 336:100, 1974.

45. Jackson, D.S., Mechanic, G.: BBA 336:228, 1974.

46. Comninou, M., Yannas, I.V.: J. Biomech. 9:427, 1976.

47. Rudowski, W.: Burn Therapy and Research, Johns Hopkins, Baltimore, 1976.

48. Bondoc, C.C., Burke, J.F.: Ann. Surg. 158:371, 1971.

49. Guthy, E.A., Billotte, J.B., Burke, J.F.: Chirurgia Plastica (Berlin) 2:263, 1974.

50. Song, I.C., Bromberg, B.E.: "Pig Skin Biologic Dressings on Burn Wounds", In: Research in Burns, Matter, P., Barclay, T.L., Konichova, Z. (eds), Stuttgart, Hans Huber, p. 285, 1971.

51. Yannas, I.V.: "Use of Artificial Skin in Wound Management", In The Surgical Wound, Dineen, P. (ed), Lea and Febiger, Philadelphia, 1981.

52. Yannas, IV., Burke, J.F.: J. Biomed. Mater. Res. 14: 65, 1980.

53. Yannas, I.V., Burke, J.F., Gordon, P.L., Huang, C., Rubenstein, R.H.: J. Biomed. Mater. Res. 14:107, 1980.

54. Dagalakis, N., Flink, J., Stasikelis, P., Burke, J.F., Yannas, I.V.: J. Biomed. Mater. Res. 14:511, 1980.

55. Burke, J.F., Yannas, I.V., Quinby, W.C., Bondoc, C.C., Jung, W.K.: Ann. Surg. 194:413, 1981.

56. Chen, E.H.: Masters Thesis, Department of Mechanical Engineering, M.I.T., 1982.

57. Flynn, S.: Bachelors Thesis, Department of Mechanical Engineering, M.I.T., 1983.

58. Okun, M.R., Edelstein, L.M.: Gross and Microscopic Pathology of the Skin, Dermatology Foundation Press, 1976.

59. Lever, W.F., Schaumburg-Lever, G.: Histopathology of the Skin, Lippincott, Philadelphia, 1975.

60. Pinkus, H., Mehregem, A.H.: A Guide to Dermatohistopathology, Appleton Century-Crofts, New York, 1981.

61. Ackerman, A.B.: Histologic Diagnosis of Inflammatory Skin Diseases, Lea and Fabiger, Philadelphia, 1978.

62. Herschman, H.R., Lusis, A.J., Groopman, J.E.: Ann. Intern. Med. 92:650, 1980.

63. O'Connor, N.E., Mulliken, J.B., Banks-Schlegel, S., Dehinde, O., Green, H.: Lancet 1981-I:75, 1981.

64. Bell, E., Ehrlich, H.P., Buttle, D.J., Nakatsuji, T.: Science 211:1052, 1981.

65. Eisinger, M., Monden, M., Raaf, J.F., Fotner, J.G.: Surgery 88:287, 1980.

66. Yannas, I.V., Burke, J.F., Orgill, D.P., Skrabut, E.M.: Science 215:174, 1982.

67. Yannas, I.V., Burke, J.F., Orgill, D.P.: Trans. Soc. Biomaterials 5:1, 1982.

68. Yannas, I.V., Burke, J.F., Warpehoski, M., Stasikelis, P., Skrabut, E.M., Orgill, D.P., Giard, D.: "Design Principles and Preliminary Clinical Performance of an Artificial Skin", In: Biomaterials: Interfacial Phenomena and Applications, Peppas, N., Cooper, S.L. (eds), Advances in Chemistry Series, ACS, Washington, 1982.

69. Yannas, I.V., Burke, J.F., Warpehoski, M., Stasikelis, P., Skrabut, E.M., Orgill, D.P., Giard, D.: Trans. Am. Soc. Artificial Int. Organs 17:19, 1981.

70. Yannas, I.V., Burke, J.F., Chen, E., Orgill, D.P., Skrabut, E.M.: IUPAC Proceedings, 28th Macromolecular Symposium, Amherst, Massachusetts, July 1982.

71. Yannas, I.V., Burke, J.F., Orgill, D.P., Skrabut, E.M.: American Chemical Society Meeting, Seattle, Washington, 1983.

72. Rogers, B.O.: Plast. Reconst. Surg. 5:269, 1950.

73. Barker, C.F., Billingham, R.E.: Ann. of Surg. 176:597, 1972.

74. Roitt, I.M.: Essential Immunology, Third Edition, Blackwell Scientific, Oxford, 1977.

75. Morhenn, V.B., Starr, E.D., Terrell, C., Cox, A.J., Engleman, E.G.: J. Investig. Dermatol. 78:319, 1982.

76. Faure, M., Eisenger, M., Bystryn, J.C.: J. Investig. Dermatol. 76:347, 1981.

77. Elmets, C.A., Bergstresser, P.R., Streilein, J.W.: J. Investig. Dermatol. 79:340, 1982.

78. Streilein, J.W., Lonsberry, L.W., Bergstresser, P.R.: J. Exp. Med. 155:863, 1982.

79. Dubertret, L., Picard, O., Bagot, M., Tulliez, M., Fosse, M., Aubert, C., Touraine, R.: Br. J. Dermatol. 106:287, 1982.

80. Holden, C.A., Morgan, E.W., MacDonald, D.M.: J. Investig. Dermatol. 79:382, 1982.

81. Fithian, E., Kung, P., Goldstein, G., Rubenfeld, M., Fenoglio, C., Edelson, R.: Proc. Nat'l. Acad. Sci. USA 78:2541, 1982.

82. Morhenn, V.B., Benike, C.J., Charron, D.J., Cox, A., Mahrle, G., Wood, G.S., Engleman, E.G.: J. Investig. Dermatol. 79:277, 1982.

83. Aberer, W., Stingl, G., Stingl-Gazze, L.A., Wolff, K.: J. Investig. Dermatol. 79:129, 1982.

84. Belsito, D.V., Flotte, T.J., Lim, H.W., Baer, R.L., Thorbecke, G.J., Gigli, I.: J. Exp. Med. 155:291, 1982.

85. Regnier, M., Delescluse, C., Prunieras, M.: Acta Dermatol. Venereol. 53;241, 1973.

86. Prunieras, M., Delescluse, C., Regnier, M.: J. Invest. Dermatol. 67:58, 1976.

87. Jepsen, A.: Scand. J. Dent. Res. 82:144, 1974.

88. Eisenger, M., Lee, J.S., Hefton, J.M., Darzynkiewicz, Z., Chiao, J.W., DeHarven, E.: Proc. Nat'l. Acad. Sci. USA 76:5340, 1979.

89. Rheinwald, J.G., Green, H.: Cell 6:331, 1975.

90. DeGowin, E.L., DeGowin, R.L.: Bedside Diagnostic Examination, Third Edition, Macmillan, New York, 1976.

91. Skrabut, E.M.: Personal Communication, 1983.

92. Ridge, M.D., Wright, V.: Biorheology 2:67, 1974.

93. Nilsson, G.E.: Med. & Biol. Eng. & Comput. 15:209, 1977.

94. Wheldon, A.E., Monteith, J.L.: Med. & Biol. Eng. & Comput. 18:201, 1980.

95. Scheuplein, R.J., Blank, I.H.: Physiol. Rev. 51:702, 1971.

96. Murthy, S.: Personal Communication, 1981.

97. Chardack, W.M., Martin, M.M., Jewett, T.C., Boyer, B.E.: Plast. Reconstr. Surg. 43:625, 1962.

98. Hubacek, J., Kliment, K., Dusek, J., Hubacek, J.: J. Biomed. Mat. Res. 1:387, 1967.

99. Hall, C.W., Liotta, D., Chidoni, J.J., Debakey, M.E., Dressler, D.P.: J. Biomed. Mat. Res. 1:187, 1967.

100. Schmulka, I.R.: J. Biomed. Mat. Res. 6:571, 1972.

101. Nalbandian, R.M., Henry, R.L., Wilks, H.S.: J. Biomed. Mat. Res. 6:105, 1972.

102. Guldalian, J., Jelenko, III, C., Calloway, D., McKnight, J.T.: J. Trauma 13:32, 1973.

103. Wilkes, G.L., Samuels, S.L.: J. Biomed. Mat. Res. 7:541, 1973.

104. Principles of Surgery, Schwartz, S.I. (ed), Third Edition, McGraw-Hill Book Co., New York, 1979.

105. Oliver, R.F., Barker, H., Cooke, A., Grant, R.A.: Conn. Tissue Res. 9:59, 1981.

106. Oliver, R.F., Grant, R.A., Kent, C.M.: Br. J. Exp. Pathol. 53:540, 1972.

107. Oliver, R.F., Grant, R.A., Hulme, M.J., Mudie, A.: Clin. Orthopedics & Related Res. 115:291, 1976.

108. Oliver, R.F., Grant, R.A., Hulme, M.J., Mudie, A.: Br. J. Plast. Surg. 30:88, 1977.

109. Shakespeare, P.G., Griffiths, R.W.: Lancet 1:795, 1980.

110. Oliver, R.F., Grant, R.A.: Br. J. Plast. Surg. 32: 87, 1979.

111. Oliver, R.F., Grant, R.A., Cox, R.W., Cooke, A.: Br. J. Exp. Pathol. 61:544, 1980.

112. Barker, H., Oliver, R., Grant, R., Stephen, L.: BBA 632:589, 1980.

113. Grillo, H.C., Gross, J.: J. Surg. Res. 2:69, 1962.

114. Billingham, R.E., Reynolds, J.: Br. J. Plast. Surg. 5:25, 1952.

115. McGrath, M.H., Hundahl, S.A.: Plast. Reconstr. Surg. 69:975, 1982.

116. McGrath, M.H.: Plast. Reconstr. Surg. 69:74, 1982.

117. Rudolph, R.: Plast. Reconstr. Surg. 63:475, 1979.

118. Rudolph, R.: Surg. Gynecol. & Obst. 142:49, 1976.

119. Corps, B.V.M.: Br. J. Plast. Surg. 22:125, 1969.

120. Brown, J.B., McDowell, F.: Skin Grafting, Third Edition, J.B. Lippincott Co., Philadelphia, 1959.

121. Li, A.K.C., Ehrlich, H.P., Relstad, R.L. Koroly, M.J., Schattenkerk, M.E., Malt, R.A.: Ann. Surg. 191:244, 1980.

122. Orgill, D.P.,: Thesis Proposal, Doctoral Thesis, M.I.T, 1981.

123. Vogel, H.G.: J. Investig. Dermatol. 76:493, 1981.

124. Mulliken, J.B., Glowacki, J., Kaban, L.B., Folkman, J., Murray, J.E.: Ann. Surg. 194:366, 1981.

125. Kueppers, F., Mills, J.: Science 291:182, 1983.

126. Wilson, R.: Bachelor's Thesis, Department of Mechanical Engineering, M.I.T., 1982.

127. Balinski, B.I.: An Introduction to Embryology, Fourth Edition, Saunders, Philadelphia, 1975.

128. Harris, A.K., Stopak, D., Wild, P.: Nature 290:249, 1981.

129. Bell, E., Ivarsson, B., Merrill, C.: Proc. Nat'l. Acad. Sci. U.S.A. 76:1274, 1979.

130. Snowden, J.M.: Australian J. Exp. Biol. Med. Sci. 59:203, 1981.